Modeling mussel bed influence on fine sediment dynamics on a Wadden Sea intertidal flat

Bas van Leeuwen

Modeling mussel bed influence on fine sediment dynamics on a Wadden Sea intertidal flat

Bas van Leeuwen

Graduation committee:

Prof. Dr. S.J.M.H. Hulscher

Dr. ir. D.C.M. Augustijn

Drs. M.B. de Vries

Dr. B.K. van Wesenbeeck

Master's Thesis

January 2008

ZZ4499

Client	University of Twente
Title	Modeling mussel bed influence on fine sediment dynamics on a Wadden Sea intertidal flat

Abstract

The influence of mussel beds on fine sediment dynamics has been well recognized in literature. Until now, no successful attempts at modeling this influence exist.

During this study a Delft3D-FLOW model implementation of young mussel bed interaction with fine sediment has been set up. Roughness and erosion behaviour have been implemented via the Delft3D trachytope functionality. The Delft3D source code has been adjusted in order to simulate active capture of suspended fine sediment by mussel filter feeding. The properties of sediment (including pseudo-faecal matter) deposited in between mussels have been taken into account by adjusting the sediment characteristics in the mussel bed.

The mussel bed implementation has been tested in a Wadden Sea intertidal mudflat model. The model domain has been based on an area south of Ameland, which is suitable mussel habitat. The model has simulated two current dominated summer months. A sensitivity analysis has been conducted on the parameters of the mussel bed implementation. Finally, different patterns, known to occur in young mussel beds, have been imposed.

It has been concluded that roughness and filtration rate of mussel beds are important factors in mussel bed influence on fine sediment. A combination of active deposition via filtration and slowdown of the flow leads to high cumulative deposition in the mussel bed. In the surrounding area deposition is also high because of a reduction of flow velocities caused by the rough mussel bed. Patchiness and specifically striped patterns in mussel bed coverage cause mussel beds to experience less sedimentation than uniformly covered beds of the same size. In a broader sense, it has been found that the ability of young mussels to quickly climb on top of deposited material, results in rapid capture and trapping of large amounts of fine sediment.

References	Z4499, biogeomorphology, fine sediment, mussel bed, Wadden Sea

Ver	Author	Date	Remarks	Review	Approved by
	B. van Leeuwen	Jan 2008	final	B.K. van Wesenbeeck	T. Schilperoort

Project number	Z4499
Keywords	Mussel
Number of pages	114
Classification	None
Status	Final

Preface

This document is my Master's Thesis for Civil Engineering and Management at the University of Twente. The project has been conducted at WL|Delft Hydraulics which has merged into Deltares in January 2008. The subject of this study is the influence of mussel beds on fine sediment dynamics and although I am not a fan of mussels in a culinary sense, I have been gripped by the sheer depth of interaction between these animals and their environment. Despite this, there have been times when I was desperately stuck. I will therefore use the rest of this preface to thank the people who have helped me come through.

First of all I would like to thank the members of my committee: Suzanne Hulscher for her constructive criticism and focus on positive results; Denie Augustijn for his guidance in keeping me on track and letting me see the way forward; Mindert de Vries for his enthusiastic support and original suggestions, especially considering the issues that have been on his mind and finally Bregje van Wesenbeeck, for providing me with meticulous feedback and suggestions during the last two months. I would also like to thank Frank Dekker, although not really part of my graduation committee, for getting me up to speed with Delft3D.

Further people that I am grateful to for letting me share in their knowledge and skills regarding a variety of subjects: Luca van Duren, Rob Uittenbogaard, Herman Kernkamp, Pieter-Koen Tonnon, Maarten van Ormondt, Norbert Dankers and Bas Borsje. Thanks goes out to my fellow graduate students and colleagues at the student square of MCM2 for the great work atmosphere they provided.

I would like to thank my parents and brother for being the wonderful people they are. Above all, Floor, thank you for your love and support during the past months, I would not know what to have done without you.

Delft, January 2008

Bas van Leeuwen

Abstract

Large aggregations of mussels, so called mussel beds, live in the Dutch Wadden Sea and the Eastern Scheldt estuary. Mussel beds can be hundreds and even thousands of meters in size. The influence of mussel beds on fine sediment dynamics has been well recognized in literature. Until now, no successful attempts at modeling this influence exist.

During this study a process-based model implementation of young mussel bed interaction with fine sediment has been set up for use in Delft3D. Roughness and erosion behavior have been implemented via the Delft3D trachytope functionality. The Delft3D source code has been adjusted in order to simulate active capture of suspended fine sediment by mussel filter feeding. The properties of sediment (including pseudo-faecal matter) deposited in between mussels have been taken into account by adjusting the sediment characteristics in the mussel bed.

The mussel bed implementation has been tested in a Wadden Sea intertidal mudflat model. The model domain has been based on an area south of Ameland, which is suitable mussel habitat. The model has simulated two current dominated summer months. A sensitivity analysis has been conducted on the parameters of the mussel bed implementation. Finally, different patterns, known to occur in young mussel beds, have been imposed.

It has been concluded that roughness and filtration rate of mussel beds are important factors in mussel bed influence on fine sediment. A combination of active deposition via filtration and slowdown of the flow leads to high cumulative deposition in the mussel bed. In the surrounding area deposition is also high because of a reduction of flow velocities caused by the rough mussel bed. Patchiness and specifically striped patterns in mussel bed coverage cause mussel beds to experience less sedimentation than uniformly covered beds of the same size. In a broader sense, it has been found that the ability of young mussels to quickly climb on top of deposited material, results in rapid capture and trapping of large amounts of fine sediment.

Contents

1 Introduction

Large aggregations of mussels live in the Dutch Wadden Sea and the Eastern Scheldt estuary, the mussel beds can stretch for kilometers. Next to the resources these shell fish offer as a local culinary delicacy, research is ongoing investigating how mussel beds can be deployed to achieve ecological and engineering aims. This graduation project aims to contribute to this research, by adding to the understanding of the influence of mussel beds on fine sediment dynamics.

Figure 1: Wadden Sea mussel bed (Photograph provided by Norbert Dankers).

1.1 Problem definition

Mytilus Edulis (Blue Mussel) is often mentioned for its role in shaping the geomorphology of its environment. Both the fact that the mussels produces (pseudo-) faeces that bind fine sediments into more erosion resistant pellets (Flemming and Delafontaine, 1994; Dame and Dankers, 1988; Oost, 1995) and the roughness of the bed and the trapping of sediment (Jumars and Nowell, 1984) are mentioned as potentially important influences. Research at WL|Delft hydraulics, RIKZ and NIOO is ongoing to survey the feasibility of mussel beds as bio-tools[1]. Examples include the use of mussels to combat turbidity, which is beneficial to for example the reintroduction of sea grasses in the Wadden Sea (Van Katwijk, 2003). Mussel beds could be used to dissipate wave energy and thereby protecting valuable salt marshes from erosion both

[1] *In the context of the Dutch Bio-Builders pilot project: "Biobouwers van de kust".*

in the Wadden Sea and in the Eastern Scheldt estuary. Mussel beds could also increase deposition in these areas by slowing down the flow. Modeling the influence of mussel beds on fine sediment dynamics will be a useful tool in predicting the effectiveness of these measures. At this moment such a model implementation does not exist.

1.2 Research objective

The goal of this graduation project is formulated as follows: *To model mussel-sediment interaction in order to study (1) the net retention and (2) the spatial distribution of fine sediment on a Wadden Sea intertidal flat*. The goal is formulated in such a way that this project can contribute to both the influence of mussel beds on large estuarine scale fine sediment dynamics (by studying the net retention of sediment) and the local effects of placing mussel beds in the vicinity of salt marshes (by investigating the influence of a mussel bed on the spatial distribution of fine sediment). The Wadden Sea has been chosen as a research area because it is both a natural habitat for mussels and a proposed location for use of mussels as bio-tools. Based on the objective the following research questions will be addressed:

1) How do mussel beds influence fine sediment dynamics and which properties of the mussel bed are important in this respect?
2) How can existing experimental data be used to assess relevant mussel bed characteristics?
3) How can mussel beds be implemented in the Delft3D hydrodynamic and morphological model?
4) What is the influence of mussel beds on net fine sediment retention on an intertidal mudflat in the Wadden Sea?
5) What is the influence of mussel beds on the spatial patterns of deposition and erosion on an intertidal mudflat in the Wadden Sea?
6) How do naturally occurring spatial patterns in mussel beds affect these influences?

1.3 Report outline

The report is structured as follows: Chapter 2 describes and analyzes the mechanisms by which mussel beds affect fine sediment dynamics with focus on the Wadden Sea habitat. Using the results from Chapter 2 a model representation of influence of mussel beds on fine sediment is proposed in Chapter 3. A Delft3D intertidal mudflat model will be set up in Chapter 4, in this model the mussel bed representation from Chapter 3 will be implemented. The results from this model study will be presented in Chapter 5. Chapter 6 is used to study the sensitivity of model results to model uncertainties and natural variability in mussel bed patterns. The research methodology and the results will be discussed in Chapter 7. Finally Chapter 8 gives the projects conclusions and offers recommendations for further research.

2 Fine sediment, mussels and mussel beds

The blue mussel (*Mytilus Edulis*) is an ecosystem-engineer (Jones *et al.*, 1994), implying that it can exert substantial effects on its surroundings. In case of the mussel, it constructs its own habitat: the mussel bed. The mussel bed influences both the amount and distribution of fine sediment on an intertidal flat. In this chapter an overview of previous research on the governing processes of this influence is presented. First, a short introduction into fine sediment dynamics is given. Second, the most essential characteristics of mussel biology are explained. Third, the influence of mussels and mussel beds on fine sediment dynamics is explained. In the fourth and last section the development of intertidal mussel beds in the Wadden Sea is explained.

2.1 Fine sediment dynamics

Before focusing on the influence of mussel beds on fine sediment dynamics, a short introduction into the fine sediment dynamics themselves is in order. Fine sediment (mud or cohesive sediment, particle diameter < 63 µm) is distinct from course non-cohesive sediment (sand, particle diameter 63 µm – 2 mm) primarily because it has much smaller particles. This difference in size brings about a distinctly different behavior of fine sediments as opposed to sands. The properties of the particles are such that electro-chemical effects play a role in binding the particles together[2]. This makes that fine sediment in a sea bed has high resistance to erosion. Also if in suspension, the small and light particles make settling of sediment a slow process[3].

2.1.1 Suspended sediment transport

Transport of fine sediment can be seen exclusively as suspended load transport, meaning that the sediment is in suspension and is transported by currents. It follows that fine sediment transport can be described by the following advection diffusion equation:

$$\frac{\partial c}{\partial t} + \underbrace{\frac{\partial uc}{\partial x} + \frac{\partial vc}{\partial y} + \frac{\partial (w - w_s)c}{\partial z}}_{advection} \underbrace{- \frac{\partial}{\partial x}\left(\varepsilon_{s,x}\frac{\partial c}{\partial x}\right) - \frac{\partial}{\partial y}\left(\varepsilon_{s,y}\frac{\partial c}{\partial y}\right) - \frac{\partial}{\partial z}\left(\varepsilon_{s,z}\frac{\partial c}{\partial z}\right)}_{diffusion} = E - D \qquad (1)$$

c = mass concentration of sediment (kg m^{-3})

u, v, w = flow velocity components (m s^{-1}) in stream wise (x), lateral (y) and vertical (z) direction

w_s = settling velocity (m s^{-1})

[2] *The cohesive behavior is caused by the overall small size of the particles, meaning that electro-chemical forces are relatively large. Also clay particles (particle diameter < 3.9 µm) consists of flakes. The large surface-to-volume-ratio and the negative charge of these flakes enhance cohesion.*

[3] *Large variation in time and space in settling velocity of fine sediment can occur due to flocculation (the fine sediment particles bind together in flocs with a larger settling velocity) and hindered settling (high sediment concentrations can inhibit overall settling velocity), see Winterwerp (2002). In this report settling velocity has been assumed to be constant in time and space.*

$\varepsilon_{s,x}$, $\varepsilon_{s,y,}$, $\varepsilon_{s,z}$ = eddy diffusivities in three directions ($m^2\ s^{-1}$)

E = erosion source term (kg $m^{-3}\ s^{-1}$)

D = deposition sink term (kg $m^{-3}\ s^{-1}$)

If vertical velocities in flow (w) can be disregarded, the distribution of fine sediment over the vertical in otherwise uniform equilibrium conditions can be described by:

$$-\frac{\partial(w_s)c}{\partial y}-\frac{\partial}{\partial z}\left(\varepsilon_{s,z}\frac{\partial c}{\partial z}\right)=0 \qquad (2)$$

As can be seen from equation (2) the distribution of suspended sediment is determined by the settling velocity causing the sediment to fall on the one hand and turbulent diffusion on the other. Suspended sediment concentrations are generally higher near the bed than higher in the vertical (because of the settling velocity) and turbulence thus has the net effect of transporting sediment upwards. Turbulence is generated by disturbances to the flow, i.e. rougher beds and high velocities cause high turbulence, causing high turbulent diffusivity. At the interface between the water and the bed, deposition (D) and erosion (E) can occur. Both can be described by the Partheniades-Krone formulations (Partheniades, 1965):

$$E = M \cdot \max\left(0, \frac{\tau_b}{\tau_{e\_crit}} - 1\right) \qquad (3)$$

$$D = w_s \cdot c_{z=0} \qquad (4)$$

Where:

E = resuspension flux (g $m^{-2}\ d^{-1}$)

M = first order erosion rate (kg $m^{-2}\ d^{-1}$)

τ_b = bed shear stress (N m^{-2})

τ_{e_crit} = critical bed shear stress for erosion (N m^{-2})

D = deposition flux of suspended matter (kg $m^{-2}\ d^{1}$)

w_s = settling velocity of suspended (m d^{-1})

$c_{z=0}$ = concentration near bed (z=0)

Bed shear stress (τ_b) is caused by shear velocity near the bed and the roughness of the bed. Currents and waves cause velocities near the bed. The higher the velocities and the rougher the bed, the higher the bed shear stress will be. Erosion is a function of this bed shear stress as soon as the latter exceeds the critical bed shear stress for erosion. Deposition is a function of the suspended sediment concentration near the bed (determined by equation (2)) and the settling velocity.

2.1.2 Lag effects

Because of the specific properties of fine sediments, two lag effects exist:

- Settling lag: when flow velocities decrease during slack tide, turbulent mixing decreases and the sediment will settle. However, the low settling velocity of fine sediment means that deposition is slow. Fine sediment can be transported for large distances after the point where the flow can no longer keep all the material in suspension.

- Scour lag. Although easily kept in suspension, once settled fine sediment is difficult to erode. Hence, flow velocities can bring in sediment at incoming tide, but the same velocities at outgoing tide may not be able to generate enough bed shear stress to erode the then settled material.

2.1.3 Fine sediment in the Wadden Sea

The Wadden Sea is a tidal inlet, i.e. a shallow sea protected by barrier islands. The area is characterized by extensive intertidal flats and intersected by narrow deep gullies (or channels). Fine sediment transport in such an area is a very complicated process, involving many factors, see for example Vermeulen (2003) and Van Ledden (2003). Here it is most relevant to explain the seasonal variation in mud content on an intertidal flat. In general it can be stated that mud accretes on the intertidal flats during summer and is eroded during late autumn and winter months (Oost, 1995). This phenomenon is the result of weather patterns. As explained in section 2.1.1 erosion is a function of bed shear stress. In summer wind speeds (and thus waves and the corresponding velocities) are low and bed shear stress is dominated by current velocities (Janssen-Stelder, 2000). Currents are highest in the channels and as a result erosion is highest there. Deposition is more or less uniformly distributed between gullies and flats, mainly occurring during flood slack tide. The resulting net effect is deposition of fine sediment on the intertidal flats in summer, hence the name 'mud flats'. In winter, wind speeds are much higher causing high waves. Waves cause orbital motions in the water, the velocities of these motions decrease with depth. The shallow intertidal flats will thus experience high bed shear stress during stormy conditions, as opposed to the deeper channels. Deposition is still more or less uniformly distributed, but erosion is now much higher on the intertidal flat. Overall the erosion has increased, leading to higher suspended sediment concentrations in winter. The net effect is that the intertidal flats erode and the fine sediment accumulates in the channels.

A final remark that needs to be made, is that the vertical distribution of sediment (in equilibrium) described by equation (2) is relatively uniform in the Wadden Sea. This has been concluded by Van Loon (2005) on theoretical grounds and measured by Ridderinkhof *et al*. (2000) on an intertidal flat. This phenomenon is caused by the low water depths and high turbulence levels in the Wadden Sea.

2.2 Blue mussel (Mytilus Edulis)

The blue mussel (*Mytilus Edulis*) is a generally well known edible shell fish. Its most important features are displayed in Figure 2. The animal is protected by a smooth shell that has concentric and sometime radial lines, but this never translates into ribbed or wave patterns seen in some other shell fish. Despite its smooth surface the hydrodynamic forces on an individual mussel can be large. Therefore byssal threads extend from the mussel to secure it in place. The foot of the mussel can provide movement if necessary, in such cases the byssal threads can be released and later reattached. The ability to move is lost with age (Dankers *et al.*, 2004b; Okamura, 1986; Hunt and Scheibling, 2002). As explained later, mussel mobility can be necessary to prevent smothering by sediment, or to gain better access to fresh water for feeding.

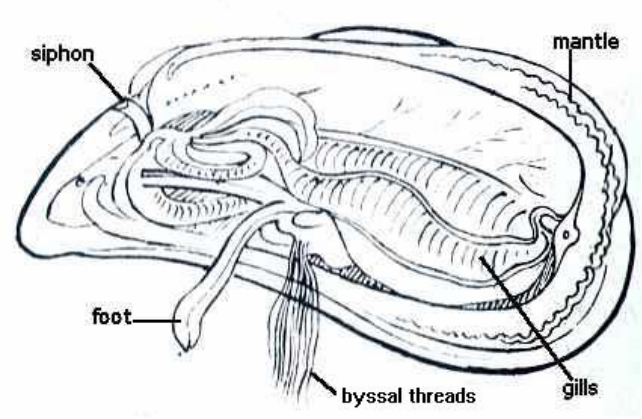

Figure 2: Mytilus Edulis selected anatomical features (image by Laura Smith, www.bumblebee.org)

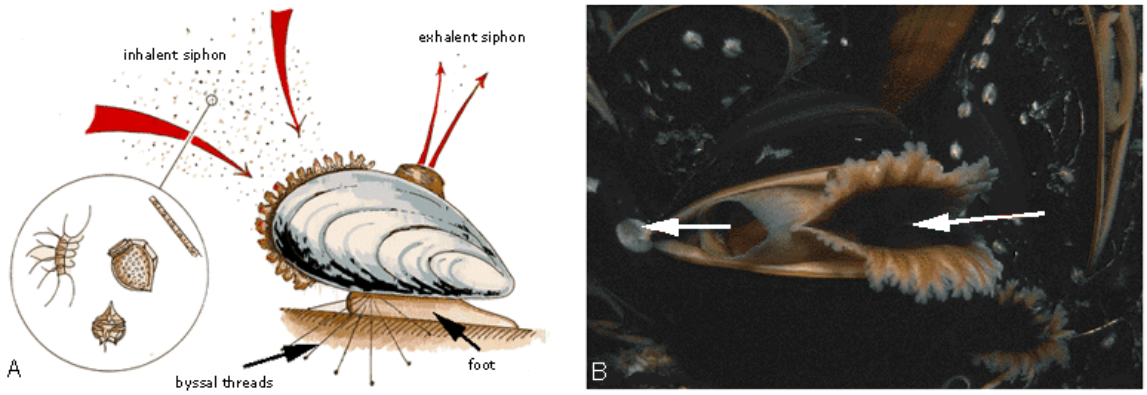

Figure 3: Mussel filter feeding, arrows give the inflow and outflow of water (source: Johannesson et al., 2000).

Mussels feed on suspended phytoplankton by filtering water with the gills. The mussel mantel opens at the right side as displayed in Figure 2, in order to inhale water into the gill system. Water is exhaled by the exhalent siphon, see Figure 3. Suspended sediment particles also taken up by filtering activity are excreted as pseudofaeces (excreted before entering the intestines) and as faeces (excreted after ingestion). The deposition of sediment in this way is an important process, especially considering the large aggregations in which mussels live.

Mussels rarely live alone, but usually form large colonies. Although mussels prefer a hard substrate to attach to, in the Wadden Sea mussel beds are found on the bare intertidal flat. Sediment can accumulate under these beds, elevating them above the rest of flat. The influence of these beds on fine sediment dynamics are explained in the next section.

2.3 Mechanisms of fine sediment influence

Mussel beds influence fine sediment dynamics by capturing and fixing sediment. Young mussel beds can rise 30-40 cm in their first months of existence (Dankers *et al.*, 2004b). The material underneath the mussels is fixed because mussels have the ability to climb on top of material deposited between them. Widdows *et al.* (2002) found that mussels can unbury themselves as much as 6 cm in a day. This is only one of the mechanisms playing a role in the influence of mussels on fine sediment.

2.3.1 Effect on hydrodynamics

Fine sediment transport is largely determined by advection of suspended sediment with the flow, as is described in section 2.1. Where flow velocities are higher, erosion may take place; if flow velocities are lower the sediment can settle to the bed. The hydrodynamics thus play a governing role in fine sediment dynamics and rough elevated mussel beds can affect these hydrodynamics in a significant way. The mechanisms via which the flow (both on a large horizontal scale and on a local vertical scale) is influenced by mussel beds are explained in this section.

2.3.1.1 Influence on flow patterns

The flow is affected in a spatial sense by mussel beds. Mussel beds can measure up to hundreds of meters and even kilometers. The increased height of mussel beds above the surrounding sediment can be up to 0.5 m. Historically far higher elevations have been recorded (Flemming and Delafontaine, 1994). However mussel beds will never increase their height above mean sea level (McGrorty *et al.*, 1993). This combined with the roughness of these beds, means that the flow is significantly impacted. The physical barrier presented by the mussel bed causes flow in front and behind the mussel bed (relative to the flow direction) to slow down. The flow is forced around the mussel bed, increasing flow velocities on the sides of the mussel bed. Faster flow causes more bed shear stress and thus more erosion, as described in section 2.1.1. The reduced flow in the wake of mussel beds means that more sediment is deposited and the potential for erosion is less. The flow over the bed is also hindered by the mussel bed roughness.

The roughness of the mussel bed is caused by roughness elements which exert drag on the fluid. The roughness elements are mussel bed patches (see Figure 10) and the roughness of the shells. The distinction between form roughness of patches and roughness of shells is similar to how roughness is described for sandy bed forms: form roughness and grain roughness. Roughness slows down the flow and generates turbulence.

2.3.1.2 Turbulence production above mussels influencing deposition

Turbulence diffuses suspended sediment and makes the water column more mixed. This has implications for the suspended sediment distribution over the vertical as explained in section 2.1.1. The sediment concentration close to the bed is an important variable determining the magnitude of deposition, see equation (4). Turbulence production is important for mussel survival. Turbulent eddies mix the lower layers of the flow (with low algae content) with higher layers (with high algae content, close to the sun light (Klausmeier and Litchman, 2001)). It has been shown by Frechette *et al.* (1989) that without the turbulent mixing the lower layers would be exhausted quickly from algae, depleting the mussels food supply. The fact that mussels are filter feeders adds to the turbulence production. The inhaled fluid is expelled through the exhalent siphon; see Figure 2. It has been shown by Van Duren *et al.* (2006) that these siphon currents have a significant impact on turbulence production. In normal conditions, without mussels, increased turbulence brings suspended sediment higher in the water column (see equation (2)). However in the case of mussels the lower regions may be exhausted of sediment because of capture by filter feeding. The combined effect of these two phenomena for deposition of fine suspended sediment is unknown[4].

[4] *In theory it is possible that filter feeding by mussels causes sediment concentrations near the bed to be lower than the sediment concentrations higher up in the vertical, exactly opposed to what is normally*

2.3.1.3 Small scale hydrodynamics in between mussels influencing erosion

In this report a distinction will be made between the sediment in between the mussels and 'mussel mud'. Mussel mud comes about as an effect of mussels climbing on top of the sediment deposited between them, thereby protecting the buried material. Figure 4 gives a cross section of a mussel bed, displaying the mussel mud and the mussel layer itself. The distinction between the mussel mud and the mussel layer is not absolute, especially for older mussel beds, dead shells will be present in the mussel mud. For a one-year-old mussel bed (as used in experiments presented by Van Duren, 2006) the (living) mussel layer is around 6 cm and has an estimated porosity of 68% (see Appendix A.2). For older or younger mussel beds these values are likely to be different. In between the mussels there is sufficient space for fine sediment.

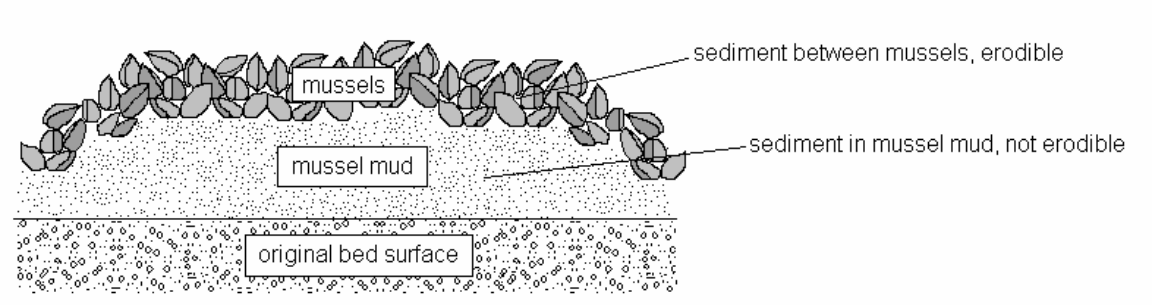

Figure 4: Mussel bed schematic displaying the layer of mussels and the underlying mussel mud.

The potential for erosion of both the sediment between the mussel and the mussel mud has been investigated in Appendix A. It has been shown that the mussel mud will never erode as long as the mussels covering it remain; the material is simply too deep relative to the mussels to be sensitive to erosive forces. If during winter storms the mussels erode (see section 2.4.2), the mussel mud underneath will become exposed and erode as well. Appendix A further focuses on the erosion of the material in between the mussels. This erosion is an effect of the force that water exerts on the sediment. For a current dominated flat bed, bed shear stress (which is the primary agent for erosion, see equation (3)) can be described as:

$$\tau_b = \frac{\rho_0 g \cdot U^2}{C^2} \qquad (5)$$

Where:

τ_b = bed shear stress (N m^{-2})

ρ_0 = density of water (kg m^{-3})

g = acceleration due to gravity (m s^{-2})

U = depth averaged velocity (m s^{-1})

C = Chézy roughness coefficient (m$^{1/2}$ s^{-1})

In case of a mussel bed most of the shear stress exerted by the flow is absorbed by the mussels themselves, not by the sediment lying in between the mussels. This can be conceptualized by relating the bed shear stress not to the depth averaged velocity as in equation (5) but to the characteristic shear velocity flowing over the sediment in

the case. In such circumstances high turbulence would actually increase the amount of sediment near the bed, by mixing the lower layers with the high concentration upper layers of the flow.

between the mussels. Also turbulent eddies in between the mussels can temporarily increase those shear velocities near the bed, increasing bed shear stress. Using a numerical point model, it is shown in Appendix A that the two determining variables - shear velocity and turbulence - are highly variable with the mussel bed characteristics. In fact, depending on where the sediment is located vertically in between the mussels (i.e. close to the mussel tops, or buried deep in between) bed shear stresses can either increase or decrease in comparison with a bed without mussels. For example after high sedimentation, sediment is stacked high between the mussels, turbulent scouring will cause high erosion. On the other hand, after such erosion the remaining sediment is left deep between the mussels, where the coverage by the mussels prevents significant further erosion (i.e. only the mussel mud remains).

2.3.2 Biodeposition as deposition flux

A major contributor to fine sediment deposition in the mussel bed and its vicinity is biodeposition. Biodeposition is the process where indigestible or otherwise rejected particles from the inhaled fluid are excreted and deposited as (pseudo-)faecal pellets. This section describes the factors influencing biodeposition and the significance of biodeposition both in and outside the actual mussel bed.

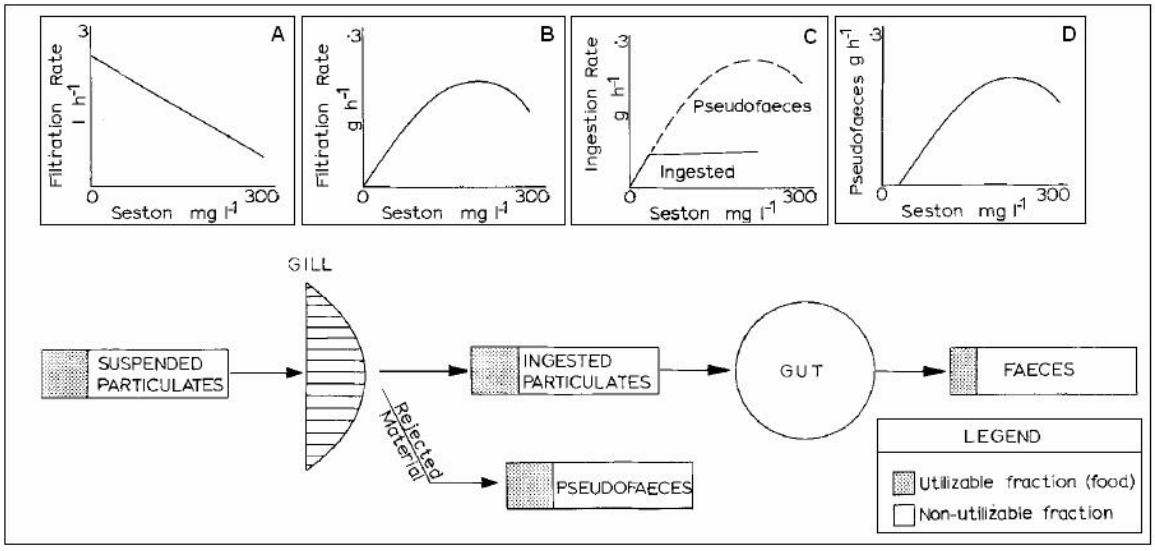

Figure 5: Fluxes of fine sediment inhaled by a mussel (adapted from Widdows et al., 1979).

In Figure 5 the phenomenon of biodeposition production in mussels is described. The figure deals with suspended particulates (or seston), which is actually a combination of organic material (partly utilizable as food) and suspended sediment. The amount of water inhaled is given as the filtration rate in l h^{-1}. It is displayed as a function of the concentration of suspended particulate material (mg l^{-1}), the higher the concentration the lower the filtration rate, see Figure 5 A. Although other factors can influence the filtration rate, the main forcing of filtration rate is the concentration of suspended material (Tsuchiya, 1980). The filtration rate multiplied with the seston concentration gives the filtration rate in mg l^{-1}, see Figure 5 B.

A pre selection is made between particles that enter the intestines and those that do not, see Figure 5 C. Actually, everything above a relatively low threshold concentration (5 mg l^{-1}) is ejected as pseudofaeces (Dankers *et al.*, 1989), see Figure 5 D. Given the normal suspended sediment concentrations in the Wadden Sea of around 50 mg l^{-1}, the

majority of excreted matter is pseudo-faeces. The rest of the material is ingested and excreted as faecal pellets.

Measurements of biodeposition rates have been carried out. A laboratory study by Tsuchiya (1980) found a result that can be translated[5] into 375 g m^{-2} d^{-1}. Field studies in the Wadden Sea and Eastern Scheldt estuary have consistently found lower values: 106-172 g m^{-2} d^{-1} by Dame and Dankers (1988)[6] and 118 g m^{-2} d^{-1} (Prins *et al.*, 1996). Using theoretical relations such as those proposed by Widdows *et al.* (1979), biodeposition flux can also be calculated by using the filtration rate, biomass per unit area, suspended sediment concentration and emersion time (when filtration is possible). Authors performing these calculations (Dankers *et al.*, 1989, De Vries, personal communication; Prins *et al.*, 1996) arrive at approximately the same values in the range 250-375 g m^{-2} d^{-1}, for similar conditions. The discrepancy between observed values in the field and laboratory and theoretical results is most likely due to erosion of deposited material in the former case. It is thus assumed that the theoretical relations can be used to predict deposition rates due to biodeposition adequately. The most consistent and complete form of these relations has been presented by Widdows *et al.* (1979) and are also displayed (in simplified form) in Figure 5. These will be used when biodeposition fluxes are to be established for specific conditions later on in this report.

2.3.3 Properties of sediment in between mussels

The forces that are available for erosion of sediment in between mussels are explained in section 2.3.1.3. However as described by equation (3), erosion is a function of both the forces available (τ_b) and the sediment properties: erosion rate M and critical bed shear stress τ_{e_crit}. Due to biodeposition the sediment in mussel beds (both in between the mussels and in the mussel mud) is composed of three parts all having their own properties: normal fine sediment, pseudofaeces and faecal pellets. It is argued by Risk and Moffat (1977) and Tsuchiya (1980) that pseudofaecal matter is relatively light and erodes more easily (smaller τ_{e_crit}) than the sediment from which it is composed. Faecal pellets on the other hand are heavier and more resistant to erosion (smaller τ_{e_crit}) (Rhoads, 1974). When erosion starts the larger pellets of the (pseudo-)faecal matter will erode faster (higher M) in comparison with normal fine sediment, simply because the 'chunks' that erode are larger. This can be summarized as follows:

- Pseudo-faecal matter: low τ_{e_crit} high M
- Faecal pellets: high τ_{e_crit} high M
- Normal fine sediment: medium τ_{e_crit} low M

The relative volume fractions of these three constituents to the total amount of material are determined by local conditions, as explained in section 2.3.2. The properties of the composite sediment between mussels are determined by the properties of the constituents. A complicating effect is that the overall properties are not a simple weighted average. Interaction such as armoring, cohesion and compaction may play an important role. This makes the overall properties difficult to quantify. Given that the majority of the excreted material will be pseudo-faecal matter as opposed to faecal

[5] *Original source 0.2 – 7.7 mg (g body mass)$^{-1}$ d^{-1}, assuming 50 kg body weight/m^2, see Tsuchiya (1980, p. 204).*

[6] *Original source: 4.4 – 7.2 g m^{-2} h^{-1}, assuming a 50 % submergence time.*

pellets (see section 2.3.2); the expectation is that the sediment between mussels erodes more easily then the same sediment without biodeposition.

If sediment from in between mussels erodes, the material can be exported beyond the boundaries of the mussel bed. As a result, the changed properties of the material can have an effect outside the mussel bed. Especially faecal pellets can hold integrity for several days and settle faster than unbound fine sediment, as described by Giles (2006) and Oost (1995). Part of the fine sediment deposited in the vicinity of mussel beds will thus be composed of (pseudo-)faecal matter. Oost (1995) suggests that this effect is a reason for the high mud concentrations that are found in de vicinity of mussel beds, see Figure 6. It is expected that the extra deposition due to a slowing of the flow (as explained in section 2.3.1.1) also contributes to this phenomenon.

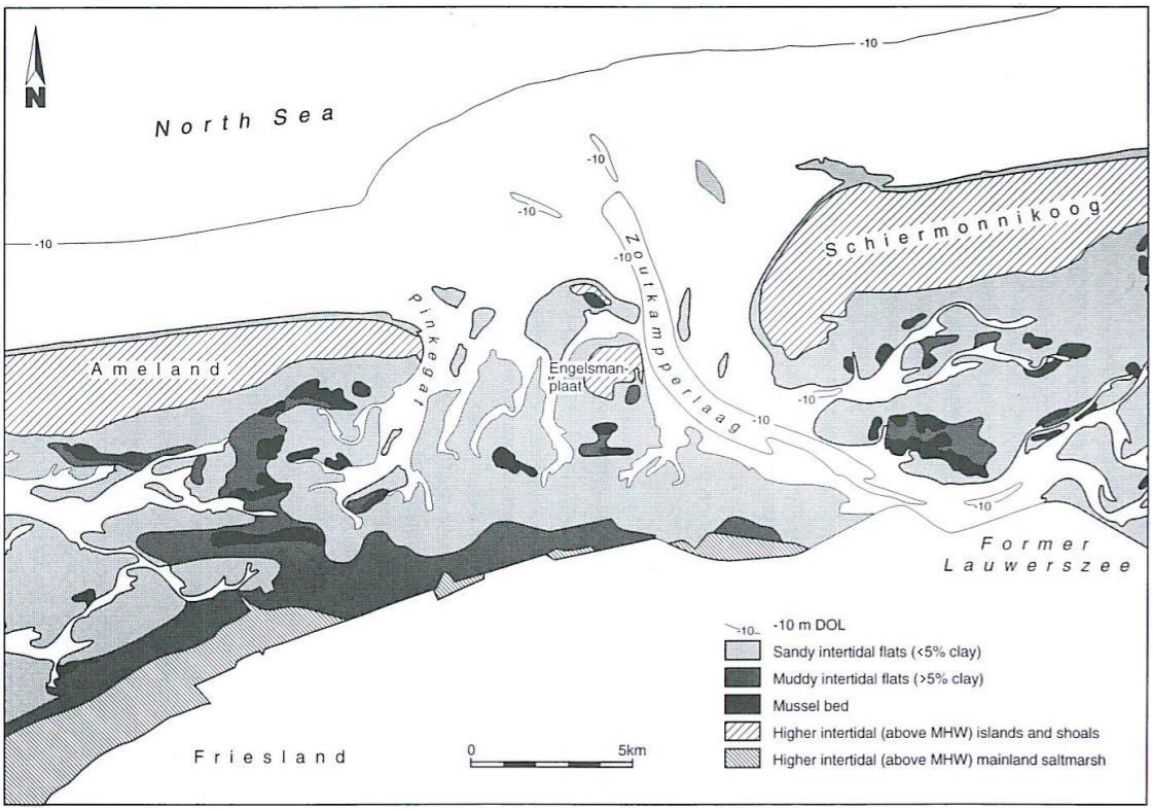

Figure 6: Sedimentary distribution relative to mussel beds during late summer in the Frisian inlet (reproduced from Oost, 1995, p. 368).

2.3.4 Conceptual model for fine sediment –mussel bed interaction

Figure 7 gives a schematic representation of the local interaction between young mussels and the sediment. A distinction is made between three stores for sediment: suspended in the water column, in between the mussels still vulnerable to erosion and below the mussels in the mussel mud. This schematic links the mechanisms presented in previous sections.

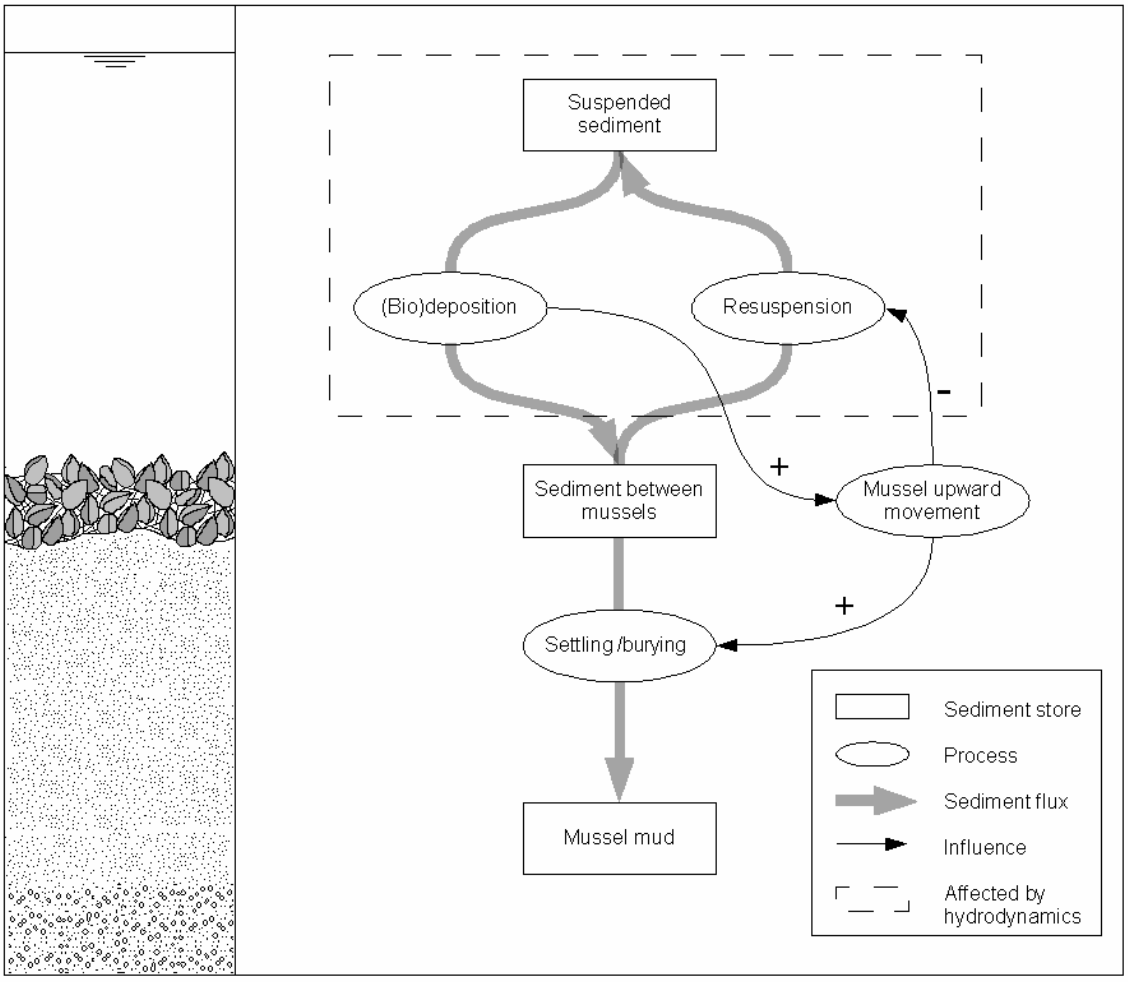

Figure 7: Schematic of mussel fine sediment interaction. On the left a schematic depiction of (from top to bottom) the water column, the mussels, the mussel mud and the original sediment.

The above figure describes how young mussels are able to create their own habitat by building and protecting a mussel mud layer. This process begins with deposition of fine sediment between the young mussels. The deposition flux is a combination of biodeposition and settling of particles without mussel influence (passive deposition). The amount of sediment available for deposition is limited by the amount that is brought in by currents; the currents in turn are influenced by the presence of the mussel bed, affecting deposition. The sediment in the mussel layer is decreased by erosion from in between the mussels.

The net amount of sediment that is deposited can be very large. Young mussels need to climb on top of the deposited material to avoid becoming smothered. Widdows *et al.* (2002) found that mussels can unbury themselves fast enough for this task. The sediment previously covering them settles down below the mussels, this is incorporated as settling/burying in Figure 7. The sediment in this mussel mud is essentially captured and will not erode as long as the mussels remain on top. Resuspension is weakened, because the sediment settles down during mussel migration upwards.

The schematic also makes clear why older mussel beds no longer heighten. Older mussels lose the ability to move and are not able to move upwards. In effect little sediment settles to the mussel mud and resuspension remains high. As a consequence

older mussels can die of smothering by sediment, especially if young mussels settle on top.

2.4 Mussel beds in the Wadden Sea

Mussels rarely live alone. Usually they form aggregations, in the Wadden Sea these aggregations are mussel beds which have settled on the soft substrate of the intertidal flat. This section gives a definition of such a mussel bed, explains how it is initiated and develops, describes the optimal conditions for a bed and finally gives an overview of the variety in coverage patterns. The development of mussel beds is relevant for the present study as the mobility of mussels determines the amount of sediment that can be deposited in the mussel mud (see section 2.3.4. The spatial patterns that mussel beds develop are also expected to play a role in sedimentation and erosion processes, as will be investigated later in this report.

2.4.1 Definition of a mussel bed

Brinkman *et al.* (2003) provide the following definition of a (mature) mussel bed (translated from Dutch):

> "A mussel bed is a benthic community in which mussels are dominant and which consists of a clearly defined area of large and small patches of mussels, rising above the surrounding area and separated by open spaces."

Mussel beds are not always continuous entities. Patchiness may break up the mussel bed into a large number of small islands. For practical purposes, mussel patches are considered part of a mussel bed when the distance between patches is no more than 25 m (Dankers *et al*., 2004b). Three stages in mussel beds can be recognized. *Seed beds* are beds newly populated by spatfall, which are very young mussels (5-10 mm). *Young beds* have survived a winter and the mussels are already much larger (2-3 cm). Finally, *old beds* have been present for multiple years and can contain more than one generation of mussels, the oldest of which are over 3 cm. Fully grown, mussels can be as large as 7 cm (Fey *et al.*, 2006). How these different stages are linked is described in the following section.

2.4.2 Development of a mussel bed

The emergence and development of mussel beds in the Wadden Sea has been described by Dankers *et al.* (2004b). Here an overview of that description is given. Mussels start their life as larvae suspended in the water column. The larvae settle on a variety of relatively hard substrates[7]: for example old mussel beds, fields of sand mason, worm or cockle grounds. At this point the young mussels measure 1-1.5 mm. The settlement of these mussels is referred to as spatfall, which usually takes place around the end of June and the beginning of July. The amount of spatfall that takes place in a year is highly variable and is in part inversely dependent on the amount of mussels already present. The more mussels are already present in an environment, the more mussel larvae are filtered from suspension and eaten.

The seed beds are initially uniformly covered. By November the beds have developed into open structures that generally cover 50-75% of the original surface. The

[7] *Often mussel larvae have two settlements. The first is only temporary and after a few weeks the mussels release their byssal threads and are washed away to settle on a permanent location.*

mechanism that drives the transition from a uniform bed to a patchy bed is still uncertain. Van de Koppel *et al.* (2005) propose that in particular cross current stripy patterns are the result of self-organization. Stripy patterns are an optimal and robust trade-off between mutual protection from erosion by waves and currents and competition between mussels for food. Dankers (personal communication) offers an alternative explanation: initial small variations in bed elevation cause small pools to form at falling tide. The remaining water is quickly depleted of food and oxygen, making it advantageous for the mussels to move to higher ground. This leads to a higher concentration of animals on the higher parts of the bed; these parts in turn are heightened further by biodeposition. Whatever the mechanism behind patterning in mussel beds is, mussel beds develop in their first few months from fully covered uniform beds, to partially covered patchy beds. Fine sediment is captured and trapped during this phase by the parts of the bed that are covered. The young and mobile mussels can climb on top of the deposited material until a layer of up to 30-40 cm above the surrounding flat has accumulated (Dankers *et al.*, 2004b). This process has been described in 2.3.4.

The very soft mud underneath the young mussel beds makes these beds very unstable. Storms during winter are responsible for the loss of many of the young beds. Actually around 50% of the new mussel beds do not make it through the first winter (Dankers *et al.*, 2004b; Steenbergen *et al.*, 2006). The beds that do survive the winter storms receive an influx of sandy material and shell remains due to conditions favoring sediment mobility. These coarse particles stabilize the material under the mussel beds, making them more resistant to erosion.

After this first winter, development is less rapid and characterized by several phenomena. Mussels become older and less mobile. The effect is that the mussels will no longer climb on top of the sediment, tempering the heightening of the bed, see also section 2.3.4. There is an advantage to not continuing to rise. Mussel beds have a more or less ideal height at mean sea level (McGrorty *et al.*, 1993). There is always a tradeoff between the amount of time emerged (not being able to feed) an the amount of time submerged, being able to feed but also at risk from starfish and crabs (Brinkman *et al.*, 2002). Mussels grow larger, but increasing mortality results in a decrease in the number of individuals per area. Incidental winter erosion or mortality means that the patches become smaller, thus overall coverage goes down. New spatfall can add a new year class to the mussel bed, increasing coverage and density.

Mussel beds usually do not reach a stable equilibrium state over time. Older parts of the mussel bed can be covered by large amounts of spatfall. In such case the deposition by the spatfall can smother the mussels below. This can lead to total erosion of the bed, as the mussels underneath die and release their byssal threads. In other cases large parts of older beds are simply lost due to erosion. However, often other parts of the bed survive and sometimes the old mud mounts are recolonized by spatfall. The changes in coverage of older mussel bed remain very dynamic and mussel beds can disappear as easily as new growth through spatfall can occur.

2.4.3 Habitat

The locations where spatfall occurs are difficult to predict. However, trends can be found in the location of older mussel beds. Brinkman *et al.* (2002) correlated the historical spatial occurrence of older mussel beds with the physical conditions in the Wadden Sea. They produced a habitat model describing the suitability of certain

locations for mussel beds, the correlations on which this model is based are presented in Figure 8.

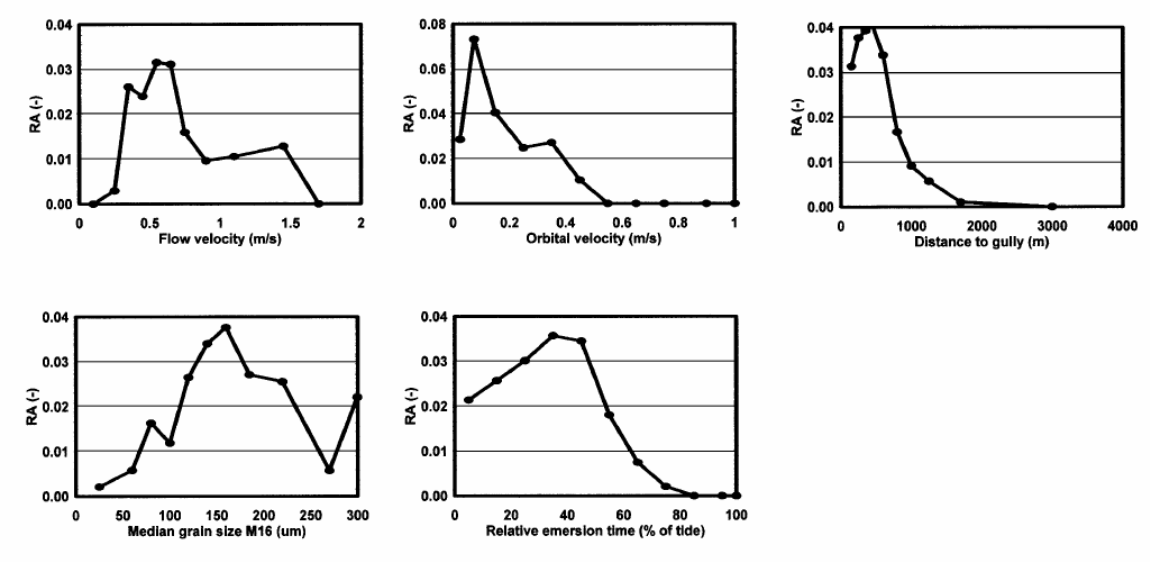

Figure 8: Relative appearance of mussel beds (m^2 m^{-2}) related to five abiotic variables. Flow velocity and orbital velocity are the maximum values attained during respectively springtide and a storm. The distance to gully is measured at mean low water level. Source: Brinkman et al. (2002, p. 67).

2.4.4 Mussel bed patterns

In the first week of existence seed beds are covered uniformly. As explained earlier, more or less unknown mechanisms cause the bed to differentiate between empty areas and densely covered mussel patches in the following months. This process is highly erratic; so many different patterns can emerge. A selection of photographs of mussel beds is given in Figure 9.

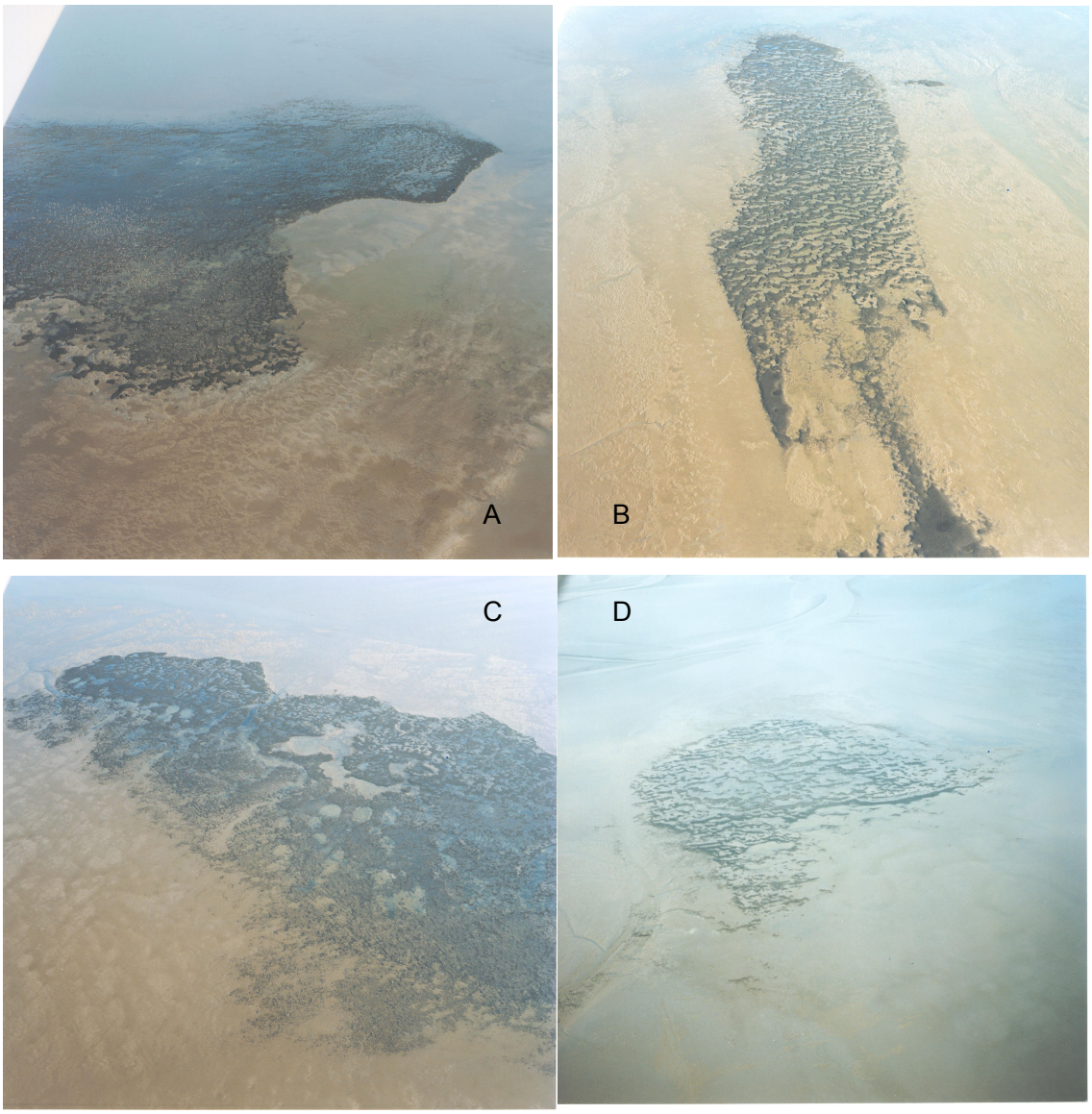

Figure 9: Selection of seed mussel beds photographed in November 1994 (except D) after dense spatfall, before winter erosion. A: near the island of Griend, south of Terschelling; B: south of Ameland. C: near the 'Molengat' gully near Ameland and D: near the 'Piet Scheve' tidal flat south of Ameland (photographed in April, 1997), photographs provided by Norbert Dankers. Depicted areas are around 500 x 500 m.

The photographs are taken from the side window of an airplane[8]. They give a good overview of the wide variety in both the patterns, configurations and forms of mussel beds. Figure 9 A B and C give seed beds before winter. The characteristic shared by these beds, is that they have a relatively high coverage. Patterns are very different, the bed in A has more or less irregular patches; the bed in B has striped features, where large areas of the bed in C are uniformly covered. Figure 9 displays another feature that is often seen in mussel beds, a uniformly covered band near the edge of the mussel

[8] *Photographs have also been taken straight down, from cameras underneath an airplane. These photographs are more suitable for analysis and have been used as such by Dankers* et al. *(2004b).*

bed. This band is often on the side of the gully. Finally photograph D has been included to give an idea of the extent of winter erosion due to storms. The mussel bed has much less coverage and the mud has been eroded, showing sandy substrate around the mussel bed.

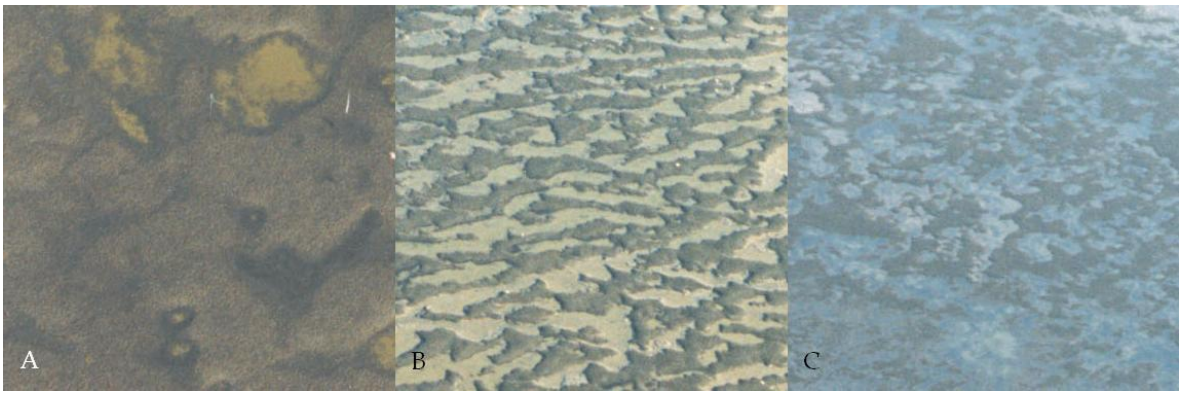

Figure 10: Patterning in seed mussel beds: A: (nearly) uniformly covered; B: striped pattern and C: random patchy pattern. Photographs provide by Norbert Dankers. Estimated dimensions A: 30 x 30 m , B and C: 75 x 75m.

Figure 10 gives zoomed images of mussel beds showing different patterns. In general the mussel bed system moves from the uniformly covered state depicted in Figure 10 A, to a partial coverage, whether this is striped as seen in B or irregular as in C. A distinction has been made between striped and random patterns. This distinction is not absolute. Many more or less random patterns show some striped features, while none of the striped beds are without irregularities (Van de Koppel *et al.*, 2005, p. E67). The cross sections in Figure 11 give an idea of both the variety and spatial scale of different patterns. Individual patches measure up to around 10 m.

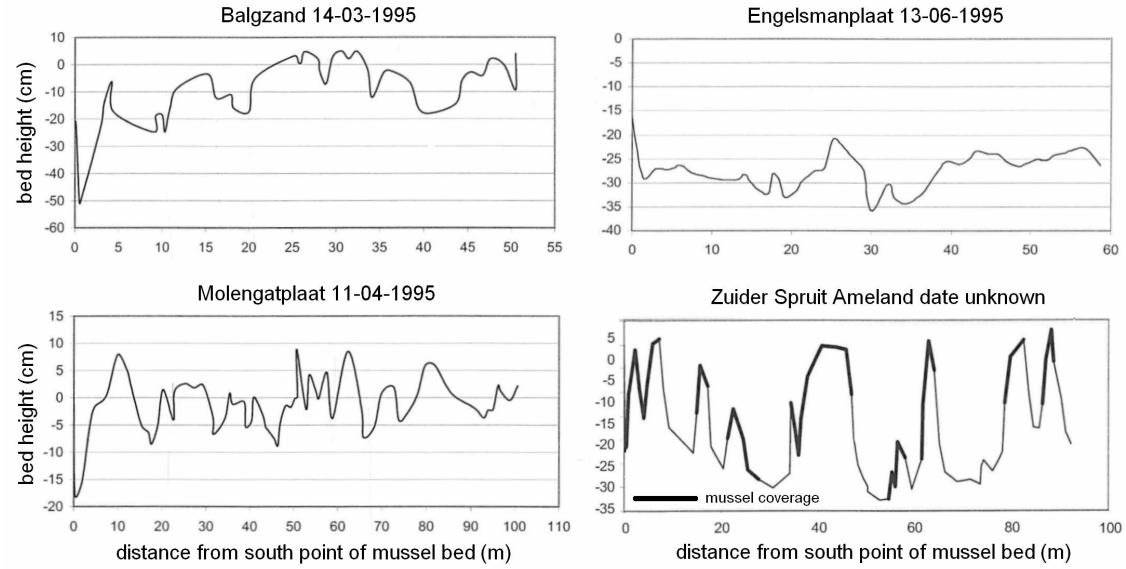

Figure 11: Mussel bed cross section along straight lines across beds. Notice the mussel coverage displayed in bold lines in figure in the right bottom corner (source: Dankers et al., 2004b, p.60-61).

2.5 Conclusions

It has been established in this chapter that there are three main mechanisms by which mussel beds influence fine sediment dynamics:

1) The first is by being a large rough obstacle in the flow, influencing horizontal flow patterns and increasing local mixing. These hydrodynamic effects force fine sediment dynamics, determining the amount of sediment available for interaction above the mussel bed. The roughness of the mussel bed is a very important variable in this process.
2) Mussels influence erosion processes. Mussel mud lying deep in between mussels cannot erode, sediment in between mussels can. Erosion from the latter source can either be faster or slower as compared with an empty bed, depending on mussel bed characteristics and the position of the sediment.
3) Biodeposition constitutes a substantial deposition flux to the bed. Tools for theoretically deriving biodeposition rates have been presented together with results from both field and laboratory experiments studying this process. The deposited pseudo-faecal matter has substantially different characteristics than normal fine sediment.

The mechanisms of fine sediment-mussel bed interaction have been brought together in a conceptual model which will be used as a guide in Chapter 3 where the mussel beds influence on fine sediment is modeled.

Next to the basic mechanism by which mussel beds interact with fine sediment, it is important to understand the development and spatial dimensions of mussel beds in the Wadden Sea. Together with the proposed conceptual model, these conclusions will be used later in this report in devising and evaluating a mussel bed model implementation and a mudflat model suitable as mussel bed habitat. It can be concluded from the second part of this chapter that:

4) The size of mussel beds ranges in the hundreds of meters and even kilometers large. The mussel bed habitat in the Wadden Sea is characterized by (among others) a maximum flow velocity of around 50 cm/s, a closeness to gullies of a few hundred meters and an emersion time of around 40%.
5) During the first months of existence (always in late summer), mussel beds capture large amounts of sediment, up to 30-40 cm in roughly four months.
6) During the same period different patterns in the covering of mussels emerge, ranging from uniform to regularly striped and randomly patchy. The scale of these patches is up to around 10 m.
7) In the first winter around 50% of young mussel beds, including the accumulated fine sediment in the mussel mud, are eroded.
8) The mussel beds that survive the first winter stabilize in the sense that they accumulate less sediment and the existing mussel mud becomes consolidated by compaction and an influx of courser material. Older mussel beds continue to experience erosion and decease of mussels and new growth by settlement of spatfall.

3 Model implementation of a mussel bed

In order to investigate the mussel beds influence on the fine sediment dynamics of an intertidal flat using a model - both with regard to net retention of sediment and the spatial pattern of that influence – a mussel bed needs to be implemented. Because it has proven difficult to establish values for important parameters such as roughness and erosion rate from theory (see Chapter 2) or empirically (see Appendix B), estimations of these values will be given. This chapter deals with the implementation of a mussel bed in Delft3D-FLOW. The spatial effects on flow and sediment dynamics will be evaluated in simulations with Delft3D-FLOW (from now on referred to as Delft3D).

The model implementation proposed here will be designed for a specific application. The implementation will be depth-averaged and thus suited for application in a depth-averaged model. This is possible for two reasons. First of all it has been shown in section 2.1.3 that the fine sediment in the Wadden Sea is generally well mixed over the vertical. Secondly, it has been demonstrated in Appendix B.4 that turbulence levels above mussels are very high. It is thus unlikely that vertical depletion of sediment near the bed will occur due to filtration, i.e. the suspended sediment over the mussel bed can also be assumed to be well mixed.

A further specification of the implementation is that it will be designed for current dominated conditions, occurring during the calm summer months. It is assumed that the phase where young mussel beds capture large amounts of sediment is most important with regard to fine sediment dynamics on an estuarine scale. The stormy winter season causes many of the young mussel beds to erode completely; this process is not considered as part of this project. As a result of the choice for current dominant conditions, the effects of waves are disregarded. It is shown in Appendix B.5 that even small waves can result in significant erosion from mussel beds. Because of the exclusive focus on currents this phenomenon is disregarded; for a further discussion of this choice also with regard to in winter erosion, see Chapter 7.

3.1 Basic implementation in Delft3D

The conceptual model introduced in Figure 7 is too complicated to implement directly in Delft3D without major revisions to the programs code. In order to avoid this, a further simplification is presented in Figure 12.

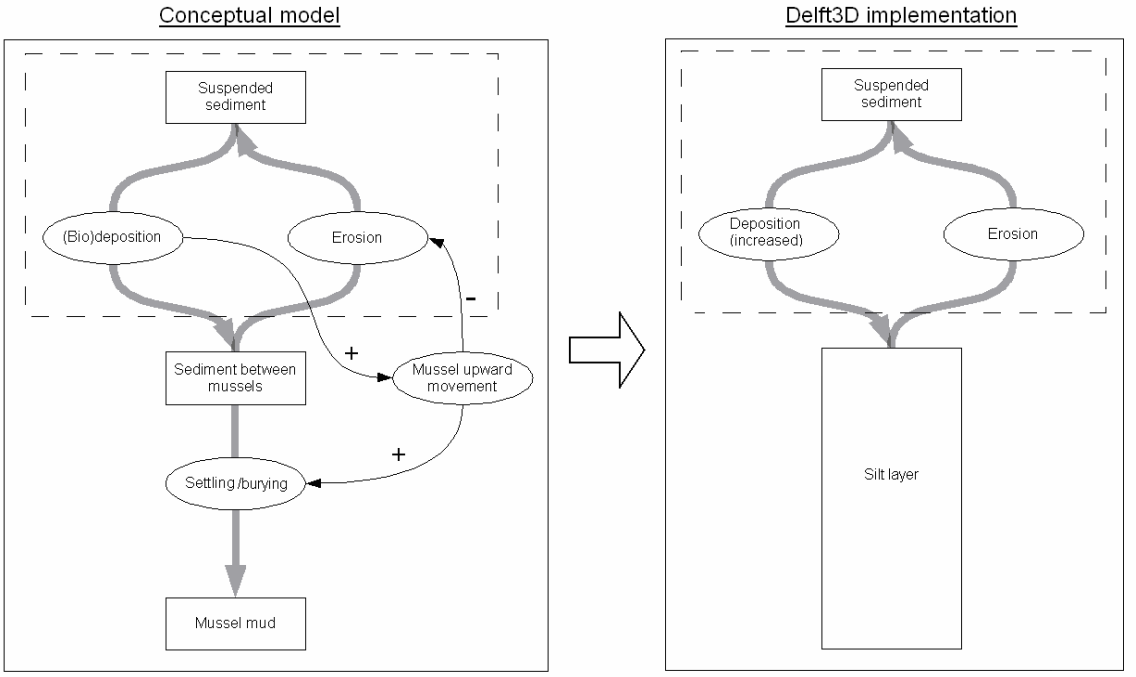

Figure 12: Conceptual model and Delft3D implementation of sediment dynamics over and in a mussel bed.

There are differences between the conceptual model of Chapter 2 and the proposed Delft3D implementation. The most obvious is the omission of the actual mussel layer. There is no difference between the sediment stored in between the mussels and the mussel mud. Furthermore the mussel upward migration is not simulated as such. This seems to be a highly simplified implementation, however given a few assumptions this system will incorporate most features of the conceptual model:

1) Mussel vertical migration instantly follows changes in bed level

The first assumption eliminates the need to simulate mussel upward migration as such. It also follows that the erosion from the bed is constant with constant velocities, as the top of the sediment remains at a constant distance from the tops of the mussels. In reality there is a limit on erosion at the moment that all erodible sediment between the mussels has gone. This is not a significant problem because of the second assumption:

2) There is significantly more sedimentation than erosion in the mussel bed

The second assumption implies that even though in principle the model implementation allows the mussel mud to erode, this will never happen in the model. In other words the limit to erosion is never reached as no extensive erosion will occur. The assumption is justified because of the choice to focus on calm summer months. It has been explained in section 2.1.3, that during such current dominated conditions, intertidal flats experience net accretion of fine sediment. A further simplification is applied which is not apparent from Figure 12: the transformation of sediment into (pseudo-)faecal pellets is not taken into account. Resuspended material enters the water column as normal sediment. Only the effect of biodeposition on sediment properties in between the mussels will be accounted for.

It is expected that the above presented implementation is an adequate approximation of a young mussel bed in its first months of existence.

3.2 Hydrodynamic implementation of a mussel bed

Hydrodynamic effects play a significant role in the system to be modeled. As has been explained in Chapter 2, there are three hydrodynamic processes influenced by mussel beds that require attention: (1) the resistance of the bed to flow (caused both by mussel bed height and roughness), (2) the high turbulence (caused by high roughness and siphon currents) mixing suspended sediment and (3) the influence of mussel shells on near bed velocities and turbulence affecting erosion. Because a depth averaged model is used, the water column is already assumed to be well mixed, which means that the second issue can be disregarded. The following three (hydrodynamic) influences remain to be implemented: an elevated mussel bed height, the mussel bed roughness and the erosive forces in between the mussels.

3.2.1 Mussel bed height

A feature of mussel beds is the increased height of the areas covered with mussels, compared to the surrounding area. The height of mussel beds can be implemented by simply elevating the bed level in the bathymetry in Delft3D at the mussel bed location. This is achieved by allowing the mussel bed to capture sediment in a morphodynamic model computation. After a given number of flow time steps, the bathymetry is automatically updated dependent on the amount of deposition and erosion. In such a computation Delft3D itself will calculate the development of a young mussel bed which will rise relative to the surrounding flat. The mussel bed height is thus both a result of the model (as it is dependent on the amount of sediment captured in the bed) and an influence (as it presents a barrier to the flow).

3.2.2 Mussel bed roughness

The roughness of a bed is usually expressed as the depth dependent Chézy coefficient (C), which determines for a given depth averaged velocity the bed shear stress. This bed shear stress is both exerted on the flow (which experiences drag) and on the bed (which can experience erosion). The roughness of the mussel bed will be implemented by the trachytope functionality. This feature of Delft3D is explained in Appendix C.4. The trachytope functionality has been designed to implement the roughness caused by vegetation in depth averaged model computations. It computes, based on certain plant characteristics a representative roughness (C_r). Combined with a certain depth average velocity Delft3D computes the total shear stress experienced by the flow (τ_t), see Appendix C.1. This total shear stress is actually composed of a bed shear stress on the vegetation (τ_v) and on the bed in between the vegetation (τ_{bv}). Only the latter is available as an erosive force on the sediment, the former is absorbed by vegetation or in this case by mussels. The combined stress (τ_t) experienced by the flow and is much larger than the shear stress the same flow would experience over an unvegetated bed, see Figure 13, because C_r is much larger than the Chézy roughness of an unvegetated bed. The trachytope functionality is used because it allows the implementation of a large roughness (of a vegetated bed simulating a bed with mussels), while simultaneously limiting the force on the sediment in between the vegetation (τ_{bv}). In other words: high roughness does not automatically lead to high erosion if the trachytope functionality is used.

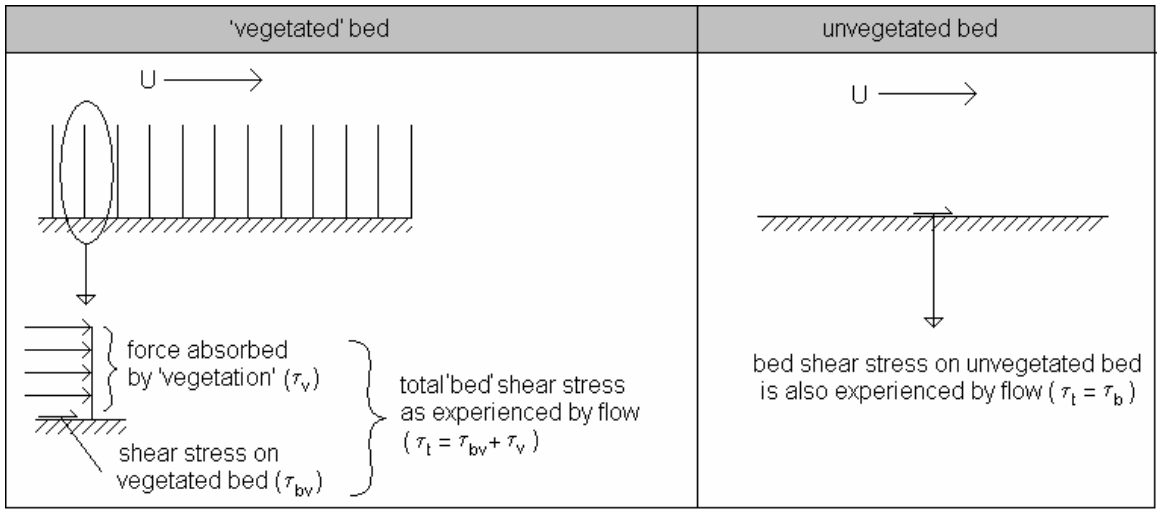

Figure 13: Shear stress on vegetation and underlying bed for a vegetated bed as compared with flow over an empty unvegetated bed.

The specific formulation proposed by Baptist (2005) will be used in the trachytope functionality (see Appendix C.4). Depending on vegetation characteristics it computes a representative roughness and uses a fixed fraction (the reduction factor, again determined by vegetation characteristics) of total stress τ_t to determine τ_{bv}, which is the force available for erosion, see equation (9). The predictive power (only validated for relatively thin long vegetation) of the equations by Baptist (2005) will not be used. Instead, by adjusting the plant characteristics, a predetermined roughness representative for mussels and a reduction factor will be imposed. The former will be determined in the remainder of this section; the latter is explained in the next section. The used plant characteristics have no bearing on mussel characteristics.

It has been attempted to establish the value of mussel bed roughness by analysis of data from experiments of flow over mussels (presented in Appendix B). This attempt has been proven unsuccessful. As a result the value of mussel bed roughness is both uncertain and variable. There is uncertainty in the sense the experiments aiming to establish the value of the roughness of mussel beds, have proven unable to do so. There is great variability in the sense that the population diversity in a mussel bed can be highly variable. Mussels grow, also older and younger mussels usually live together. As has been shown by the De Vries experiments in Appendix B, high sedimentation (of pseudo-faecal mimics) between the mussels makes the bed less rough. Because of these reasons the value of the roughness parameter will be varied later on, as part of the sensitivity analysis. In order to estimate an initial value for mussel bed roughness, it is assumed that the mussel shell roughness is similar to the roughness induced by randomly placed stones. The roughness length (z_0, which is a measure for roughness, see also equation (17)) can then be estimated using the equation suggested by Hofland (2005, p. 10):

$$z_0 \approx \frac{d}{10} \qquad (6)$$

Where:

d = height of roughness elements;

This can be rewritten in to the Nikuradse roughness height which can be implemented (via the trachytope functionality) in Delft3D:

$$k_s = 30 \cdot z_0 \approx 3 \cdot d \quad (7)$$

The above equation is similar to the equation used for estimating roughness of sandy beds: $k_s = 3 \cdot D_{90}$, where D_{90} is the grain size that is not exceeded by 90% of the sediment mixture. The height of the roughness elements (d) is assumed to correspond to the length of individual mussels. It is further assumed that the largest mussels in a bed will determine the roughness of such a bed. A young mussel has a shell length of around 30 mm, although the spatfall existing during the first weeks of the mussel bed is much smaller (5-10 mm, Dankers *et al.*, 1989). In this early stage the roughness of the bed may be determined more by the way these young mussels organize themselves and by the form of the underlying bed. For example, it is known that spatfall often settles on old shells, sand mason fields or cockle grounds (Dankers *et al.*, 2004b). In such cases the underlying roughness elements determine the roughness and have dimensions at least in the same range as the more mature mussels. As such a 30 mm roughness length is considered a good estimate in this variable and uncertain situation. Following equation (7) it is found that the Nikuradse roughness length (k_s) is then 0.09 m. This value can be imposed on the location of mussel bed via the trachytope functionality. Delft3D computes the Chézy roughness coefficient (C) from k_s following the White Colebrook equation (8).

$$C = 18 \log\left(\frac{12h}{k_s}\right) \quad (8)$$

Where:

h = water depth (m)

k_s = Nikuradse roughness length (m) = $30 \cdot z_0$

3.2.3 Bed shear stress on sediment between mussels

The erosive forces between mussels form a complex interplay of shear velocities and near bed turbulence, as presented in section 2.3.1.3 and explained in Appendix A. A mudflat model in Delft3D does not have the resolution to compute velocities and turbulence at this scale, especially not in a depth averaged model. Furthermore erosion in Delft3D is solely a function of the bed shear stress, which is caused by either currents or waves, but not enhanced by turbulence. The erosive forces are thus restricted to the bed shear stress on the sediment between the mussels. The equation for bed shear stress proposed by Baptist (2005) implemented in the trachytope functionality has the following form (see Appendix C.4 for more details):

$$\tau_{bv} = f \tau_t \quad (9)$$

Where:

τ_{bv} = bed shear stress on sediment between vegetation (N m^{-2})

f = reduction factor (-), based on vegetation characteristics.

τ_t = total shear stress (N m^{-2}) on bed and vegetation defined as: $\frac{\rho g U^2}{C_r}$

C_r = vegetated bed representative Chézy roughness coefficient (m$^{1/2}$ s^{-1})

As has been explained in section 2.3.1.3 there is no reason to assume that on average erosion from in between mussels will be either higher or lower than on a flat bed. Therefore it is assumed that bed shear stress on the sediment between mussels is as high as on an empty bed with an equal depth averaged flow velocity. The vegetation characteristics in the trachytope functionality will be chosen in such a manner that this equality is simulated[9]. In words related to Figure 13, *f* is chosen so that for an equal depth averaged velocity *U*, τ_{bv} on the vegetated bed is equal to τ_b on the unvegetated bed.

3.3 Biodeposition in Delft3D

3.3.1 Adding a biodeposition term to Delft3D

The three dimensional diffusion advection equation for suspended sediment transport, presented in section 2.1.1, is simplified in a depth averaged Delft3D model, see equation (36) in Appendix C.5. Deposition is represented as a sink term (*D*). In the case of a mussel bed an extra term D_{bio} is added to simulate biodeposition:

$$\underbrace{\frac{\partial c}{\partial t}+\frac{\partial uc}{\partial x}+\frac{\partial vc}{\partial y}}_{advection}\underbrace{-\frac{\partial}{\partial x}\left(\varepsilon_{s,x}\frac{\partial c}{\partial x}\right)-\frac{\partial}{\partial y}\left(\varepsilon_{s,y}\frac{\partial c}{\partial y}\right)}_{diffusion}=E-D-D_{bio} \qquad (10)$$

Where:

c = mass concentration of sediment (kg m^{-3})

u, v = flow velocity components (m s^{-1})

$\varepsilon_{s,x}, \varepsilon_{s,y}$ = eddy diffusivities in three directions (m^2 s^{-1})

E = erosion (kg m^{-3} s^{-1})

D = deposition (kg m^{-3} s^{-1})

D_{bio} = biodeposition (kg m^{-3} s^{-1})

Deposition is described in Delft3D as:

$$D = w_s \cdot c \qquad (11)$$

Where:

w_s = settling velocity (m s^{-1})

Biodeposition can be defined in a similar form. Defining a filtration rate *fr* as a volume per time per area, the biodeposition term becomes:

$$D_{bio} = fr \cdot c \qquad (12)$$

Where:

[9] *The total bed shear stress on a mussel bed and the bed shear stress on an empty bed computed via Delft3D calculations are not linearly related with varying water depths. Therefore it is not possible to derive vegetation characteristics so that the ratio between bed shear stress between mussels and on an empty bed is constant. Instead, the ratio will be set at 1 for the water depth where velocities are at maximum. Deviations with changing water depth from this ratio are small, i.e. maxima around 10%.*

fr = filtration rate ($m^3\ s^{-1}\ m^{-2}$, or $m\ s^{-1}$)

Note that in both deposition terms the depth averaged concentration is used, i.e. the suspended sediment concentration is assumed uniform over the vertical. The similar form of equations (11) and (12) makes it possible to add the two terms together, into a combined deposition term:

$$D_{total} = D + D_{bio} = w_s \cdot c + fr \cdot c = (w_s + fr) \cdot c \qquad (13)$$

If the filtration rate is taken as a constant - which is a slight simplification as in reality it varies with amount of suspended material – and the settling velocity as well (neglecting hindered settling and flocculation), the two can be added together. Biodeposition can thus be simulated by locally (over the mussel bed) increasing the settling velocity with the filtration rate *fr*. The source code of Delft3D has been adapted in order to simulate biodeposition in this manner.

3.3.2 Estimating filtration rate

Filtration rate is inversely related with the suspended material concentration. Also it is the case that many seed mussel beds have a higher combined filtration rate than the lower densities of young and mature mussels (Dankers, personal communication). The latter phenomenon is neglected simply due to a lack of information. Instead the mussel bed used in the experiments by Van Duren (2006) will be taken as a guideline and it is assumed that this also represents biodeposition for very young mussel beds.

Relations between sediment concentration and filtration rates are displayed in Figure 14. There are other sources treating filtration rate, for an overview see Jörgensen (1996). The laboratory studies carried out by Widdows *et al.* (1979) are used here because they incorporate the relevant variables: suspended particulate matter and mussel size. Jörgensen (1996) compares laboratory measurements with field experiments and shows that in laboratories clearance rates (not pumping rates) are overestimated, because refiltration of water can occur in dense mussel beds. From analysis of the data mentioned by Jörgensen (1996) it can be deduced that the overestimation is around 50%.

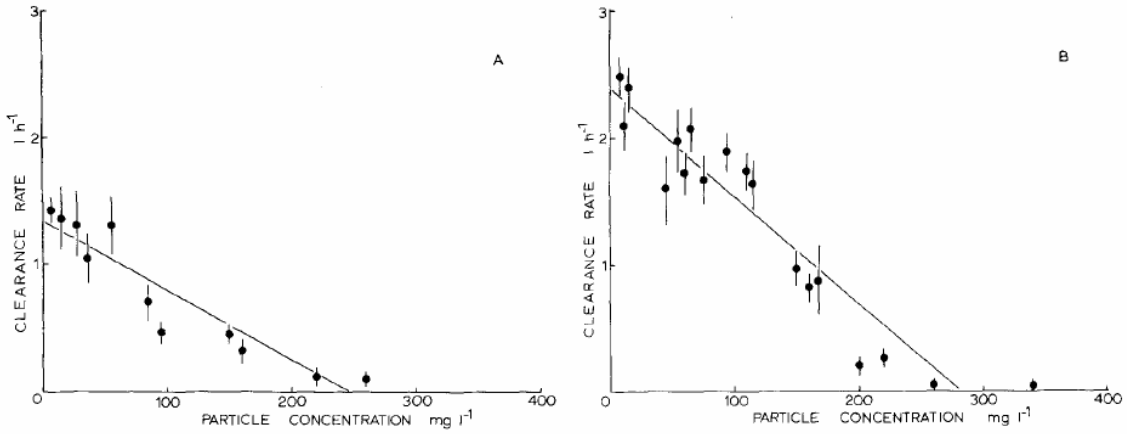

Figure 14: Filtration rates of individual mussel as a function of particle concentration; A: mussel length = 3 cm; B: mussel length =5 cm (adapted from Widdows et al., 1979).

The suspended sediment concentration that will be applied in the model has a maximum of 50 mg l^{-1} (see Chapter 4). As the mussels used by Van Duren were on average 38 mm long, a filtration rate of 2 l h^{-1} ind^{-1} will be used. Using a density of 1800 ind m^{-2}, this gives a filtration rate of 3600 l h^{-1} m^{-2}, or 0.001 m^3 s^{-1} m^{-2} or 1 mm s^{-1}. Considering that some of the filtered water will be re-filtered, the effective filtration rate is lower: 0.5 mm s^{-1}. This value is similar to settling velocities often used for Wadden Sea fine sediment: 0.5 mm s^{-1} (see Chapter 4). The observation by Ten Brinke *et al.* (1995) that biodeposition and passive deposition contribute roughly equal amounts to total deposition is here confirmed.

3.3.3 Implementing properties of (pseudo-)faecal matter in sediment

Biodeposition is more than an extra sediment flux to the bed as presented in the previous section, the properties of (pseudo-)faecal matter are very different compared to normal sediment. This will be simulated by adjusting the sediment properties in the mussel bed. Erosion at a given bed shear stress is determined by Delft3D by two such properties: the critical bed shear stress (τ_{e_crit}) which determines whether the sediment erodes and the erosion rate (M) which determines how quickly the sediment will erode, see section 2.1.1. The sediment in between mussels is composed of roughly 50% biodeposited material[10], which is built up out of pseudofaeces and faecal pellets. The properties of these constituents are presented in section 2.3.3. In relation to sediment without biodeposited material, pseudo-faecal and faecal pellets have a high erosion rate and have respectively a low and high critical bed shear stress. As a first estimate it is thus assumed that the critical bed shear stress of the average behavior of sediment in between mussels is equal to that of normal sediment. The erosion rate is chosen higher. For fine sediment in the Wadden Sea values of τ_{e_crit} = 0.5 N m^{-2} and $M = 1 \cdot 10^{-4}$ kg m^{-2} s^{-1} are used (see Chapter 4). For the sediment in between mussels τ_{e_crit} = 0.5 N m^{-2} and $M = 4 \cdot 10^{-4}$ kg m^{-2} s^{-1} are used. Delft3D provides the option to spatially vary erosion rate and critical bed shear stress.

[10] *Considering that the biodeposition flux is roughly equal in size to the normal deposition flux (both characterized by w_s = 0.5 mm s^{-1}), it can be expected that an equal ratio of (pseido-)faecal pellets to normal sediment is deposited in between the mussels. However it has been found by Ten Brinke et al. (1995) by sampling of the top layer, that only around 15-40% of the material consisted of identifiable (pseudo-)faecal pellets. Regardless, the precise ration of (pseudo-)faecal pellets has no impact on the choice of sediment parameter setting.*

4 Model set-up

The model set-up as implemented in Delft3D is presented in this chapter. The model should represent a typical mussel inhabited mud flat. The model should also facilitate the investigation of the mussel bed implementation as proposed in Chapter 3. To satisfy the second objective the model should be simple enough to easily differentiate between effects on fine sediment dynamics caused by the mussel bed and those attributable to choices in the model domain and boundaries. This second requirement suggests the use of an idealized model. The goal of this chapter is therefore to set-up an idealized model of a typical mussel inhabited mud flat.

The choice for an idealized model removes the problems of obtaining data of such mussel beds (although some bathymetry readings exist (Van Eijsbergen and Veeken, 2005; Ten Haaf and Karels, 2005)). However it also gives a great range of freedom in choosing the characteristics of the model area. This range is somewhat constricted by the stated goal of modeling a typical mussel inhabited mudflat. Brinkman *et al.* (2002) correlated the historical spatial occurrence of mussel beds with the physical conditions in the Wadden Sea. The results of this study are presented in Figure 8 in Chapter 2. In order to justify the qualification of the used idealized model as a typical mussel habitat, it should as a minimum conform to the habitat demands posed by mussels. The mussel habitat demands have also been translated into habitat suitability maps by Brinkman *et al.* (2002). These maps combined with historical records of mussel bed locations show that the area of the Wadden Sea south of Ameland is a fertile ground for mussel beds. The area is displayed in Figure 15. The mussel grounds on the south coast of Ameland will serve as a guideline for designing an idealized mudflat model.

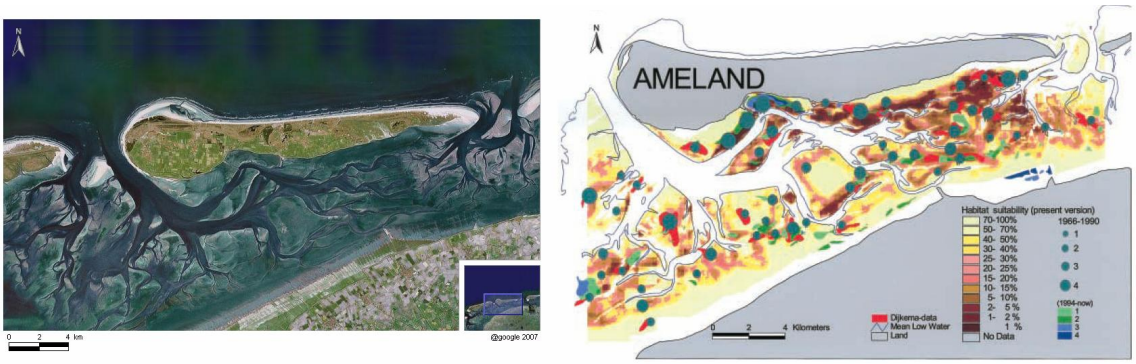

Figure 15: Left: aerial photograph of the Wadden Sea south of the barrier island Ameland (source: Google.maps). Right: the suitability of this area for mussel beds as predicted by Brinkman et al. (2002). The colors give the suitability where as the dots give known (historical) mussel bed sites.

The rest of this chapter describes the model set-up of this idealized mudflat in Delft3D FLOW. This model will be used for combined hydrodynamic and morphological computations, simulating two summer months (60 days). Waves will not be implemented. All input variables (except the bathymetry) are also given in Appendix D.

A distinction is made between the reference situation of an empty mudflat and the spatial implementation of the mussel bed. This chapter treats the reference situation first; in the last section the implementation of mussel beds in the reference situation is explained.

4.1 Model area

4.1.1 Model location and dimensions

An area of the south coast of Ameland is used as an example of a suitable mussel habitat. Figure 16 shows bathymetric data of this area. A transect of the mudflat bordering the south coast of Ameland is selected and presented separately in the same figure. This transect is chosen because of the simple geometry and the suitability as habitat for mussels. The transect shows two distinct sections, the mudflat with a gradient of approximately 1:1000 and the channel with a much steeper gradient (approximately 1:50).

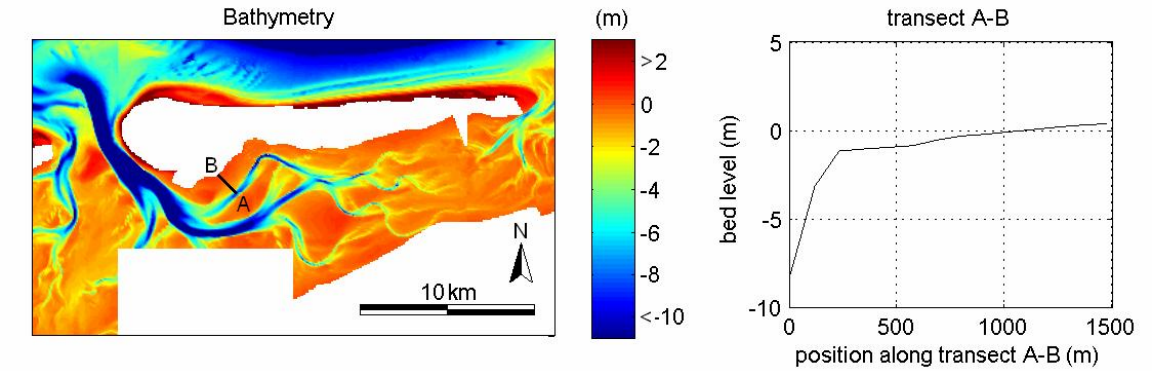

Figure 16: Left: bathymetry of area around Ameland relative to mean sea level. Bathymetry from JARKUS (yearly coastal measurement program in the Netherlands), combined measurements from the summers of 2005 and 2006. Right: bed level along transect.

Only a section of the above presented area will be modeled in this study. Mussel beds are found near the edge of the flat near the channel. This is important, as close to the channel the flooding and drying tide is forced from the deeper channel. A bed can have a length of over a kilometer, however usually the dimensions range in the hundreds of meters (see Dankers *et al.*, 2004b). Here a relatively small mussel bed will be implemented with maximum dimensions of 150x50 m. This size is the result of practical considerations of computation time and of the expectation that a much larger bed will not yield additional insights.

The dimensions of the model area should be large enough to avoid boundary effects influencing the area of interest. Boundary effects are influences of discrepancy between imposed boundary conditions and processes computed in the model near the boundaries. The dominant boundary effect in this particular situation is the suspended sediment concentration. Concentrations uniform in time will be imposed at the model boundaries; these do not match the model behavior where concentrations vary with flow velocities. This means that the suspended sediment concentrations need space to adjust to the flow conditions. The model domain should allow room for the adjustment length over which the concentrations adapt. Considering these processes and the planned properties of the model the dimensions are chosen as 2250 x 300 m (see Appendix D.1 for the calculation of the adjustment lengths).

4.1.2 Grid and Bathymetry

The model grid provides the dimensions of the control volumes for which the model equations are solved. Two grids have been set-up. One with 10x10 m grid dimensions

in the model center. The second grid has grid size of 2x2 m so that it can be used to model mussel bed patches as small as 10 m (bathymetric features should be covered by at least 5 grid cells). The disadvantage of the second grid is that computation time is increased by more than an order of magnitude. Both grids have a decreasing resolution when approaching the model boundaries. The two grids are presented in Appendix D.1 and pass the applying quality criteria as defined by WL|Delft Hydraulics (2006, p. 4-13).

A mudflat profile is set-up that will be applied uniformly in the long shore direction. The near channel part of the tidal flat (slope 1:1000) and a part of the channel have been incorporated (slope 1:50) in this profile, similar to the transect shown in Figure 16. The channel has been incorporated for a number of reasons. A tidal wave propagation velocity is limited by the available flow depth. This means that the tidal wave will travel faster in the channel than on the flat, resulting in higher velocities in the channel. Advection will ensure that on near channel flats high velocities will also occur. Mussel beds are located in this area and thus experience relatively high velocities. Also, by including the channel, the flat will flood from the channel, instead of directly following the imposed boundary conditions. This has the advantage that errors in the boundary conditions have a more limited influence on the processes on the flat. The entire profile and the cross section are presented in Figure 17 below.

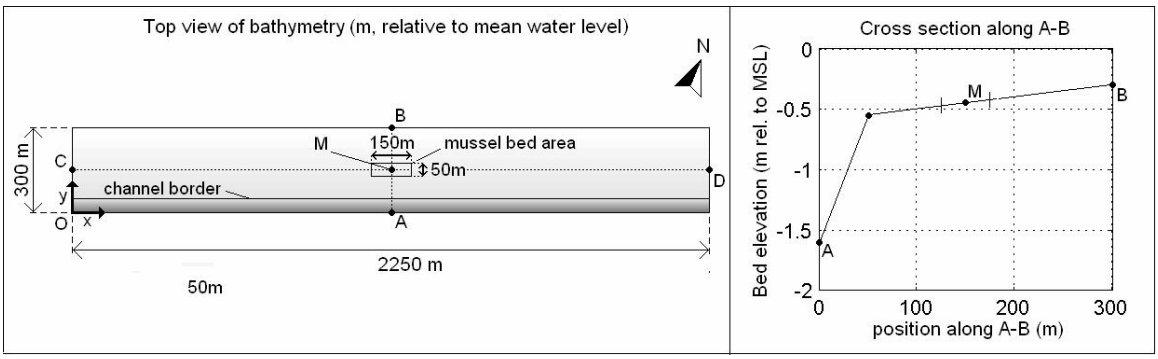

Figure 17: Left: overview of model area with the channel to the south. Right: cross section of bed level with the channel on the left. Cross section A-B and C-D and point M are included for later reference. Note the definition of x and y-axis and (x,y) = (0,0) at origin (O). Lower left corner of the mussel bed is located at (x, y) = (1050, 125).

The above presented combination of the bathymetry and the computational grid means that the mussel bed will lie around 100 m from the gully. According to Brinkman *et al.* (2002) mussel beds are located close to channels, where according to his analysis this closeness is in the order of hundreds of meters. The distance of 100 m falls within this range.

4.2 Hydrodynamic model set-up

4.2.1 Hydrodynamic boundary conditions

The mudflat model is a rectangle and thus has four boundaries. Three of these boundaries have been specified as open water level boundaries, the fourth (Northern) is closed, see Figure 18. The northern boundary is closed for a number of reasons. The model behavior is forced from the channel, through which the tidal wave enters the model. How this tidal wave propagates over the flat is difficult to predict, especially in the case of a rough mussel bed. Keeping the model closed in the north solves this problem by letting the model determine the water level on that boundary itself. The closed boundary constricts flow in northern and southern direction over that boundary.

When an open north boundary is used the velocities over that boundary remain very small (results not shown here), the error induced by keeping the boundary closed is thus small.

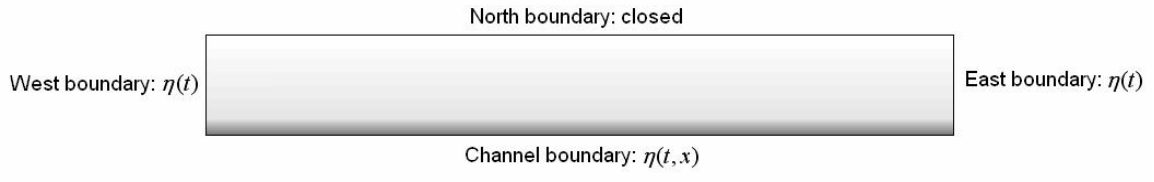

Figure 18: Water level, η (m), boundaries.

Because in tidal inlets the tide comes in following the tidal channels, main flooding velocities are parallel to the channel[11]. A simple harmonic tide will thus be imposed propagating from west to east. At a specific point at the boundary the imposed water level is described by the following equation:

$$\eta(x,t) = A\cos(\omega t + kx) \qquad (14)$$

Where:

η = water level relative to reference plane (m)

A = tidal amplitude (m)

ω = tidal frequency = 2π/T (rad s^{-1})

T = tidal period (s)

k = tidal wave number = 2π/L (rad m^{-1})

L = tidal wave length (m)

x = distance parallel to channel, refer to Figure 17 (m)

The tidal forcing is uniform in y-direction, as can be concluded from the absence of y in equation (14). The West and East boundaries are thus spatially uniform and only time dependent[12]. The channel boundary is situated in x direction and is both time and spatially variable, forcing the tidal wave along the model domain. A period (T) of 12 hours for the tide is chosen and an amplitude (A) of 1.5 m. The tide in the Wadden Sea is not harmonic, but the values represent an approximation of Wadden Sea conditions. The tidal wave length (L) has been calibrated to generate current velocities of 0.5 m s^{-1} (corresponding with mussel habitat optimum, see Figure 8) at the mussel bed location: L = 147 km. Equation (14) can thus be applied using, A=1.5 m, $\omega=1.45\cdot10^{-4}$ rad s^{-1} and $k=4.27\cdot10^{-5}$. With these tidal characteristics the wave is forced at the desired speed trough the model. Furthermore the channel position 1.6 m below reference will always carry water, which is desirable for numerical reasons.

[11] *This has been checked by using the Wadden Sea model used in the study of Borsje (2006) and in flow computations presented in RIKZ (1998).*

[12] *As explained earlier the tidal wave is forced from the channel and as an effect it is expected that the wave will thus pass the flat somewhat later., also because a wave propagates slower over shallower ground, The uniform forcing on the West and East boundaries thus introduces a boundary effect, i.e. the imposed boundaries do not correspond to the system simulated in the model. It is assumed that the length of the model in West-East direction will render this effect negligible in the area of interest.*

4.2.2 Physical parameters

Delft3D resolves the water motion based on the presented bathymetry and boundary conditions and is further determined by the setting of a range of physical parameters. The parameter values are listed in Appendix D. Here the parameters that require justification are treated.

A uniform bottom roughness is implemented. This value is overruled in those cells where the trachytope functionality is imposed. A Nikuradse roughness length (k_s) of 0.005 m, or 5 mm, is used. This implies that the model computes bed resistance using the White Colebrook formulation, see equation (8). The chosen roughness length is relatively smooth, which corresponds with the slick surface of a mud flat. Paarlberg *et al*. (2005) used the same roughness length for a muddy intertidal flat in the Western Scheldt estuary.

Horizontal viscosity (u_h) determines the diffusive part of the impulse equations given in Appendix C.1 as equations (25) and (26). The parameters should take into account the grid size dimensions. Small grid cells can resolve advection at finer scales and thus require less compensation by horizontal viscosity. For models of the scale used here (order of tens of meters grid size), uniform horizontal viscosities of 1-10 $m^2\ s^{-1}$ are recommended (WL|Delft Hydraulics, 2006, p 4-60). A value of 1 $m^2\ s^{-1}$ has been chosen, it has been found that a value of 10 $m^2\ s^{-1}$ does not lead to significant changes in the resulting hydrodynamics. It has also been investigated whether the abrupt edges of the mussel bed create horizontal turbulence that should be accounted for. A Large Eddy Simulation (LES, described and tested by Uittenbogaard (1998) and Van Vossen (2000)) was used in a normal model run with a rough and heightened (40 cm) mussel bed. The LES resolves sub grid eddies and computes the resulting horizontal viscosities. The maximum values for u_h were in the order of 0.01 $m^2\ s^{-1}$. The addition of this turbulent viscosity is thus relatively small and can be disregarded. For the horizontal diffusivity, which governs not the diffusion of momentum but of substances, the same considerations apply: a value of 1 $m^2\ s^{-1}$ has been chosen.

4.3 Morphology

4.3.1 Fine sediment

In reality sediment in a system consists of a continuous distribution ranging from sands (or even larger particles) all the way down to clay. For model purposes such a continuous spectrum is replaced by discrete groups of sediments with certain properties. In this case one fine sediment fraction is used. It is a challenge to capture the diversity of fine sediments into a sediment type with single values for important properties like grain size, settling velocity and critical bed shear stress. Previous authors provide examples regarding this process. Here the properties are derived from the work of both Van Ledden (2003) and Paarlberg *et al*. (2005). The most important properties of this silt is a settling velocity of 0.5 mm s^{-1}, a critical bed shear stress of 0.5 N m^{-2} and an erosion coefficient of $1 \cdot 10^{-4}$ kg $m^{-2}\ s^{-1}$. The density of the sediment is 2650 kg m^{-3}, however when deposited the bed density is only 500 kg m^{-3}. Such a low density corresponds to a very loose bed. Over time mud will consolidate, time scales modeled here are too short for consolidation to play an important role, the process is thus disregarded.

4.3.2 Initial and boundary suspended sediment concentrations

Because of the settling lag in fine sediment (see section 2.1.2), it is not possible to impose equilibrium conditions on the model boundaries. Because of the uniform implementation of the flow and bathymetry in east-west direction, it is expected that deposition and erosion effects will also be uniform in that direction. This requirement has been used in a calibration process. It was found that concentrations in the order of 40 mg l^{-1} give more or less uniform distribution. Furthermore the lower velocities on the higher parts of the tidal flat mean that lower concentrations can be carried. To account for this, lower concentrations (30 mg l^{-1}, increasing linearly to 40 mg l^{-1} in the channel) have been applied in the north of the western boundary. Finally it should be considered that the tidal channels at incoming tide will carry much higher concentrations than the return flow at falling tide from the flats, caused by the earlier mentioned scour lag (see section 2.1.2). This has been simulated by applying a reduced inflow concentration on the eastern boundary to 75% of the western boundary setting. Although these values are based on the model behavior, they are consistent with measured concentrations in the Wadden Sea (see Oost, 1995). Finally a Thatcher-Harleman time lag of 90 minutes has been imposed on all boundaries. After flow reversal on a certain boundary, the concentrations is gradually adjusted (over the specified time) from the last concentration leaving the model to the imposed boundary concentration. This prevents unrealistic discontinuities in concentrations at boundaries at reversing flow.

Although care has been taken to choose suitable boundary conditions, apart from the Thatcher Harleman time lag, they have not been varied in time. At low flow velocities this results in high deposition rates at the model boundaries, somewhat compensated by erosion at high velocities. This is exactly why the stretched model domain is used: to allow the model to compute fitting sediment concentrations itself.

The mudflat is modeled to represent a period in summer; net deposition should thus take place (as explained in section 2.1.3). For this reason it is chosen to start from an empty bed. Fine sediment is deposited and can erode if necessary. Because deposition exceeds erosion no sources of sediment are disregarded. As initial condition a uniform suspended sediment concentration of 0.4 mg l^{-1} is chosen.

4.3.3 Morphological parameter settings

The morphological parameters have been displayed in Appendix D.5. It is the aim of the model to simulate sixty days of morphological changes. Flow will be computed for six days. This means that a morphological multiplication factor of ten will be applied, multiplying changes in bed level by erosion and deposition by ten. This technique of multiplying the bathymetrical changes is well validated (see for example Van Ledden, 2003).

4.4 Spatial implementation of mussel bed

How the mussel bed is modeled is presented in Chapter 3, here the spatial pattern of the mussel bed will be explained. Regarding the location of the mussel bed it is known that optimal mussel habitat conditions include an emersion time of around 40% (see Figure 8). This is modeled by placing the bed level of the mussel bed location at -0.45 m relative to mean tide. With the given tidal forcing with a amplitude of 1.5 m, this results in an submersion time of 60%. Mussel beds can vary in height, but will never become higher than the mean water level. The location and dimensions of the largest implemented mussel bed are displayed in Figure 17

In order to investigate the influence of mussel bed patterning as described in section 2.4.4, different configurations of the mussel bed are implemented. Naturally occurring patterns are depicted in Figure 10; uniformly covered, striped and random patterns have been identified. These three types have been translated in four different mussel bed configurations: uniform, patchy (modeled as checkerboard), stripes transverse and stripes parallel to the channel. The patchy configuration simulates the random pattern and the striped configurations simulate the naturally occurring striped patterns. The mussel bed configurations are displayed in Figure 19. Using these patterns both the size of the mussel bed (ranging from 7500 to 1875 m^2) and pattern type are varied. Because of the restriction in grid size, only the uniform and (adjusted) patchy patterns are applied for the smallest mussel bed.

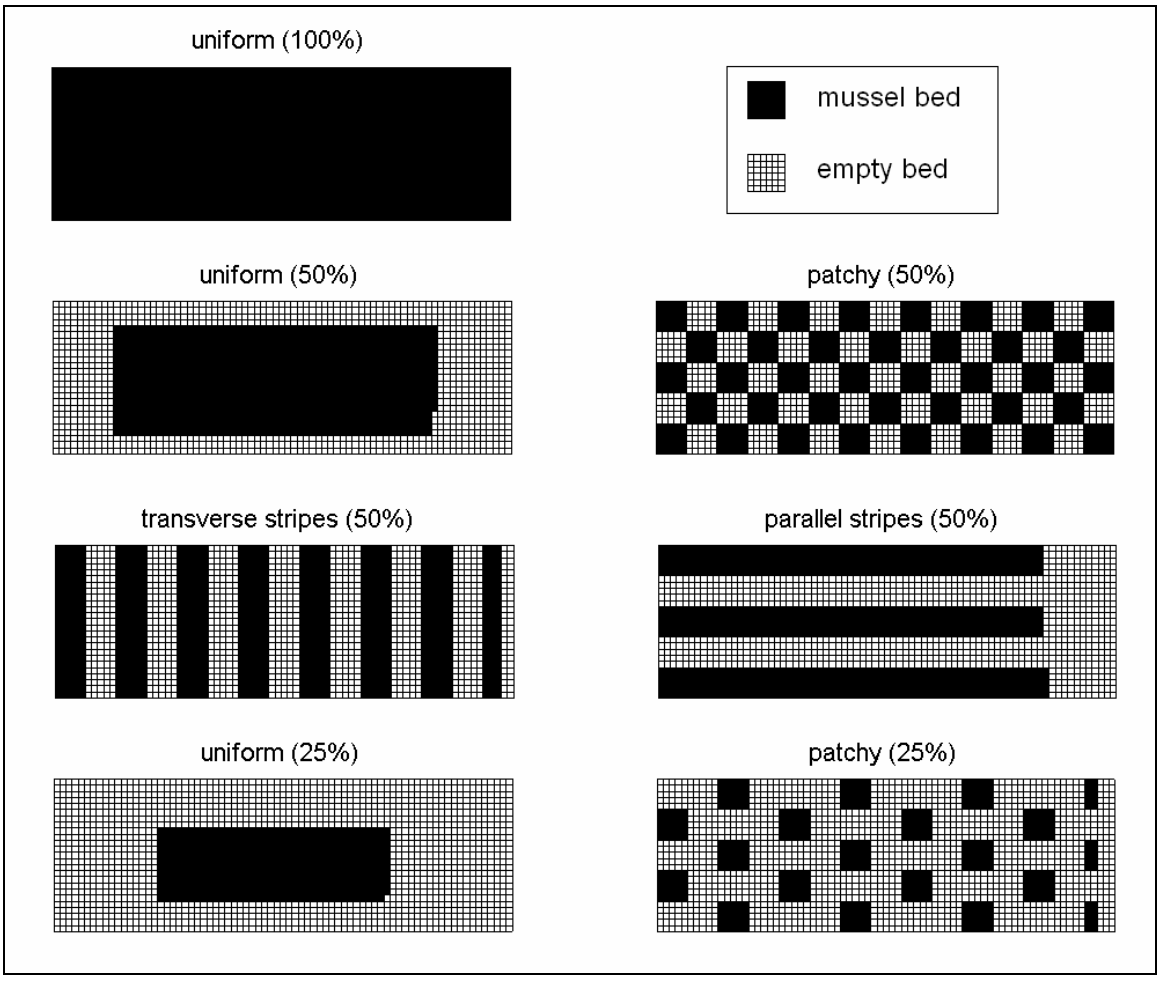

Figure 19: Mussel bed area with the coverage configurations applied in this study. The surface of the 100% uniform mussel bed is 7500 m^2, which implies 3750 m^2 for 50% and 1875 m^{-2} for 25% coverage. Note that some of the configurations have been adjusted in order to keep the surface area constant.

5 Simulation results

A reference situation and a situation with a standard mussel bed have been set up in the previous chapter. The results from the model runs corresponding with these situations are presented in this chapter. It is evaluated whether the imposed boundary conditions indeed translate into model conditions corresponding to mussel habitat needs, whether the reference run simulates an accreting summer mudflat (accretion rate in the order of mm/months) and whether the standard mussel bed implementation shows phenomenon consistent with real mussel beds.

5.1 Reference model results

5.1.1 Flow conditions and suspended sediment concentration at model center

The center of the model – denoted as M in Figure 17 - is situated in the most important area of the model. This area will be the location of the mussel bed and should thus conform to the requirements set by the habitat guidelines presented in Chapter 2. In Figure 20 four quantities recorded at M are displayed: water levels, flow velocities, suspended sediment concentrations and cumulative erosion/deposition (hereafter called cumulative deposition). Cumulative deposition is displayed for later reference. Figures displaying the conditions for other observation points in the model domain are displayed in Appendix E.

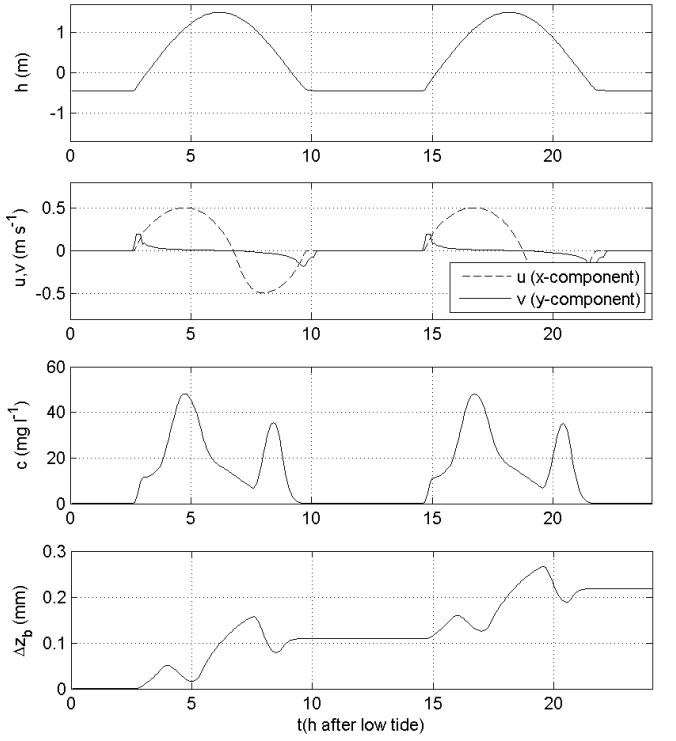

Figure 20: Water level (h), flow velocity components (u, v), suspended sediment concentration (c) and cumulative deposition (Δz_b) in M during a double tidal cycle following low tide in the reference situation. Note that the change in bed levels has been divided by 10 to compensate for the morphological multiplication factor.

The water levels closely follow the imposed water level boundary conditions. A harmonic tide with an amplitude of 1.5 m and a 12 hour period is clearly visible. The model bathymetry at point M is located 40 cm below mean water level, which brings about an emergence time of 40%. Maximum flow velocities occur in west and eastward direction, parallel to the channel and achieve maxima of 50 cm s^{-1}. Both emersion time and maximum flow velocity are important factors in mussel habitat in the Wadden Sea. The values observed in the model comply with habitat requirements as found by Brinkman *et al*. (2002).

The second flow velocity component (*v*) – directed along y, transverse to the channel – shows peaks during initial stages of rising (incoming) and falling (outgoing) tide. The *v*-components are most prolonged during outgoing tide. The reason for this asymmetry is that at incoming tide the *v* components are directed against the tidal flat gradient, whereas at outgoing tide this component is directed with the gradient. As a direct effect of the asymmetry in y velocities, more water leaves the model via the channel and the channel boundary at outgoing tide than enters it at incoming tide. The same amount of water has to travel less distance to leave the model via the channel and channel boundary at outgoing tide in comparison with incoming tide, where the water has to travel the length of the model. The same amount of water, traveling less distance, results – on average – in lower velocities. This is indeed the case, as can be seen in the *u* velocity component in Figure 20. Although maximum velocities are equal at in- and outgoing tide (0.5 m s^{-1}), the average velocities are larger at the inflowing stage. The development over time of velocity vectors along the transect AB (which includes M at y=150, see Figure 17) is presented in Figure 21. Figure 21 further makes clear that velocities in the channel are higher than those on the flat. It can be stated in conclusion that the model is forced from the channel where velocities are highest. The tidal flow on the intertidal flat is flood dominant in the sense that high velocities are most prolonged at incoming tide. Tidal asymmetry (both flood and ebb dominated depending on location) is a well known feature of intertidal flats in the Wadden Sea (see for example Van Ledden, 2003).

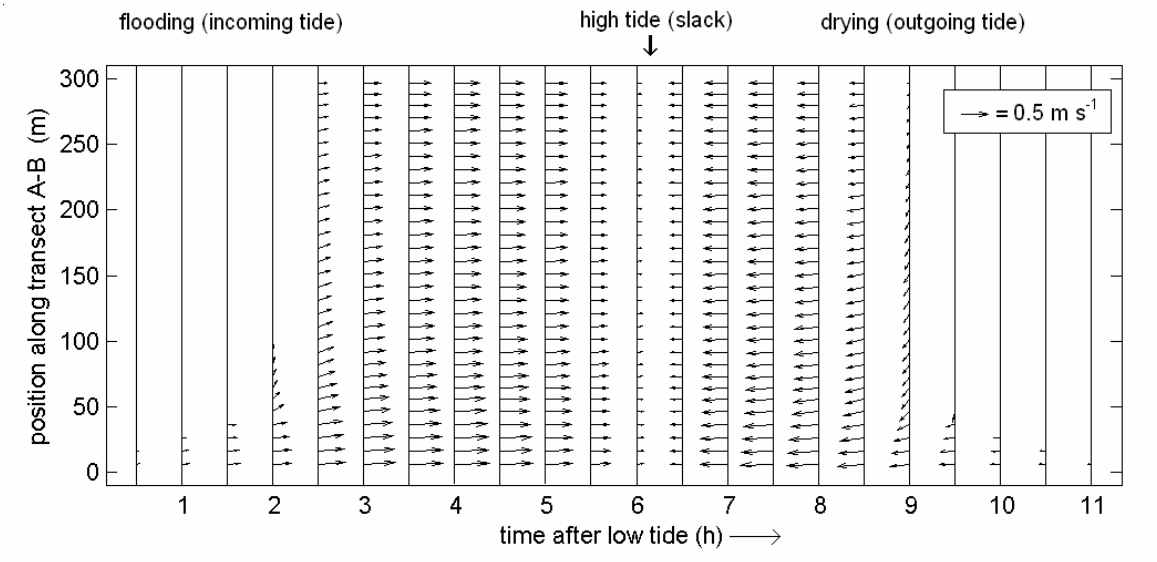

Figure 21: Velocity vector over AB as varying over a tidal cycle.

Suspended sediment concentrations have also been displayed in Figure 20. The concentrations show a dual peak over a tidal cycle. The peaks in concentration correspond to peaks in flow velocities causing bed shear stress which brings sediment

in suspension. Faster flow also allows less time for sediment to settle to the bed. The asymmetry in the flow velocities as explained above is thus carried through into the suspended sediment concentrations, with higher concentrations carried at incoming tide. The higher suspended sediment concentration at the western (incoming tide) boundary also adds to this model behavior. Finally incoming tide comes partially from the channel (high suspended sediment concentration) whereas outgoing tide comes from the low concentration flat. The combined effect of velocity asymmetry, imposed boundary conditions and channel/flat effects cause the suspended sediment to be flood dominant. Higher concentrations are carried over the flat at incoming tide and lower concentrations during outgoing tide. This effect has been explained in section 2.1.3 and is expected on an accreting intertidal flat.

5.1.2 Accretion and erosion in model domain

Not all fine sediment carried into the model can be kept in suspension, a certain amount will be deposited. At high velocities some of the deposited sediment is eroded again. However flow velocities bringing in suspended sediment that is deposited, do not have enough force to erode it again, this is called the scour lag (see section 2.1.2). In this model the phenomenon can be observed and has been displayed in Figure 20. The figure relates the cumulative deposition to the other conditions in M. Material can only accrete or erode if water is present, hence the absence of either erosion or accretion (horizontal line) every twelve hours. At all other times deposition takes place when velocities are low, erosion takes place when velocities are high. High erosion occurs twice every tidal cycle, corresponding to two peaks in velocity (at incoming tide and at outgoing tide). This behavior is depicted as two depressions every tidal cycle (12 hours) interrupting otherwise continuous accretion when the flat is submerged. Because of differences in velocities and location relative to the boundaries, accretion is not uniform. The spatial pattern of accretion after 60 simulated days is presented in Figure 22.

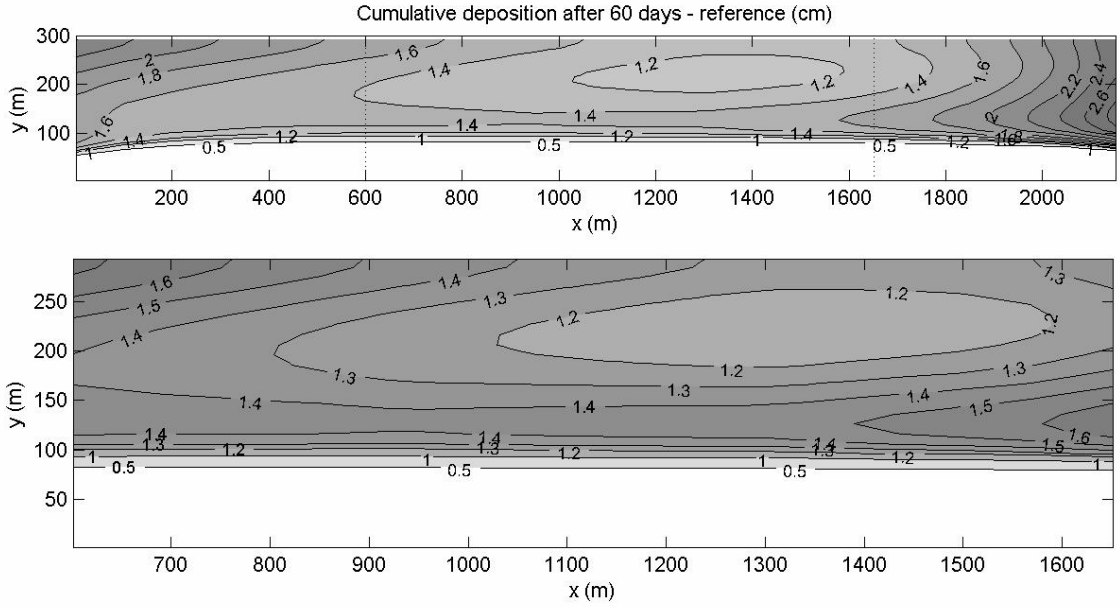

Figure 22: Deposition after 60 days in cm. The upper figure displays the entire domain. The lower figure focuses on the area of interest located between the dotted lines in the top figure. From here on all figures plot only the area of interest.

Figure 22 makes clear that there is no sedimentation in the channel. The high flow velocities there (see Figure 21) favor erosion over deposition. The mud has accreted around 1.5 cm, corresponding to an accretion rate in the order of mm/month as is normal for mudflats during summer. Accretion is highest near the east and west boundaries as result of boundary effects. It should be noted that these effects were expected and the reason for the elongated design of the model domain. Because the boundary effects do not impact the - relatively uniformly accreted - area of interest, the boundary effects are deemed acceptable.

5.2 Standard mussel bed

5.2.1 Impact on flow velocities

The standard mussel bed has been implemented following the proposed values in Chapter 3. The values of which will be varied in the sensitivity analysis presented in Chapter 6. The standard mussel bed is 150 m in x-direction and 50 m in y-direction and is positioned with the center on point M. Difference in sediment accretion and erosion are due to the spatial hydrodynamic influence and biodeposition. The effect of the mussel bed presence on hydrodynamics is treated in this sub section.

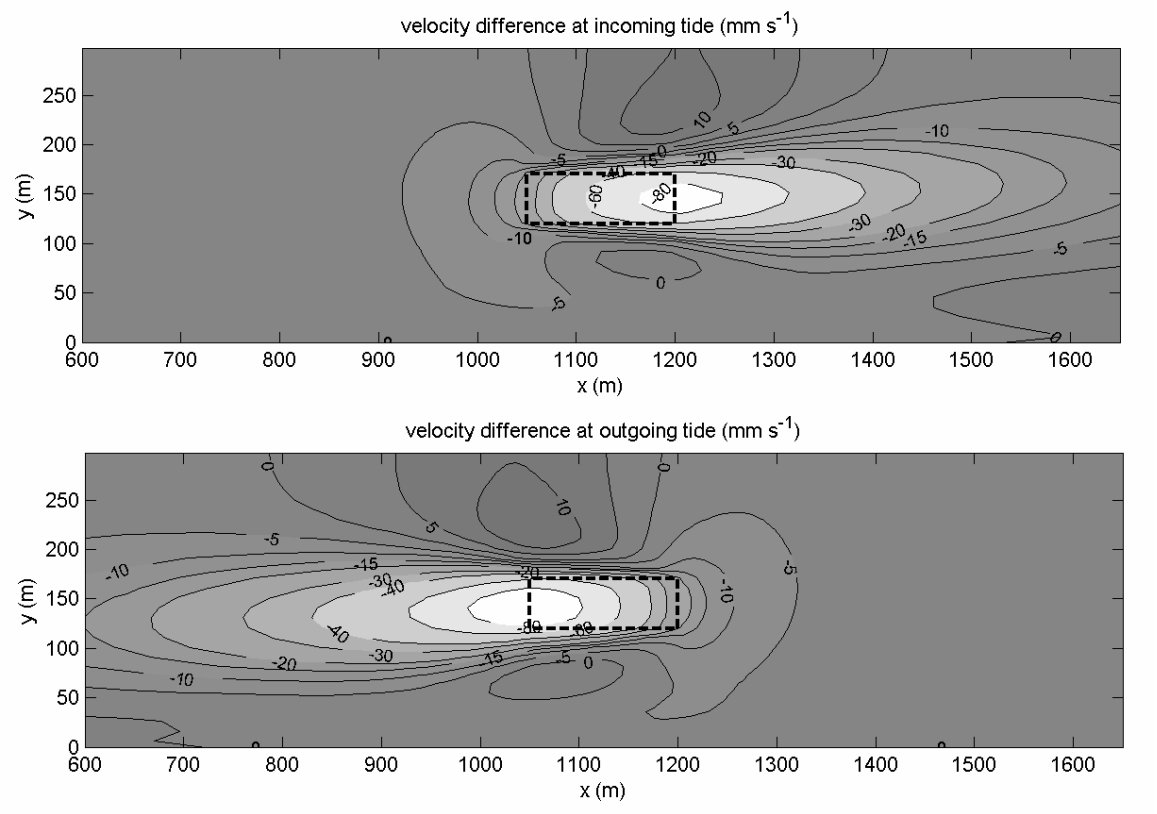

Figure 23: Spatial difference in maximum flow velocity between the standard mussel bed case and the reference case (negative values denote a relative decrease in maximum velocity in the former), during incoming (upper) and outgoing (lower) tide. The mussel bed area is depicted by a thick dotted line.

The presence of a mussel bed has two distinct effects, as can be seen in Figure 23. The velocities in front, on top and in the wake of the mussel bed, show a decrease in comparison to the situation without the mussel bed. The water, forced to find another way, flows around the sides of the mussel bed increasing flow velocities there.

Velocities over the flat, north of the mussel bed, experience the largest increase. The limited flow depth on the flat means that small increases in discharge, cause relatively high increases in velocities.

5.2.2 Mussel bed effects on net retention of sediment

In comparison to the reference situation sediment is retained. A comparison between the deposited amount in the mussel bed location with and without the mussel bed gives an added deposition of $390 \cdot 10^3$ kg. The area of interest as defined in Figure 22 accumulates an added $565 \cdot 10^3$ kg. The sediment amount deposited inside the mussel bed and around it due to a decrease in overall flow velocity are thus of the same order of magnitude.

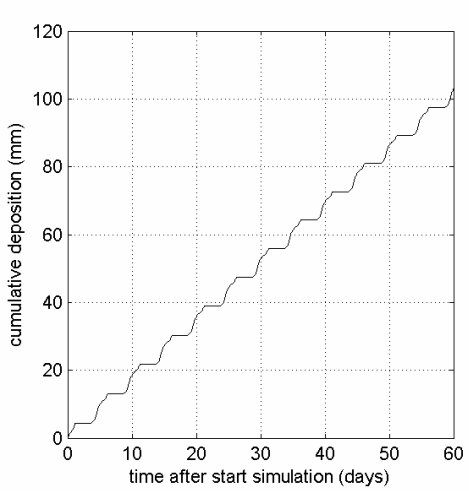

Figure 24: Cumulative deposition in M (see Figure 17) for the standards mussel bed. Note that the morphological factor of 10 has been applied, and that the simulated time scale has been displayed (60 days). The phase of deposition still follows the 6 day actual simulation time.

Figure 24 gives the cumulative deposition in M for the standard mussel case. It is clear that the mussel bed elevates itself to around 10 cm. Also note that cumulative deposition hardly diminishes over the simulated time. It appears that the current model implementation does not have a strong negative feedback between mussel bed elevation and deposition (or a positive feedback with erosion). Apparently there must be other mechanisms that halt mussel bed elevation, see for discussion Chapter 7.

5.2.3 Mussel bed effects on accretion patterns

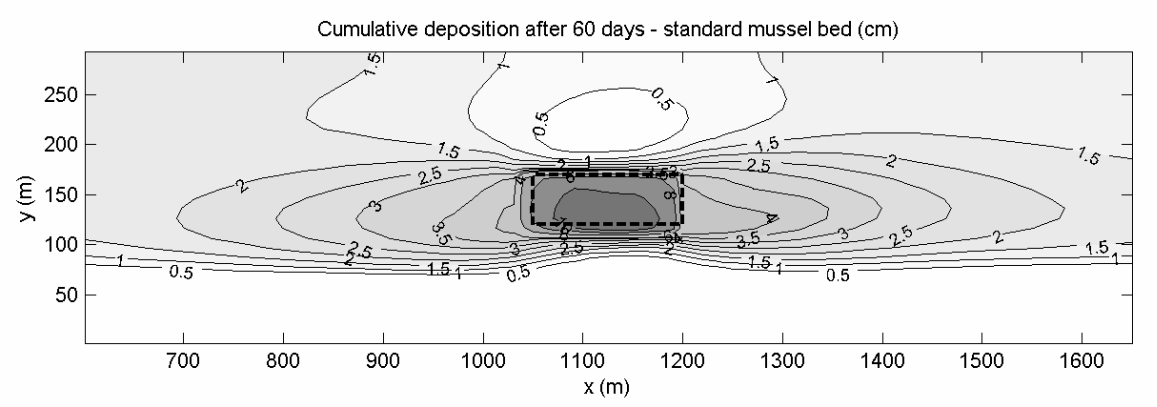

Figure 25: Accretion in the area of interest in case of the standard mussel bed. Note the changed shading scale in comparison with Figure 22. The mussel bed area is depicted by a thick dotted line.

Figure 25 shows that accretion – outside the mussel bed area - occurs in the wake of the mussel bed, during both incoming and outgoing tide. Relatively little deposition has occurred north of the mussel bed, where flow has accelerated. The area clear of mud bordering the channel has been expanded towards the mussel bed area.

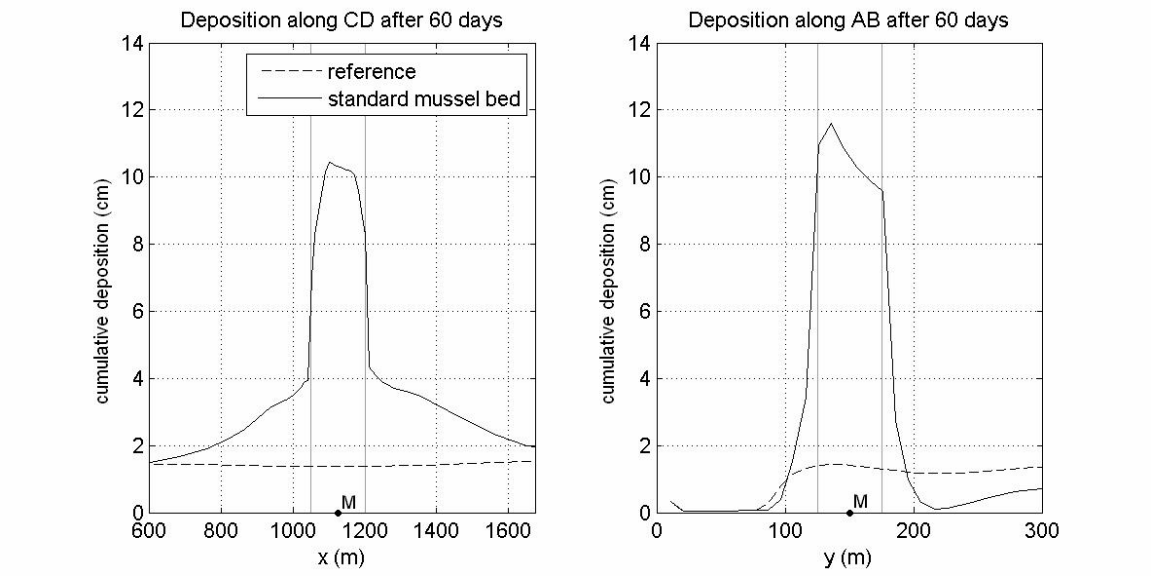

Figure 26: Accretion along cross section CD (left) and AB (right) after 60 simulated days. Cross sections are defined in Figure 17. The mussel bed location is marked by two vertical grey lines. Note the scaling of the figure; no gradients exceeding 1/100 are present in the results.

Accretion along cross sections has been displayed in Figure 26. These graphs make clear the extent of the differences in accretion between the situation with and without a mussel bed. Also the deposition in the wakes on both sides of the mussel bed is substantial, showing accretion of up to twice that of the reference situation. Deposition east of the mussel bed is slightly higher than in the west, as a result of the wake in the sediment rich incoming tide. Reduction of deposition south and especially north of the mussel bed location is substantial. However, spatially the effect is less significant as seen in Figure 25.

The accretion inside the mussel bed is very high, elevating the mussel bed location by more than 10 cm in 60 days. Such a rise is comparable with the 30-40 cm as mentioned by Dankers *et al.* (2004) for young mussel beds over the first months of their existence (July-November: 6-8 cm month^{-1}). The sharp curves in accretion inside the mussel bed, suggest that discontinuous effects play a role. Indeed, the rough mussel bed caused flow velocities to reduce below those necessary for critical bed shear stress. The result is that the middle parts of the mussel bed do not erode and net accretion is exclusively due to deposition.

5.2.4 Decomposition of causes

One of the advantages of model simulations is that certain processes can easily be turned off in order to asses their importance. In this subsection processes by which the mussel bed is defined are excluded in order to conduct a preliminary investigation into their respective importance. The processes excluded are, the filtration of sediment causing biodeposition, the increased erosion coefficient of (pseudo-)faeces rich sediment and finally the elevation of the mussel bed relative to the surrounding flat. The latter effect is the result of feedback of morphological changes, which can simply be switched off in Delft3D. In that mode the model keeps track of bathymetric changes, but no longer feeds this back into the hydrodynamics equations. As far as the hydrodynamics are concerned the mussel bed remains at the height it has at t=0: i.e. no elevation relative to the surrounding bathymetry. Comparisons between the runs have been displayed in Figure 27.

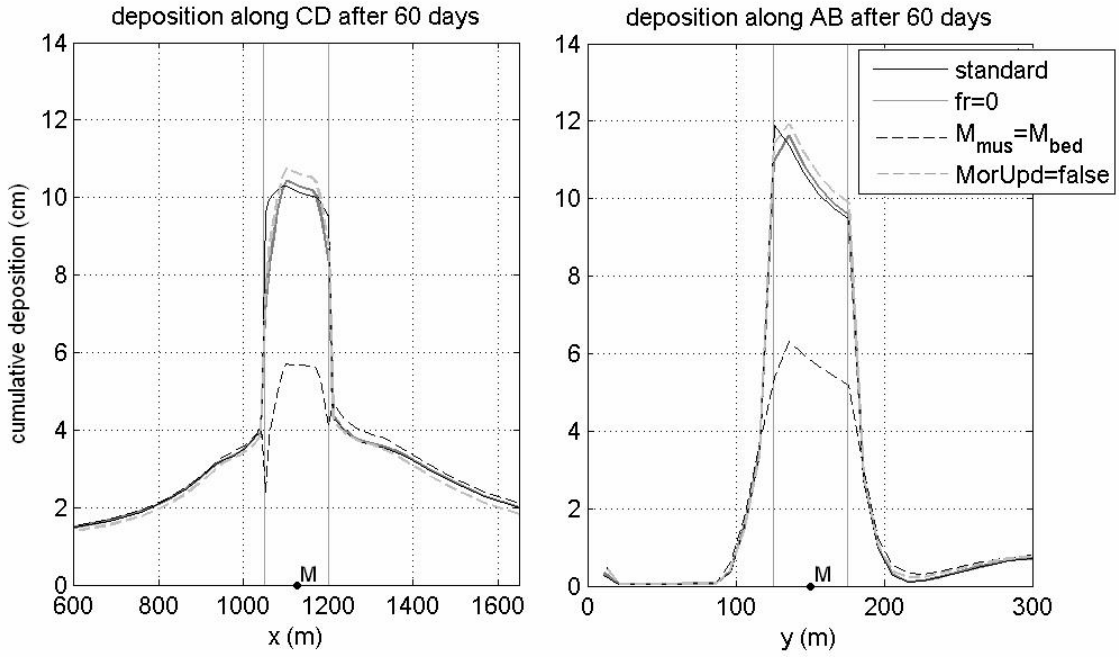

Figure 27: Standard mussel bed cross sections compared with similar runs without biodeposition (filtration rate fr = 0); without increased erosion rate $M_{mus}=M_{bed}=1{\cdot}10^{-4}$ kg m^{-2} s^{-1} and without the mussel bed elevation influencing the hydrodynamics respectively. Cross sections are defined in Figure 17. The mussel bed location is marked by two vertical grey lines.

Biodeposition has a marked influence on the final results. As biodeposition is modeled as a doubling of the settling velocity, the elevation of the mussel model is drastically reduced. More sediment can pass over the mussel bed leading to a slight increase in accretion around the model, i.e. because it is not captured by the bed it accretes after

passing the bed. The amount of deposition (both biodeposition and passive deposition) almost exclusively defines the amount of sediment captured in the mussel bed; erosion only has a limited effect at the mussel bed edges. The effect of the bathymetric updating is surprisingly small, as has already been observed in section 5.2.2. Ten centimeters extra height apparently does not have a significant effect on overall accretion patterns. For possible future modeling this leads to the conclusion that it is much more important to determine roughness and filtration rates, than to correctly estimate mussel bed heights. It is also shown in Figure 27 that increased height decreases deposited material. Apparently the influence of height on deposition (more flow resistance, lower velocities and more deposition) is outweighed by the decrease in flow height (lower depth, more velocity to carry similar discharges, which in turn lead to higher bed shear stress and more erosion).

5.3 Conclusion

The model has been shown to represent realistic fine sediment dynamics on a Wadden Sea intertidal flat: no deposition in the channel and slow accretion of the flat itself. The location of the mussel bed experiences conditions that suit mussel bed habitat needs. It can thus be concluded that this model is suitable for investigating the influence of a mussel bed on fine sediment dynamics on an intertidal flat in the Wadden Sea.

The standard mussel bed shows high accretion, in accordance with observed rates for young mussel beds. Deposition also occurs in the wake of the mussel bed, variable with the amount of sediment carried by the flow. In comparison with the reference situation without the mussel bed, the mudflat experiences increased erosion north and south of the mussel bed as flow velocities are increased in those areas. The increased deposition in the wake of the mussel bed, is much higher than the decreased deposition north and south. In effect the area around the mussel bed retains a large amount of sediment.

Finally it can be stated that, in the model, high accretion in the mussel bed is determined mainly by (1) the roughness of the bed slowing down the flow and thus increasing deposition and (2) by biodeposition. The heightened bed in itself does not represent a significant influence, nor does erosion from in between mussels.

6 Sensitivity analysis

The results presented in the previous chapter are based on a certain set of parameter values. These parameters are to an extent uncertain. Three types of uncertainty are identified: (1) the location of the mussel bed. Although the mudflat model has been designed to match mussel habitat, there is a certain spread in where mussel beds will actually be able to survive. It will be investigated in this chapter how the mussel bed implementation will perform under different model conditions. (2) The parameters by which the mussel bed model is defined are also uncertain. The second part of this chapter will treat variations in these parameters. The results of this analysis can provide guidance for further research, specifically which parameters determine the system most. (3) Finally mussel beds have a large variation in form and pattern, as explained in section 2.4.4. The third section of this chapter presents the effects of different patterns on the amount of sediment that is retained in the mussel bed area.

6.1 Variations in mudflat slope

The mudflat model as presented in Chapter 4 is defined by characteristics that are interrelated. This is in accordance with an actual mud flat. For example the amount of sediment that can be carried by the flow is dependent on the current velocities. Furthermore the edge of the channel should correspond more or less to the boundary of fine sediment deposition. This makes it difficult to simply vary one characteristic of the model, without this resulting in model conditions that are unrealistic. To give an example, for the reference situation without a mussel bed, the mudflat slope has been adjusted, the cross sections of resulting cumulative deposition are given in Figure 28.

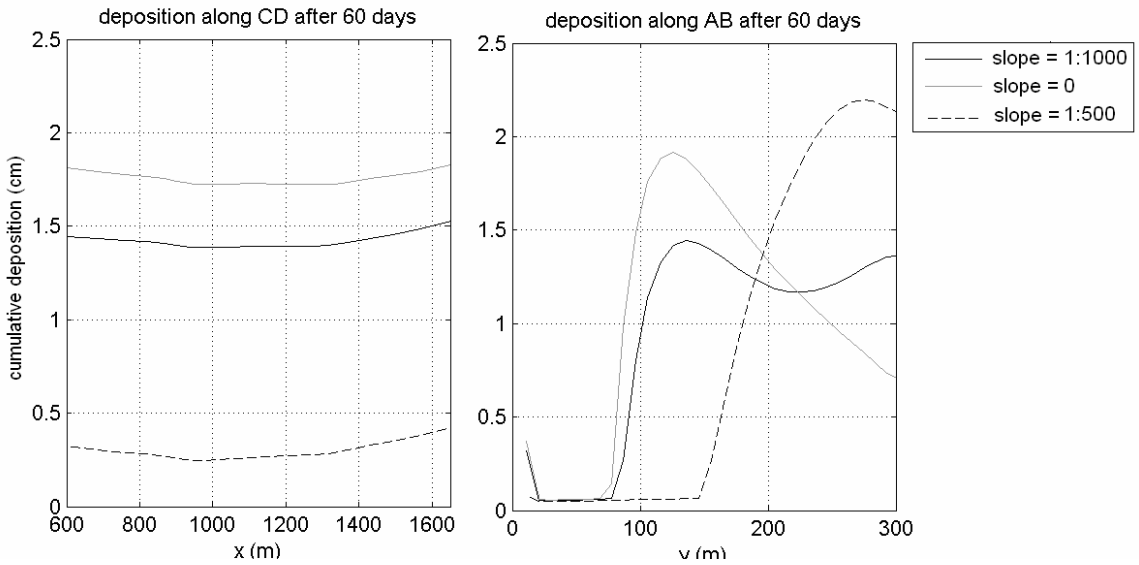

Figure 28: Reference situation with three different intertidal flat slopes. In case of a steeper slope the mussel bed is no longer positioned in an area that is accreting. In case of an absence of bed slope, high sedimentation occurs on the channel boundary creating a levee. Cross sections are defined in Figure 17.

It is becomes clear from Figure 28 that with changing a parameter such as the bed slope the entire model behavior changes and this means that the model no longer describes a mud flat. The same kind of large shifts in model behavior occur when other

individual parameters are changed. In fact in order to significantly vary conditions, whole new models need to be set up. This goes beyond the time restraints of this study.

An alternative is found in variations in the settling velocity. In fact the settling velocity determines the relative importance of erosion, it determines the relative importance of active filtration by mussels and it changes the effects of variations in flow velocities. Variations in settling velocity are more easily achieved and still represent a large spectrum in intertidal flat conditions. Thus, the sensitivity analysis in the next section will also incorporate differences in settling velocities in order to show that the found relations are not determined solely by model conditions and are instead a property of the mussel bed implementation. The standard settling velocity of the fine sediment used here is 0.5 mm s^{-1}. To represent different conditions 0.35 and 0.65 mm s^{-1} will be used.

6.2 Sensitivity for mussel bed parameters

The mussel bed is characterized by the mussel bed elevation and roughness, by the filtration rate and by the erosion behavior. The latter is determined by three further parameters: the erosion rate and critical bed shear stress of the sediment in between the mussels and the amount of force available for the erosion in the form of the bed shear stress. As explained in section 3.2.3 the mussel bed has been implemented such that the bed shear stress between mussels is equal to that on an empty bed under the same conditions. Following equation (3), erosion is determined by the erosion rate and the *ratio* between bed shear stress and critical bed shear stress. Only variation in one of the latter two parameters is needed to account for uncertainty in both. Therefore sensitivity for variation in erosion rate and critical bed shear stress is tested, also capturing the uncertainty in the bed shear stress between mussels.

6.2.1 Analysis method

The sediment is captured in the mussel bed itself and in the wake of the mussel bed. The erosion around the edges has been shown to be irrelevant in terms of volume in section 5.2.2 and will be disregarded as a separate result. The results – the sensitivity of which will be tested – are thus summarized as the amount of sediment captured in the mussel bed area (MA) and the amount of sediment captured in the area around the mussel bed area (AMA). The former area is defined as the 150x50 m area where the mussel bed is located; the latter corresponds to the area of interest as defined in Figure 22 measuring 1050x300m, excluding MA. The result will be displayed as the difference with the reference situation, i.e. the excess sediment as compared to a situation without the mussel bed. The amount of sediment of MA and AMA combined is defined as the total amount of sediment captured by the mussel bed. By specifying the MA and AMA separately the effect of variations on both the total net accretion and on the amount of accretion outside the mussel bed can be investigated.

6.2.2 Sensitivity to mussel bed roughness

The mussel bed roughness has been determined using the size of roughness elements. The value of k_s = 90 mm has been chosen based on roughness elements of 30 mm. Because the latter size is both variable as mussels grow and depending on the seed mussel configuration, a considerable amount of variation can occur in this parameter. In Figure 29 the Nikuradse roughness length of the mussel bed has been varied to 50% below and above the initial value.

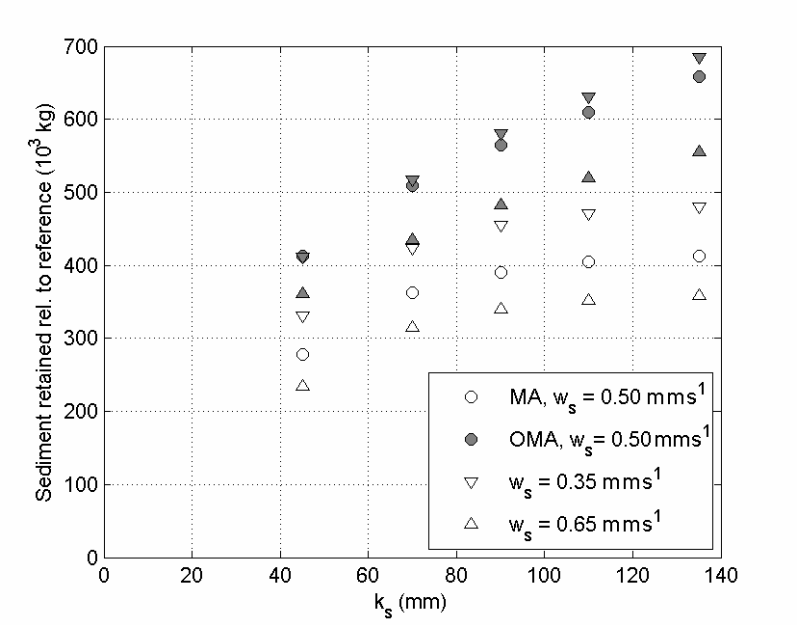

Figure 29: Sensitivity of model results to variations in mussel bed roughness, presented as the amount of sediment retained in the mussel bed area (MA) and in the area around the mussel bed area (AMA) relative to reference situation without a mussel bed. Note that the reference situations are also run with the respective settling velocities.

It can be seen in Figure 29 that the combined amount of retained sediment will rise as the mussel bed is rougher. In particular the amount of sediment deposited in the wake of the mussel bed rapidly increases with increasing roughness. The deposited sediment in this area is determined by the decrease in flow velocity and is thus directly related to how much resistance the mussel bed poses to the flow. As expected from the results presented in the previous chapter, the increase in deposited sediment in the wake of the bed outweighs any effect of increased erosion around the side. The amount of sediment deposited in the mussel bed also increases with the higher roughness but this increase is limited. Apparently most of sediment has already settled from the slow current over the mussel bed at lower roughness values.

The effect of changes in settling velocity on the sensitivity for roughness is surprisingly limited. Actually, relatively little extra sediment is retained in case of higher settling velocities. Because more sediment has already been deposited in the reference case, a further slow down of the flow has relatively less effect.

6.2.3 Sensitivity to filtration rate

The filtration rate in the standard mussel bed has been estimated based on laboratory experiments, model conditions and has been corrected for refiltration in a dense mussel bed (see section 3.3.2). Especially the latter correction is very uncertain. For this reason filtration rate has been varied over a wide range from 0.25 to 1.5 mm s^{-1}. The results of the model runs are displayed in Figure 30.

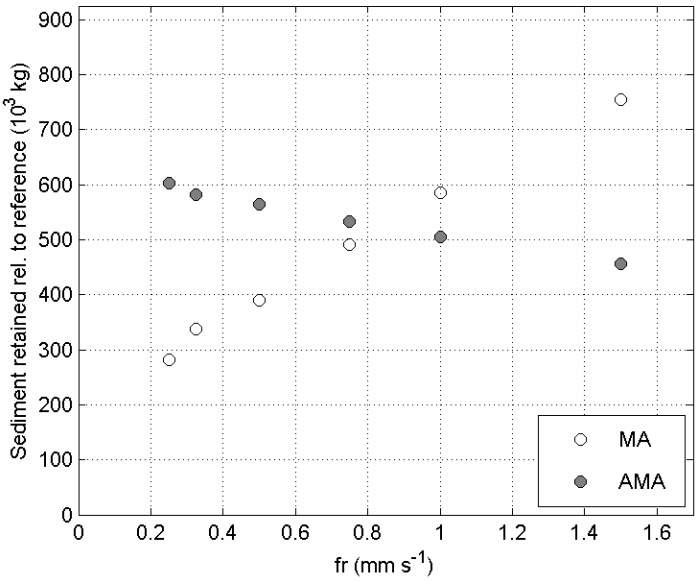

Figure 30: Sensitivity of model results to variations in mussel bed filtration rate, presented as the amount of sediment retained in the mussel bed area (MA) and in the area around the mussel bed area (AMA) relative to reference situation without a mussel bed.

It is shown that especially the amount of sediment captured by the bed is extremely variable with changing filtration rate. The extra elevation caused by deposition does not provide significant feedback in the form of increased erosion as shown in section 5.2.4. Therefore extra deposition caused by filtration is directly added to the amount captured by the bed. Because of the large quantities captured by the bed less sediment is available for sedimentation in the wake of the mussel bed. At high filtration rates, the amount of sediment captured by the mussel bed can actually exceed the amount settling in the area around the mussel bed. The settling velocity has not been varied because the filtration rate itself is modeled as an increase in settling velocity. Consequently it can easily be understood that if settling velocity is lower, the relative influence of biodeposition becomes higher.

6.2.4 Sensitivity to erosion behavior

The amount of erosion that takes place from in between the mussels is determined by both the properties of the sediment and the forces exerted on the bed. As has been explained in sections 3.2.3 and 3.3.3 there is little data available for estimating these values. The result is that there is large uncertainty in the parameters. In the standard model erosion is not a large factor (see section 5.2.4). Inhibiting erosion further will not have large results. The critical bed shear stress has thus been chosen at two lower values of 0.3 and 0.4 N m^{-2}, these values also represent the uncertainty in the bed shear stress acting on the sediment. The erosion rate has been varied from half that of the original sediment (actually erosion rate is expected to be higher, see section 2.3.3) and ten times as high. The results are presented in Figure 31.

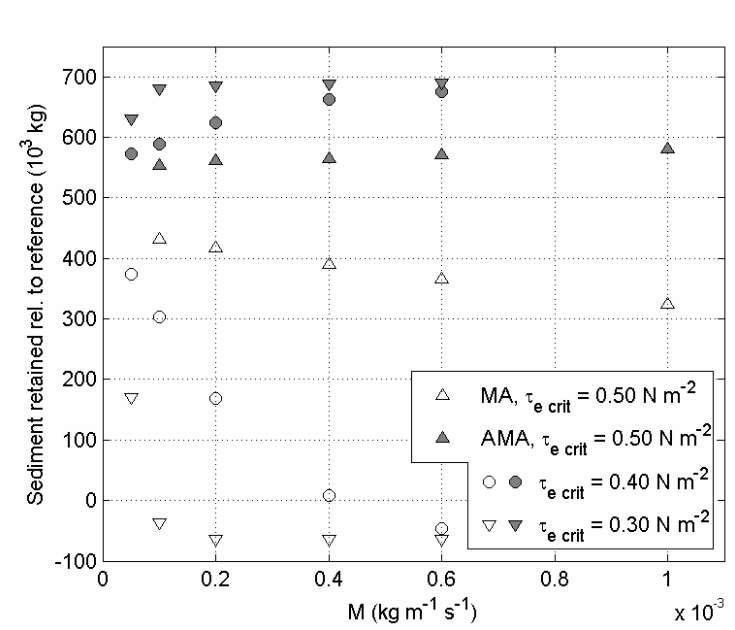

Figure 31: Sensitivity of model results to variations in erosion rate and critical bed shear stress, presented as the amount of sediment retained in the mussel bed area (MA) and in the area around the mussel bed area (AMA) relative to reference situation without a mussel bed.

There is little influence of the erosion behavior on sediment outside the mussel bed area. However increased erosion quickly yields unrealistic results for the mussel bed itself. One of the assumptions on which the mussel bed implementation is based, is that deposition is dominant over erosion. It is clear that this assumption is not met for the model runs with lower critical bed shear stress. It could be stated that the model parameters are restricted by what is expected of the model, i.e. a mussel bed that is elevating itself. Most results with the decreased critical bed shear stress result in bed levels in the mussel bed that are lower than the surrounding area, which is clearly unrealistic. Erosion from a mussel bed that is much higher than that of the surrounding sediment is simply not observed in the field and the chosen parameters should reflect this. This means that in a summer situation where deposition is already dominant on the empty bed, the same will apply for the mussel bed, i.e. erosion will be relatively small. As a result the net accretion rates will not be significantly impacted by erosion processes.

6.2.5 Conclusion

Because of the relative unimportance of erosion, the behavior of the mussel bed is determined by its roughness and the filtration rate. It can be concluded from the relative sensitivity to these parameters, that the amount accreted inside the mussel bed is mostly variable with the filtration rate. The amount deposited in the wake is more sensitive to changes in mussel bed roughness.

6.3 Patterning in young mussel beds

The mussel bed patterns as presented in section 4.4 have been implemented in the mudflat model. The resulting influence on deposition in and outside the mussel bed in those cases is presented in this section. Contour plots have been made of sedimentation for all mussel bed patterns, these figures are displayed in Appendix F.

6.3.1 Cross sections of mussel bed accretion in case of different patterns

In order to study the deposition distributions inside the differently patterned mussel beds, cross sections of cumulative deposition are given for the different patterns in Figure 32, Figure 33 and Figure 34.

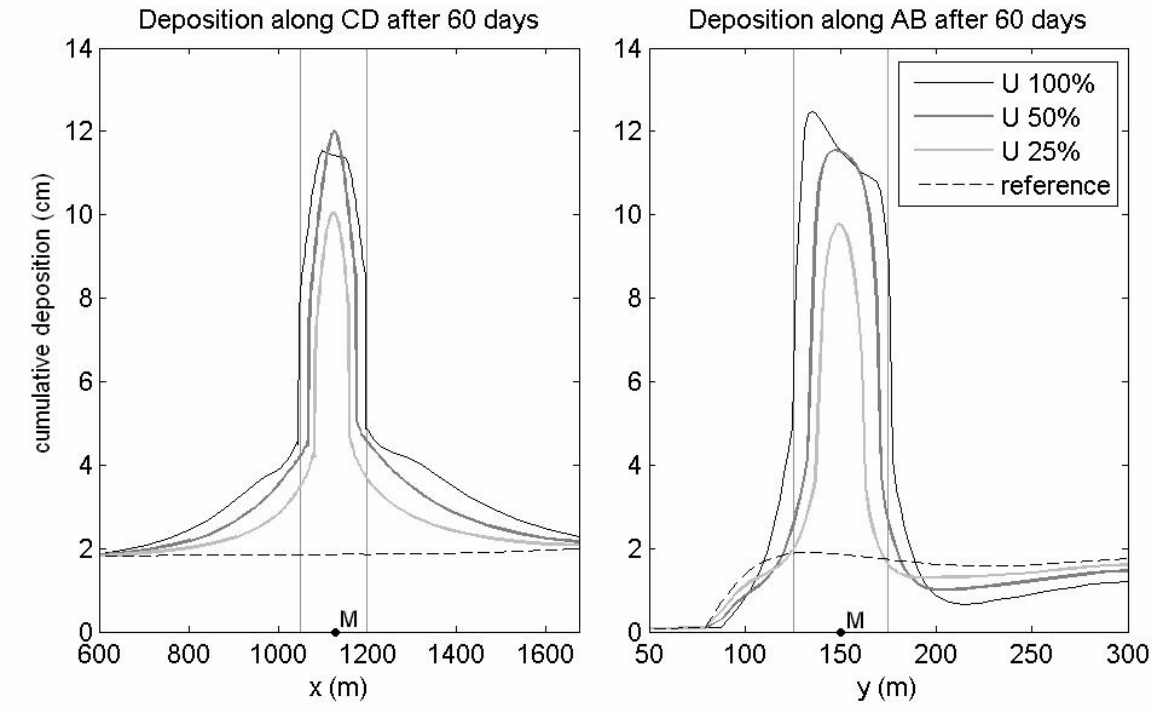

Figure 32: Cross section of cumulative deposition in case of uniform mussel bed patterns. Cross sections are defined in Figure 17. The mussel bed location is marked by two vertical grey lines.

Erosion, although not dominant, plays an important part in the differences between the different patterns. As can be seen in Figure 32, the standard mussel bed no longer experiences erosion in the middle, i.e. the bed shear stress does not exceed the critical bed shear stress. For the smaller uniform beds this is not the case, the rough area posed by these smaller beds is not large enough to decrease velocities to the same degree, erosion still takes place. In the right hand side plot of Figure 32, it can be seen that the larger mussel plots cause more relative erosion north of the mussel bed.

Figure 33 displays a similar figure, now for the patterns covering 50%. It is apparent that the uniform pattern is elevated more than the other patterns. The latter show much lower maxima in accretion. Although the patchy patterns pose larger resistance to the flow, the decrease in deposition north of the mussel area is actually decreased. On closer inspection it can be seen that the maxima of the transverse striped patterns (TS) are lowest. Apparently this pattern allows slightly higher flow velocities causing slightly higher erosion. In the case of parallel stripes (PS) the mussel bed is in its own wake at dominant velocity in x direction, reducing erosion. The checker board pattern (P) shows similar maxima to PS.

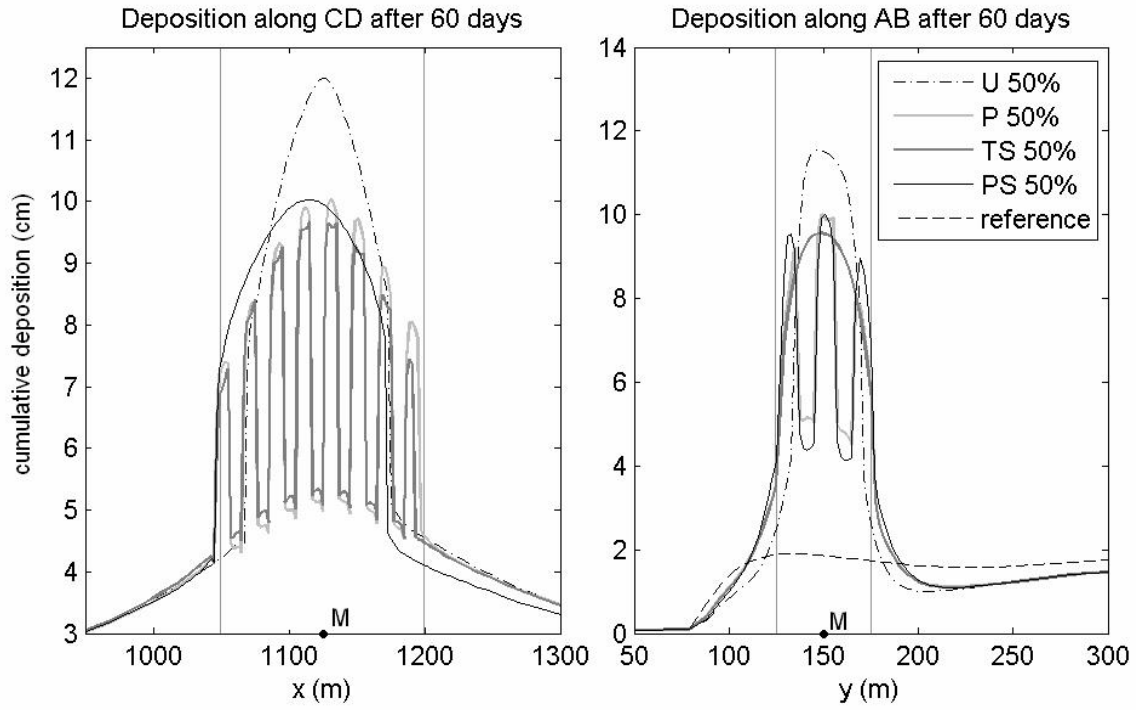

Figure 33: Cross section of cumulative deposition in case of mussel bed patterns covering 50% of surface of standard mussel bed. Cross sections are defined in Figure 17. The mussel bed location is marked by two vertical grey lines.

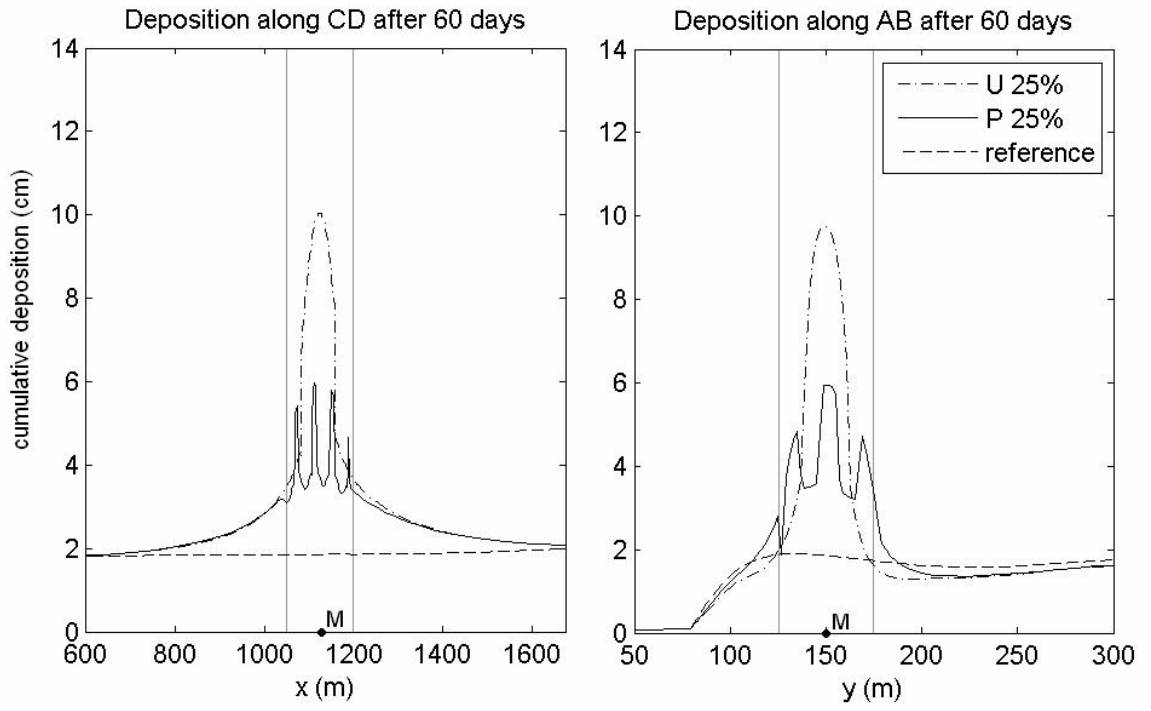

Figure 34: Cross section of cumulative deposition in case mussel bed patterns covering 25% of surface of standard mussel bed. Cross sections are defined in Figure 17. The mussel bed location is marked by two vertical grey lines.

Finally the 25 % coverage patterns are presented in Figure 34. Here the difference between the patchy mussel bed and the uniform pattern is even more distinct. The uniform pattern elevates itself almost twice as high as the patchy pattern. The very

open structure of 25% patchy pattern, allows for relatively high velocities and thus relatively high erosion.

6.3.2 Deposition in and around mussel bed in case of different patterns

The cumulative deposition results are aggregated along whether the material has been deposited inside the mussel bed area (MA) or around it (AMA). A comparison of the found values is displayed in Figure 35. It is clear that the patchy patterns catch less sediment inside the mussel bed and more in the wake. This effect can be explained by considering that an open structure will allow higher velocities than a concentrated uniform mussel bed. Higher velocities result in higher erosion from in between the mussels. Furthermore the flow as a whole experiences more drag from such a patchy structure. Velocities are higher and shear stress experienced by the flow is related to the velocity squared, see equation (5). The flow is - on average -.slower in the mussel bed wake in case of the patchy beds, resulting in more sedimentation there. Patchy structures thus capture less sediment, but have a larger influence on the surrounding mudflat than the same surface of mussel bed concentrated in a uniform bed.

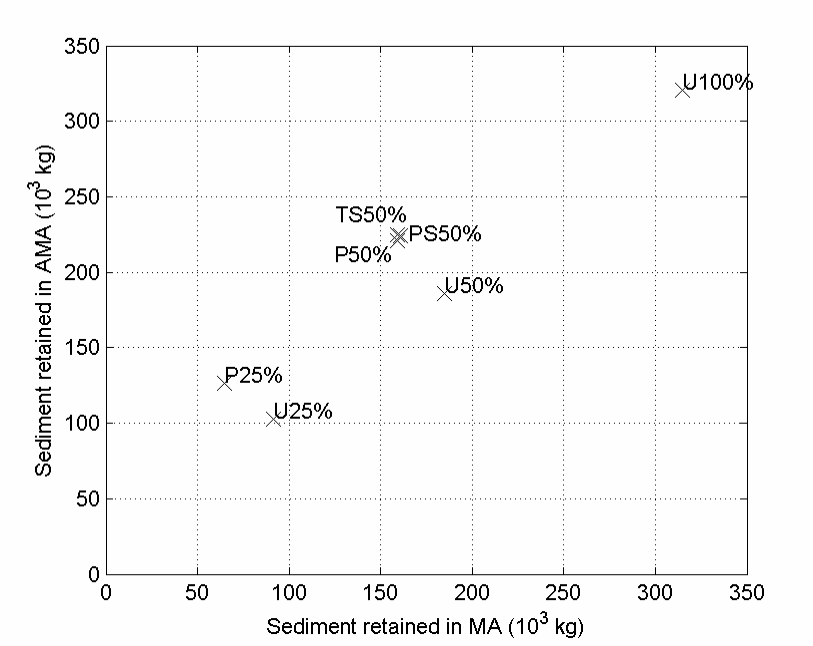

Figure 35: Influence of patterning on deposition inside (MA) and outside the mussel bed (AMA). U stands for uniform, P for the checker board pattern, TS for transverse stripes and PS for parallel stripes. Note that the MA is the same area for all patterns, i.e. only in U100% is MA fully covered by mussels.

6.4 Relating fine sediment influence to mussel biology

A significant result of the first part of this chapter is that increased roughness actually increases deposition in a mussel bed. With regard to the difference between reefs of mussels and the pacific oyster (*Crassostrea gigas*), it is sometimes argued that the latter are very rough in order to reduce deposition (De Vries, personal communication). If the present result is applied to that case it can be stated that although high roughness may, on a small scale, increase turbulent erosion, on a larger scale such rough beds are likely to increase the amount of sedimentation.

Elevating their surroundings can be advantageous to mussels as has been explained in section 2.4.2. The higher elevation puts the entire bed out of reach of predators such as crabs and for individual mussels being high in the flow gives a feeding advantage relative to the other mussels. However the high sedimentation with which this elevation necessarily corresponds can also have negative effects. It has been shown by Ten Brinke *et al.* (1995) that mussel beds can actually be smothered as a result of high sedimentation. Even if not fatal, constantly having to crawl out of the sediment and having to reattach to other mussels will be a drain on mussel energy levels. Finally quick deposition will result in highly unconsolidated sediment, making it easier for the entire bed (including mussels) to erode. Therefore it can well be argued that it is advantageous for mussel to rise up slowly and the waste products such as (pseudo-) faecal pellets should be resuspended as much as possible. The transverse striped pattern is most efficient at allowing the flow to take away the excess in waste products. If rising slowly is indeed advantageous to mussels, this study gives an additional reason[13] why it is in the mussel beds interest to arrange into stripes transverse to the flow.

[13] *See section 2.4.2 for the theory by Van de Koppel et al. (2005) on patterning in young mussel beds. This issue will be further discussed in the next chapter.*

7 Discussion

This study has provided a first implementation of the influence of mussel beds on fine sediment dynamics in a process based model. A conceptual model has been set-up in order to provide insight in this system. The conceptual model has been translated into a young mussel bed model implementation for Delft3D. Both literature research and experimental data analysis have been employed to estimate the relevant parameters of this implementation. The modeled mussel bed has been deployed in a summer intertidal mudflat model, characteristic for mussel habitat in the Wadden Sea. The model results showed that mussel bed roughness and filtration rate are very important parameters in determining the amount of sediment deposited in the mussel bed and around it. Erosion from the mussel bed itself proved relatively insignificant. It has also been shown that patchy beds collect less sediment than uniform bed.

7.1 Discussion of methodology

The large amount of variables related to a mussel bed and its interaction with fine sediment dynamics, mean that many choices have to be made before such a system can be modeled. As a result, questions will come up regarding the validity of the results. Although most of the model choices have been defended in the main text of this report, here some particularly fundamental issues will be discussed.

7.1.1 Mussel upward migration (climbing)

The fact that mussels climb on top of the sediment that has been deposited is not incorporated in the model implementation. It has been assumed that the mussel layer will simply follow the bed surface as it develops as a result of deposition and erosion. In reality this is not the case. No more sediment can be eroded than is actually in between the mussels; the mussel mud below will remain in place as long as the mussels are present. However the question that is relevant to this study is: do young mussels actually protect the sediment during calm summer conditions? It has been shown in this study that - assuming sediment characteristics that actually favor erosion (high erosion rate) but are otherwise comparative to characteristics of normal sediment - very little erosion will take place from the mussel bed. This is realistic, considering the rate at which young mussels collect sediment, erosion cannot play a large role. It would follow that mussels are actually irrelevant to erosion during summer conditions; the fact that no erosion takes place would solely be the result of limited bed shear stress. However there is an indication that this is not the case.

Adult mussel beds will experience similar deposition as compared to young mussel beds. However it is known that these older beds do not gather as much sediment and do not continue to elevate themselves. Actually, mussel beds will never become higher than mean sea level (McGrorty *et al.*, 1993). Apparently mature mussel beds do experience erosion of the material deposited between the mussels. The difference between the erosion in young and mature mussels beds is best explained by the known fact that young mussels are very mobile and climb on top of the sediment[14]. Mature

14. It has been shown that the elevation of a mussel bed does not provide a significant feedback in the form of extra erosion, so this cannot alone be a reason in reduced elevation rate for mature mussel beds.

mussels have lost this ability to climb and sediment is thus deposited between them, however high flow velocities are apparently sufficient to erode this material again. The answer to the question posed in the previous section is thus that young mussels do in fact protect deposited material. This answer is confirmed by the fact that when new spatfall settles on top of mature mussel beds, the young mussels deposit large amounts of sediment and climb on top. The underlying mussels are smothered and die. The destabilizing effect of this can cause whole sections of mussel bed to detach (Newell, 1989).

The model implementation does not model the climbing of young mussels. Nonetheless erosion does not have a significant effect. To summarize: the process of the reduction of erosion for a young mussel bed (mussel climbing) is not incorporated in the present model implementation; however the actual result (no erosion) is correctly simulated. A final recommendation that follows from this is that for mature mussel beds, it is needed to simulate the high potential for erosion. This can be done by adjusting the sediment characteristics. In reality the erosion of this material must be caused by small scale turbulence between the shells, possibly also related to small waves.

7.1.2 (Pseudo-)faecal pellets as export product of mussel bed

The mussel bed implementation as used in this study has intentionally been kept simple. One process that has not been included is that sediment eroding from the mussel bed has different properties because of the (pseudo-)faecal pellets. Oost (1995) has shown that faecal pellets can be transported for a long distance after resuspension from the model, influencing sediment transport over distances much larger than the mud flat. It has been shown in this study that faecal pellets are actually only a small part of the biodeposited material. The deposition close to the bed of resuspended material close to the bed is likely to be more influential. For example, it has also been argued by Oost (1995), that (pseudo-)faecal pellets have a high organic content. If this material is deposited in the wake of the mussel bed after resuspension, organic content will be high there as well. As an effect biological activity in the area surrounding mussel beds is high, leading to large amounts of surface deposit feeders such as the lugworm. Bioturbation brought about by such organisms stimulates erosion. Such secondary effects can be incorporated in model studies as has been done by Herman *et al* (2001). This has not been pursued in this study.

7.1.3 Waves

It has been shown in appendix B.5 that even small waves may be very important in causing erosion from in between mussels. This effect exceeds what would be expected based on the bed shear stress of those small waves, apparently turbulent processes play a role. During summer, as modeled in this study, conditions are usually calm, however small waves will always occur. It may therefore not be defensible to ignore waves and focus on currents only. Small waves can be modeled as an extra bed shear stress source specifically concentrated in the mussel bed. If it is assumed that this force acts more or less uniform on the mussel bed and is more or less constant over time, the erosive force can be seen as an increased erodibility of the mussel bed. This erodibility has been included in the sensitivity analysis in changes in M and τ_{crit}. It has become apparent that under the used model conditions erosion can not play an important role. It can thus be argued that the effect of small waves has already been incorporated in the analysis. However, on the other hand, as waves dissipate over the rough mussel bed and have a certain direction the influence of waves is not actually spatially uniform or

constant over time. It would be interesting to introduce waves in the model analysis generated using a specialized wave model such as SWAN.

Larger waves, such as those that would result from storms would have a different effect. In summer such storms are rare and the calm weather makes the fine sediment dynamics on a mudflat current dominant (Janssen-Stelder, 2000). Storms do occur however – even in summer – and can quickly erode the sediment on the bare mudflat. This is the reason why mud is transported back to the channels in winter (Oost, 1995). As long as a mussel bed survives the storm the mussel mud will be unaffected. No information is available on erosion of mussels in summer; it is not expected to be common occurrence.

7.1.4 Sand-silt interaction

In the model used in this study the interaction between sand and silt is not taken into account. In fact, sands have not been included at all. In reality, in systems containing both fine sediment (cohesive) and sands (non-cohesive) the interaction between these two sediment types can have a substantial influence on the overall behavior of the system (see Van Ledden, 2003). In essence, when fine sediment concentrations are low, the non cohesive behavior is dominant: erosion rate and critical bed shear stress of the sediment mixture are those of sand (Van Ledden, 2003). If, on the other hand, silt concentrations are above a certain threshold, the properties of the mixture become cohesive, increasing critical bed shear stress and decreasing erosion rate (Van Ledden, 2003). Areas can thus become either muddy and difficult to erode, or sandy and easy to erode. The former will continue to collect fine sediment, where the latter will remain sandy.

Because sand is not included in the model in this study, it is effectively assumed that cohesive behavior is always dominant. This will lead to an underestimation of the erosion of fine sediment in sandy areas such as the channel. The model area has been chosen as an intertidal mudflat; in fact the state of the flat as cohesively dominated has thus been imposed from the outset. Further, as there is no ‘store’ of fine sediment available to erode from the channel, underestimating erosion is not considered problematic. However it would be interesting to investigate how the influence of a mussel bed on fine sediment would be on a sandy flat. It is known that mussel beds are located on average in areas with high mud content (Brinkman *et al.*, 2002; Oost, 1995). It may be the case that mussels themselves are a cause behind the muddy nature of their habitat, this has also been suggested by Flemming and Delafontaine (1994).

7.1.5 Boundary conditions and nesting

Relatively simple boundary conditions have been imposed in this study in order to simulate an accreting mudflat suitable as mussel habitat. More realistic boundary conditions can be obtained by nesting the model area in a larger tidal inlet model, which can be validated by measurements. The boundary conditions generated by such a large scale model make a better ‘fit’ with the small scale area of interest, reducing the boundary effects observed in this study.

More importantly is the question to what extend the chosen model conditions affect the mussel bed influence. Although the choice in the model conditions for testing the mussel bed implementation has been made with care, mussels live under a variety if conditions. Actually the spread in the conditions where mussel beds occur (as presented in Figure 8) is relatively large. It is suggested by explorative model analysis during the final stages of this project (not displayed in this report) that especially the

area around the mussel bed may be influenced differently under different conditions. Changing the flow velocities and suspended sediment concentrations has been shown to be difficult however. By implementing a mussel bed in different nested locations in a larger model, the effects of different conditions can be researched in a more reliable manner.

7.2 Discussion of results

This section discusses how the results of this project relate to other research. Furthermore the implications of the research are discussed.

7.2.1 Implications of the relative importance of roughness and filtration rate

It has been shown in this report that roughness and filtration rate are important factors for mussel bed influence. Biodeposition was responsible for more or less half of the sediment in between the mussels, depending on the choice in parameters. This is comparable to field observations by Prins (1996) and Kautsky and Evans (1987) who found respectively roughly half and 24% of deposited material to be deposited via biodeposition. In a mussel bed the percentage of identifiable (pseudo-)faecal pellets is about 15-40% (Ten Brinke *et al.*, 1995). This relatively low percentage may be a result of disproportionate erosion of this material, or degradation of the pellets (Prins *et al.*, 1996). The biodeposition rate in this study has been estimated using the filtration rate of mussels; it is thus encouraging that it also corresponds to field observations of actual deposits.

The roughness of mussel beds has to the author's knowledge not previously been identified as a major factor in both the deposition inside the mussel bed and the area around it. The large decreases in flow conditions generated by mussel presence allow significantly more sediment to settle as compared to a situation without a mussel bed.

One important thing is the relative unimportance of erosion. If erosion had been significant, the young mussel bed would not have elevated as they are known to do by observations (Dankers *et al.*, 2004b). It has been established in the first part of this discussion that the fact that young mussels climb on top of newly deposited material is the reason behind the limited erosion.

Further implications follow when these results are projected on another reef building shell fish species: the pacific oyster (*Crassostrea gigas*). The pacific oyster is not a native species but has invaded the Wadden Sea (Reise, 1998). These animals are much larger and have rougher shells in comparison with mussels. Also filtration rate is at least as high as that of mussels (Smaal *et al.*, 2005). Higher roughness and equal filtration rate will, based on the results found in this report, lead to the expectation of higher deposition. However oyster beds do not show rapid sedimentation as young mussel beds do. This has everything to do with the lack of mobility of an oyster. The oyster is fixed on a certain position and does not climb on top of - and thus does not protect - settled material, i.e. there is not such thing as 'oyster mud'. Over time oysters can form high reefs, however this is the result of physical growth of the oyster itself, they can grow as large as 33 cm (Dankers *et al.*, 2004a). Oysters resemble mature mussels in their relation to fine sediment. Erosion should play a part to avoid becoming smothering by sediment. Sediment erosion for oyster reefs may be facilitated by two characteristics, (1) oysters form open aggregations, with clusters of shells separated by bare bed and (2) oyster (pseudo-)faecal material is very light and easy to suspend. The open structure of the oyster reef can be seen as similar to the patchy nature of mussel beds, albeit on a smaller scale: both facilitate erosion.

7.2.2 The advantage of a patchy bed

It is striking that during this project the striped patterns transverse to the dominant currents were found to be most efficient (although by a thin margin) in facilitating erosion. There are good reasons that mussels indeed want to limit deposition and thus promote erosion from the bed, see section 6.4. Van de Koppel *et al.* (2005) have shown by means of a model analysis that the same patterns are the result of self-organization by young mussels. Such a wave-like pattern (in this case in space) is a well known phenomenon in ecology, and usually arises from resource limitations, see Van de Koppel *et al.* (2005) for an overview. The self-organization of young mussels is a reaction to on the one hand erosion from waves and currents if a mussel is alone or in a small patch and on the other hand starvation if the mussels group is too large (i.e. food supply is depleted). Removal of waste products could be an additional motivation of this behavior as it is also a negative effect of living in large groups, i.e. large aggregations of mussels experience high deposition and may become smothered. What does this hypothesis mean for oysters, which - as mentioned in the previous section - occur in much smaller patchy pattern (clusters of a few shells)? Perhaps facilitation of erosion by oysters is more important because they do not have the means to climb on top of sediment and would get smothered by high sedimentation. Further research in this area along the lines of the article by Van de Koppel *et al.* (2005) may yield interesting results.

7.2.3 Seasonal variation versus long term morphological influence

During this study the influence of a young mussel bed during the first summer months of its existence has been modeled. What is the significance of this period, especially considering the fact that 50% of mussel beds do not make it through the winter (Steenbergen *et al.*, 2006). If a young mussel bed is eroded during a storm, the mussel mud will also erode. Even if the mussel bed survives the material deposited in the wake of the mussel bed will likely erode during winter (see section 2.1.3). What do the results of this project mean considering this limited scope?

First of all it has been shown that there is seasonal influence. Young mussel beds capture large amounts of sediment in late summer. During winter storms much of this material is resuspended. The seasonal influence enforces the seasonal variation that already exists in the Wadden Sea: low suspended sediment concentrations in summer, high concentrations in winter. In this respect the influence of mussels is similar to another biological stabilizer: microphytobenthos which form algal mats (Andersen, 2001). Algal mats occur on the higher intertidal areas of the Wadden Sea (above mean sea level). In addition, the area of mussel beds surviving each winter form a more or less stable store of sediment (mussel mud). As has been found in this study and the above discussion, the mature mussel beds actually have a smaller influence on fine sediment deposition in summer. However the mussel mud is more consolidated in mature beds, if mussels are eroded the bare mud mounts can persist for multiple years (Dankers, personal communication).

In order to asses the amount of sediment stored in summer and released in winter by mussel beds the surface area of mussel beds is required. Figure 36 gives the surface area of mussel beds in the Wadden Sea. Over a given year there is around 2000 ha of mussel bed area. Each winter on average 40% will be eroded (of all beds, of the young beds more than 50% erodes). Only the sediment in the mussel bed itself is considered and it is assumed that all of this material erodes (neglecting consolidated mussel mud mounts). A density of 500 kg/m^3 for the mussel mud (as is normal for unconsolidated mud, see Van Ledden, 2003) and an average mussel bed thickness of 30 cm are assumed. It is then found that on average $1.2 \cdot 10^9$ kg of material is fixed in summer

and released in winter. A further $1.8 \cdot 10^9$ kg is on average stored inside mussel beds. The yearly import into the Wadden Sea is much higher: around $70 \cdot 10^9$ kg yr^{-1} (Postma, 1981), however only around 5% of this material is net import: $3.5 \cdot 10^9$ kg yr^{-1} (Eisma, 1979). It can thus be concluded that the estimated amounts of fine sediment stored in mussel beds and the amount fixed in summer and released in winter by mussel beds is - on the Wadden Sea scale - in the same order of magnitude as the net import of sediment.

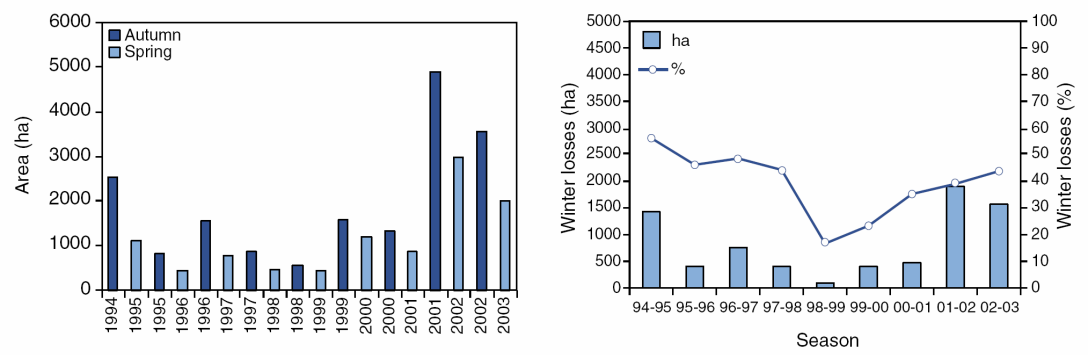

Figure 36: Left: total area of mussel bed in autumn and spring from 1994-2003; Right: area and percentage of total of winter loss of mussel bed (figures adapted from Steenbergen et al., 2006).

In the Wadden Sea system sediment that is stored is not available for dynamic processes. For example it is not available for export to the Wadden Sea, or for deposition in a tidal marsh. As long as this store of sediment is more or less stable over time, their will not be a significant long term influence on the system. However there are indications that the dominant reef building bivalve population in the Wadden Sea is shifting from mussels to the earlier mentioned pacific oyster (Reise, 1998). This may be a result of the changing climate. It is suggested that the pacific oyster (which is best suited to warmer climates) thrives because of increasingly warm summers (Diederich, 2006). Oysters do not quickly capture sediment. Furthermore the total store of sediment in oyster beds is much lower than in mussel beds (some material can be present between the shells of oysters). A species shift from mussels to oysters would thus make a large part of $1.8 \cdot 10^9$ kg of fine sediment available for interaction, and seasonal deposition and erosion will also likely be less. Considering the net deposition rate of $3.5 \cdot 10^9$ kg yr^{-1}, a species shift from mussels to oysters can have a significant consequence for the net behavior of the system. Because significantly less sediment is stored in mussel beds, export can be assumed to be higher and the net import of the Wadden Sea could well be reduced. A link may thus exist between the seasonal influence of mussel beds and the long term morphological processes in the Wadden Sea.

7.2.4 Implications for use of mussels as bio-tools.

The introduction of this report mentions two distinct ways in which mussel beds can be used to achieve ecological objectives. The first is to locate mussel beds in front of salt marshes in order to protect them. Secondly, mussels could play a role in reducing turbidity in the Wadden Sea, improving light penetration during summer. Turbidity is thought to be an important factor in limiting the survival of the sea grass population in the Wadden Sea (Van Katwijk, 2003). In order to investigate such effects the results of this study should be implemented on Wadden Sea or tidal inlet scale.

7.2.4.1 Implementing mussel beds in estuarine basin scale models

It has been shown in the previous section that mussel beds fix and interact with a significant amount of fine sediment. It is hypothesized that this could affect turbidity levels in the Wadden Sea (De Vries, personal communication). However considering the total amount of suspended sediment of $70 \cdot 10^9$ kg yr^{-1} the amount fixed by mussel beds is not very high. The surface area of mussel beds will have to be increased in order to significantly impact turbidity levels on a Wadden Sea scale.

However if not over the entire Wadden Sea, then perhaps mussel beds can reduce turbidity levels locally. This could be investigated using a tidal inlet scale model. In such tidal basin models, mussel beds become sub grid phenomena, meaning that entire beds may fall into one grid cell. Mussel beds can be simulated by tweaking parameters governing erosion and deposition as has been done in the study presented in this report. These parameter adjustments can be implemented to vary both in space and time, as has been shown by Borsje (2006). A prerequisite for implementation is the existence of a model for mussel settlement and winter loss. Research in this latter area is ongoing and has resulted for example in the work of Brinkman et al. (2002). In order to model these effects a probabilistic approach would have to be taken to account for the shear variability in mussel settlement and subsequent winter erosion.

7.2.4.2 Mussel beds in relation with salt marshes

It has been proposed to construct mussel beds in order to protect salt marshes. It is hypothesized that mussel beds are beneficial to salt marshes because they promote deposition. Salt marshes exist at the interface between land and sea. Flooded only very shortly or occasionally, the salt marsh is a result of slow accretion of fine sediment. This fine sediment comes from the mud flat. During winter erosion of mud flats some of the sediment is transported towards the salt marsh, while most is transported back into the channel (see Oost 1995). Mussels fit in by allowing more sediment to settle on the intertidal flat and thus facilitate the first step towards transportation to the salt marsh.

It has been shown in this report that mussels indeed promote deposition on the mud flat. However it has also been shown that in certain areas a reduction in deposition is caused as a result of increased flow velocities. When planning to construct mussel beds (or other shell fish colonies) on an intertidal flat it is thus important to first analyze dominant current directions. For example in case of the Paulina polder as studied by Paarlberg *et al.* (2005), currents are directed parallel to the coast (and the salt marsh). Positioning a mussel bed simply in front of the salt marsh may actually decrease deposition between the mussel bed and the salt marsh, the direct opposite of the objective.

Positioning regarding deposition may actually be at odds with the other proposed function of a mussel bed: decreasing erosive wave action and thus protecting the salt marsh. One can even wonder whether decreasing waves over the intertidal flat will be beneficial to the salt marsh. The erosive forces of the waves are required to erode the settled material and allowing it to be transported to the salt marsh. Similarly, break waters positioned in front of mangrove forests in South East Asia, actually cause mangrove forest degeneration as the small waves necessary for sediment transport are suppressed (Winterwerp *et al.*, 2005).

8 Conclusion and recommendations

8.1 Conclusion

The goal of this project is formulated as follows: *To model mussel bed-sediment interaction in order to study (1) the net retention and (2) the spatial distribution of fine sediment on a Wadden Sea intertidal flat*. It has been shown in this thesis that modeling the influence of a young mussel bed on fine sediment dynamics is possible. The answers to the research questions constitute the projects conclusions:

1) How do mussel beds influence fine sediment dynamics and which properties of the mussel bed are important in this respect?

Mussel beds influence fine sediment by affecting (1) both large scale hydrodynamics and small scale flow between the mussels and (2) by actively filtering sediment from suspension and (3) depositing this material between the mussels as (pseudo-)faecal pellets. These processes are described by the mussel bed roughness, the bed shear stress, the near bed turbulence between mussels, the mussel filtration rate and finally by the properties of the deposited material. How much sediment can erode from mussel beds is determined by how quickly mussels can and do climb on top of the sediment.

2) How can existing experimental data be used to assess relevant mussel bed characteristics?

Two experimental data sets were analyzed and it has been shown that, at this moment, it is not possible to derive a reliable mussel bed roughness. It has been established that turbulence resulting from roughness and filtering activity, is high compared to flat beds. Turbulence causes the water column to be well mixed above the mussel bed.

3) How can mussel beds be implemented in the Delft3D hydrodynamic and morphological model?

The mussel beds influence on hydrodynamics and fine sediment has been implemented in a depth averaged Delft3D model as follows: The trachytope vegetation roughness functionality has been used to implement the roughness of a mussel bed, as well as the fact that only a fraction of the force exerted by the flow on the mussel bed is available for erosion of sediment from in between the mussels. An extra term modeling biodeposition as a function of filtration rate has been implemented in the Delft3D transport equation. Finally properties of the sediment in between mussels (consisting partly of (pseudo-) faecal pellets) can be implemented by spatially varying critical bed shear stress for erosion and erosion rate. The implementation is suited for modeling mussel bed dynamics in summer. The parameters required for the implementation are to a certain extent uncertain. This makes an extensive sensitivity analysis a necessity in order to investigate the relative importance of different mussel bed characteristics.

4) What is the influence of mussel beds on net fine sediment retention on an intertidal mudflat in the Wadden Sea?

Fine sediment is captured and retained in the mussel bed itself. This process is mainly determined by the filtration rate of mussels and a slow down of the flow

over the rough bed, erosion behavior is less important. A roughly equal amount of sediment as is retained in the mussel bed itself is deposited in the wake of the mussel bed due to reduced flow velocities. The deposition around the bed is determined mainly by the mussel bed roughness, although high filtration rates can reduce the amount deposited in the wake of the mussel bed. The elevation of the mussel bed does not have a significant influence on the model results.

5) What is the influence of mussel beds on the spatial patterns of deposition and erosion on an intertidal mudflat in the Wadden Sea?

Sediment is deposited in the wake of the mussel bed. The location of this wake is dependent on direction of dominant flow and sediment import. In case of a Wadden Sea intertidal flat, sediment is brought in with the incoming tide and the most prominent deposition will develop in the downstream direction from incoming tidal currents. Because of the reduction in flow velocities in the mussel beds wake, higher flow velocities occur on the sides of the mussel bed, decreasing deposition there. This decrease in deposition along the sides of the mussel bed is limited, mainly because flow velocities remain low in comparison with critical values for erosion.

6) How do naturally occurring spatial patterns in mussel beds affect the influences on fine sediment dynamics?

In their first year of existence, mussel beds develop from uniform into patchy structures. Generally it can be concluded that the more open these structures are, the lower deposition is inside the mussel bed and the higher deposition is in the wake of the mussel bed. Different patterns in mussel beds have little effect on the total amount of sediment retained. However it appears that a striped pattern oriented transverse to the flow leads to the lowest deposition.

As has been established in the discussion a new insight in mussel bed influence on fine sediment has been obtained. The mobility of young mussels and their ability to climb on top of the sediment is the key characteristic that allows young mussel beds to quickly capture sediment. This makes them different from mature mussel beds and for example oyster beds.

All in all, modeling biological influences remains a challenge. The behavior of organisms can be very complex and incorporate many variables. In this report a necessary selection of the processes regarding mussel behavior has been made resulting in an implementation of this behavior that is both simple and captures the most important features. One can continue to add processes, while at each step also introducing new uncertainties.

8.2 Recommendations

8.2.1 Recommendations for future experiments

The experimental data sets analyzed in this report did not yield the expected results. The following recommendations are made for future experimental research:

- Mussel bed roughness has been shown to be an important characteristic with regard to the influence of mussel beds on fine sediment. Mussel bed roughness can be derived from flume experiments by either precisely measuring the water surface slope of a flow over mussels, or measuring the flow profile in flow over a mussel bed in conditions where logarithmic flow profiles occur.

- Field measurements seem to be most important. Young mussel beds (as opposed to mature mussel beds) have the largest influence on fine sediment dynamics and should be the focus of a measurement campaign. The amount of sediment in the mussel mud tracked during the early stages of a mussel bed development would provide a wealth of information for comparison with model simulations. Experimental techniques have been presented by Flemming and Delafontaine (1994).
- Mussel upward movement (climb rate) has been shown to be an important mussel characteristic with regard to the amount of sediment that is retained by a mussel bed. Simple experiments focusing on the time it takes for mussels of different ages to climb out of a certain layer of sediment could provide invaluable data.

8.2.2 Recommendations regarding the mussel bed model implementation

A number of possible additions for the mussel bed implementation have been proposed in the discussion of this report. Two of these deserve priority; together they will make it possible to simulate mussel beds under a variety of conditions, including winter:

- Simulating the mussel layer as a limit to erosion is important. Mussel beds should not experience erosion if all material between mussels has already eroded. The implementation of a mussel layer can be achieved by dynamically varying the erosion rate (M), i.e. high M after a period of deposition and a low M after a period of erosion. Such an algorithm would have to be written into the Delft3D code. The precise behavior of the system could be informed by experimental results regarding mussel climb rate as proposed in the previous subsection.
- The effect of waves has been shown to be very relevant with regard to erosion from in between mussels. Waves are also important as a cause for erosion of the bare intertidal flat surrounding a mussel bed. The dissipation of wave energy over mussel bed can be predicted using an empirical equation based on bed roughness (Madsen *et al.*, 1988) The erosion of sediment in between mussels as a result of waves is still highly uncertain, a good start would be to apply standard erosion equations and settings.

8.2.3 Recommendations regarding model application

The above model implementation can be used to predict the influence of mussels in actual situations. The following applications are recommended.

- It will be very interesting to see how a mussel bed will influence the sedimentation in a salt marsh. Such an analysis should constitute a year round analysis using both waves and currents. If this type of application is performed nested in a larger model, different locations for the mussel bed can be used to asses the influence of varying conditions on the mussel beds interaction with fine sediment dynamics.
- At this moment the model implementation as proposed in this report cannot be directly implemented in a large estuarine scale model such as a Wadden Sea model. In such a model the mussel bed should be parameterized by quick deposition and resistance against erosion in the first few months of existence and by extensive erosion in subsequent winters should the mussel bed be

eroded. Mussel bed settlement and winter erosion may be modeled as a statistic process as no exact predictive tools exist.

References

Andersen, T. J. (2001). "Seasonal Variation in Erodibility of Two Temperate, Microtidal Mudflats". *Estuarine, Coastal and Shelf Science* 53: 1-12.

Baptist, M. J. (2005). *Modelling Floodplain Biogeomorphology*. DUP Science, Delft.

Baptist, M. J., Babobic, V., Rodriguez Uthurburu, J., Keijzer, M., Uittenbogaard, R., Mynett, A., Verwey, A. (2006). "On inducing equations for vegetation resistance". *Journal of Hydraulic Research* 45: 1-16.

Borsje, B. W. (2006). "Biological influence on sediment transport and bed composition for the Western Wadden Sea". Master's thesis, University of Twente.

Brinkman, A. G., T. P. Bult, N. M. J. A. Dankers, A. Meijboom, D. Os, M. R. Stralen and J. Vlas (2003). "Mosselbanken: kenmerken, oppervlaktebepaling en beoordeling van stabiliteit". Alterra

Brinkman, A. G., Dankers, N. M. J. A., Van Stralen, M. R. (2002). "An analysis of mussel bed habitats in the Dutch Wadden Sea". *Helgoland Marine Research* 56: 59-75.

Dame, R. F., Dankers, N. M. J. A. (1988). "Uptake and release of materials by a Wadden sea mussel bed". *Journal of Experimental Marine Biology and Ecology* 118: 207-216.

Dankers, N. M. J. A., Dijkman, E. M., De Jong, M. L., De Kort, G., Meijboom, A. (2004a). "De verspreiding en uitbreiding van de Japanse Oester in de Nederlandse Waddenzee". Alterra, Report No. 909. Wageningen.

Dankers, N. M. J. A., Koelemaij, K., Zegers, J. (1989). *De rol van de mossel en de mosselcultuur in het ecosysteem van de Waddenzee*. Rijksinstituut voor Natuurbeheer,

Dankers, N. M. J. A., A. Meijboom, M. L. Jong, E. M. Dijkman, J. S. M. Cremer and S. Sluis (2004b). "Het ontstaan en verdwijnen van droogvallende mosselbanken in de Nederlandse Waddenzee". Alterra

Delvigne, G. A. L. (1984). "Laboratory facility for the simulation of the natural and chemical dispersion of oil". WL|Delft Hydraulics, Report No. M 1933.

Diederich, S. (2006). "High survival and growth rates of introduced Pacific oysters may cause restrictions on habitat use by native mussels in the Wadden Sea". *Journal of Experimental Marine Biology and Ecology* 328: 211-227.

Eisma, D. (1979). "Supply and deposition of suspended matter in the North Sea". *Int.Assoc.Sedimentol.Int.Meet.Holoscene Sedimentation North Sea Basin.* (Special publication).

Fey, F., Dankers, N. M. J. A., Meijboom, A., Van Leeuwen, P. W., Verdaat, H., De Jong, M. L., Dijkman, E. M., Cremer, J. S. M. (2006). "Ontwikkeling van mosselbanken in de Nederlandse Waddenzee situatie 2006". Imares, internal report, No. 07.006.

Flemming, B., Delafontaine, M. (1994). "Biodeposition in a juvenile mussel bed of the east Frisian Wadden Sea (Southern North Sea)". *Aquatic Ecology* 28: 289-297.

Frechette, M., Butman, C. A., Geyer, W. R. (1989). "The Importance of Boundary-Layer Flows in Supplying Phytoplankton to the Benthic Suspension Feeder, Mytilus edulis L". *Limnology and Oceanography* 34: 19-36.

Giles, H. (2006). "Dispersal and remineralisation of biodeposits: Ecosystem impacts of mussel aquaculture".The University of Waikato.

Hofland, B. (2005). "Rock & Roll: Turbulence-induced Damage to Granular Bed Protections". PhD thesis, Department of Civil Engineering and Geosciences, Delft University of Technology.

Hofland, B., Battjes, J. A. (2006). "Probability Density Function of Instantaneous Drag Forces and Shear Stresses on a Bed". *Journal of Hydraulic Research* 132: 1169.

Hunt, H. L., Scheibling, R. E. (2002). "Movement and wave dislodgment of mussels on a wave-exposed rocky shore". *The Veliger* 45: 273-277.

Janssen-Stelder, B. (2000). "The effect of different hydrodynamic conditions on the morphodynamics of a tidal mudflat in the Dutch Wadden Sea". *Continental Shelf Research* 20: 1461-1478.

Johannesson, B., M. Larsvik, L. Loo and H. Samuelsson (2000). "Blue mussel". *Aquascope [on line]* . (Accessed on 30-05-07). Tjärnö Marine Biological Laboratory, Strömstad, Sweden. <www.vattenkikaren.gu.se/fakta/arter/mollusca/bivalvia/mytiedul/mytiede.html>.

Jones, C. G., Lawton, J. H., Shachak, M. (1994). "Organisms as Ecosystem Engineers". *Oikos* 69: 373-386.

Jörgensen, C. B. (1996). "Bivalve filter feeding revisited". *Marine Ecology Progress Series* 142: 287-302.

Jumars, P. A., Nowell, A. R. M. (1984). "Effects of benthos on sediment transport: difficulties with functional grouping". *Continental Shelf Research* 3: 115-130.

Kautsky, N., Evans, S. (1987). "Role of biodeposition by Mytilus edulis in the circulation of matter and nutrients in a Baltic coastal ecosystem". *Mar.Ecol.Prog.Ser* 38: 201-212.

Klausmeier, C. A., Litchman, E. (2001). "Algal Games: The Vertical Distribution of Phytoplankton in Poorly Mixed Water Columns". *Limnology and Oceanography* 46: 1998-2007.

Madsen, O. S., Poon, Y. K., Graber, H. C. (1988). "Spectral wave attenuation by bottom friction: Theory". *Proceedings of the 21st International Conference on Coastal Engineering* 492.

McGrorty, S., Goss-Custard, J. D., Clarke, R. T. (1993). "Mussel *Mytilus edulis (Mytilacea)* dynamics in relation to environmental gradients and intraspecific interactions". *Aquatic Ecology* 27: 163-171.

Nepf, H. M., Vivoni, E. R. (2000). "Flow structure in depth-limited, vegetated flow". *Journal of Geophysical Research* 105: 28527-28546.

Newell, R. I. E. (1989). "Species profiles: life histories and environmental requirements of coastal fishes and invertebrates (north and Mid-Atlantic)--blue mussel". *United States Fish and Wildlife Service Biological Report* 82.

Okamura, B. (1986). "Group living and the effects of spatial position in aggregations of Mytilus edulis". *Oecologia* 69: 341-347.

Oost, A. P. (1995). *Dynamics and sedimentary development of the Dutch Wadden Sea, with emphasis on the Frisian inlet: a study of the barrier islands, ebb-tidal deltas, inlets, and drainage basins*. Faculteit Aardwetenschappen, Universiteit Utrecht,

Partheniades, E. (1965). "Erosion and deposition of cohesive soils". *Journal of the Hydraulics Division, ASCE* 91: 105-139.

Postma, H. (1981). "Exchange of materials between the North Sea and the Wadden Sea". *Marine Geology* 40: 199-213.

Prins, T. C., Smaal, A. C., Pouwer, A. J., Dankers, N. M. J. A. (1996). "Filtration and resuspension of particulate matter and phytoplankton on an intertidal mussel bed in the Oosterschelde estuary (SW Netherlands)". *Marine Ecology Progress Series* 142: 121.

Reise, K. (1998). "Pacific Oysters Invade Mussel Beds in the European Wadden Sea". *Senckenbergiana maritima* 28: 167-175.

Rhoads, D. C. (1974). "Organism-sediment relations on the muddy sea floor". *Oceanographic Marine Biology Annual Review* 12: 263-300.

Ridderinkhof, H., Van der Ham, R., Van der Lee, W. (2000). "Temporal variations in concentration and transport of suspended sediments in a channelûflat system in the Ems-Dollard estuary". *Continental Shelf Research* 20: 1479-1493.

RIKZ (1998). "Sedimentatlas Waddenzee". Rijksinstituut voor kust en zee, CD-Rom, Haren.

Risk, M. J., Moffat, J. S. (1977). "Sedimentological significance of fecal pellets of Macoma balthica in the Minas Basin, Bay of Fundy". *Jounal of Sedimentary Research* 47: 1425-1436.

Smaal, A. C., Stralen, M., Craeymeersch, J. A. (2005). "Does the Introduction of the Pacific Oyster Crassostrea gigas Lead to Species Shifts in the Wadden Sea?". In R. F. Dame and S. Olenin (eds). *The Comparative Roles of Suspension-Feeders in Ecosystems.* pp. 277-289. Kluwer Academic Publishers, Dordrecht.

Steenbergen, J., J. Baars, M. R. Van Stralen and J. A. Craeymeersch (2006). "Winter survival of mussel beds in the intertidal part of the Dutch Wadden Sea". Ed. K.Laursen. *Monitoring and Assessment in the Wadden Sea, Proceedings from the 11th Scientific Wadden Sea Symposium Esbjerg, Denmark 4-8 april 2005.NERI Technical Report,* 573: 107-111.

Ten Brinke, W. B. M., Augustinus, P. G. E. F., Berger, G. W. (1995). "Fine-grained sediment deposition on mussel beds in the oosterschelde (The Netherlands), determined from echosoundings, radio-isotopes and biodeposition field experiments". *Estuarine, Coastal and Shelf Science* 40: 195-217.

Ten Haaf, M., Karels, P. (2005). "The relationship between the stability of a mussel bed in the Dutch Wadden Sea and its morphological, sedimentological and biological characteristics". Student report, Utrecht University.

Tsuchiya, M. (1980). "Biodeposit production by the mussel Mytilus edulis L. on rocky shores". *Journal of Experimental Marine Biology and Ecology* 47: 203-222.

Van de Koppel, J., Rietkerk, M., Herman, P. M. J. (2005). "Scale-dependent feedback and regular spatial patterns in young mussel beds". *The American naturalist* 165: E66-E77.

Van Duren, L. A., Herman, P. M. J., Sandee, A. J. J., Heip, C. H. R. (2006). "Effects of mussel filtering activity on boundary layer structure". *Journal of Sea Research*.

Van Eijsbergen, E., Veeken, E. M. W. (2005). "The influence of hydrodynamics on the stability of mussel beds". Student report, Utrecht University.

Van Katwijk, M. M. (2003). "Reintroduction of eelgrass (*Zostera marine L.*) in the Dutch Wadden Sea: a research overview and management vision". Eds W. J. Wolff, K. Essink, A. Kellermann, and M. A. Van Leeuwe. *Proceedings of the 10th International Scientific Wadden Sea Symposium*: 173-197. University of Groningen, Groningen.

Van Ledden, M. (2003). *Sand-mud Segregation in Estuaries and Tidal Basins*. Dept. of Civil Engineering and Geosciences, Delft University of Technology, Delft.

Van Loon (2005). "Modelling the long-term fine sediment balance in the Western Wadden Sea". Master's Thesis, University of Wageningen.

Vermeulen, T. (2003). "Sensitivity Analysis of Fine Sediment Transport in the Humber Estuary". Master's thesis, TU Delft.

Widdows, J., Fieth, P., Worrall, C. M. (1979). "Relationships between seston, available food and feeding activity in the common mussel Mytilus edulis". *Marine Biology* 50: 195-207.

Widdows, J., Lucas, J. S., Brinsley, M. D., Salkeld, P. N., Staff, F. J. (2002). "Investigation of the effects of current velocity on mussel feeding and mussel bed stability using an annular flume". *Helgoland Marine Research* 56: 3-12.

Winterwerp, J. C. (2002). "On the flocculation and settling velocity of estuarine mud". *Continental Shelf Research* 22: 1339-1360.

Winterwerp, J. C., Borst, W. G., De Vries, M. B. (2005). "Pilot Study on the Erosion and Rehabilitation of a Mangrove Mud Coast". *Journal of Coastal Research* 21: 223-230.

Winterwerp, J. C., Van Kesteren, W. G. M. (2004). *Introduction to the physics of cohesive sediment in the marine environment*. Elsevier, Amsterdam.

Witman, J. D., Suchanek, T. H. (1984). "Mussels in flow: drag and dislodgement by epizoans". *Mar.Ecol.Prog.Ser* 16: 259-268.

WL|Delft Hydraulics (1990). "Electromagnetic velocity and direction meter". Report No. N 0056.

WL|Delft Hydraulics (2006). "User Manual Delft3D-FLOW". WL|Delft Hydraulics, Delft.

A Investigating erosion in a mussel bed with DPM vegetation model

This appendix deals with the erosion from mussel beds. Mussel beds consist of more than one layer of mussels directly on the original bed surface. The deposition – in part biodeposition – settles between the mussels, which in turn can climb on top of that sediment. This forms a layer of very fine (because it consists mainly of formerly suspended material), with a high organic content, see Figure 37. It is concluded in this appendix that it is very unlikely that sediment is eroded from this layer. This does not include erosion after mussels themselves have been eroded, or the erosion of sediment that has only recently been deposited and is located between the mussels. It is shown for the latter that erosion is a complex phenomenon.

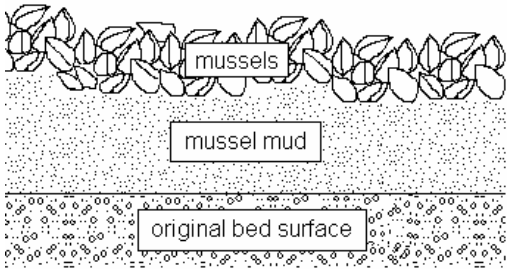

Figure 37: Schematic of a mussel bed.

It is expected that the erosion from mussel mud will be negligible (Van Duren, personal communication). Considering the thickness of a mussel bed, stacked multiple mussels thick and intertwined with byssal threads, it is difficult to imagine how any particle can be eroded successfully. Even then, it would likely be captured by the byssal threads or shells. This hypothesis is further supported by the results from the erosion experiments by De Vries presented in Appendix B.5: no matter how high flow velocities or waves were, a certain amount of pseudo-faecal pellet mimics always remained between the mussels.

Erosion from in between mussels is a more complex process; this was also studied in the experiments by De Vries but with less clear results. Widdows *et al.* (2002) studied a single layer of mussels. Depending on the density of the mussels in the single layer, erosion was both increased (25% and 50% coverage of mussels) and decreased (100% coverage) as compared to an empty bed. Apparently in between mussels both turbulent scouring (in the low coverage cases) and reduction of flow velocities (at 100% coverage) play a role. Similar processes will also be relevant in case of a multi layer mussel bed. Coverage is then always 100% and variability exists instead in where the sediment is located between the mussels. For example after high sedimentation, the mussels can be covered by sediments. However after high flow velocities and corresponding resuspension, the remaining sediment will be located deep in between the mussels.

The hypothesis that no sediment can be eroded from the mussel bed will be researched in this appendix. Also the potential of erosion in between the mussel will be researched. It is assumed that both can be modeled by changing the height of a mussel bed. If the mussel bed is very high it is as if the sediment is located deep between the mussels,

simulating mussel mud. If the mussel layer is thinner, it is as if the sediment is located in between the mussels.

A.1 Directional Point Model

The Directional Point Model (DPM) for simulating flow over and through vegetation will be used to model a mussel bed. The DPM model is in essence a model for flow through a porous medium. The properties of this medium (porosity, cavity size) are derived from an input of vertical cylinders. The model is designed to model the flow over relatively low density cylinders, representing for example grasses or trees. Here mussels are simulated and idealized in the following manner:

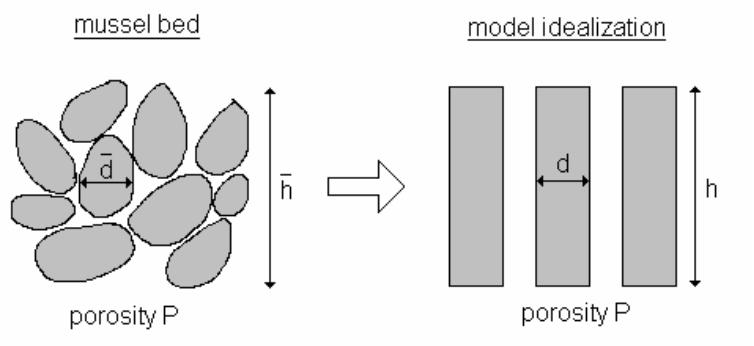

Figure 38: Cross section of schematized mussel bed and of the model implementation.

The above idealization is deemed acceptable because the layered DPM uses the horizontal dimension of the cavity space to derive turbulence dissipation. Perhaps this raises the question how a mussel bed of stacked individual shells can be simulated as a grid of vertical cylinders. Reference is made to the explanation of the DPM model as given in the literature study of this project. The model does not model individual cylinders; instead it uses derived variables for each vertical layer. In such a vertical layer, only the density and diameter of the cylinders count. Whether or not these cylinders are aligned over the different layer does not matter for the model in principle[15].

No empirical data is available to effectively validate the model results. Also the model results are rather uncertain as is the nature of many turbulence calculations. The modeling results generated below should thus be seen as a rough approximation of the actual system.

A.2 Input

For now, the mussel bed used in the experiments by Van Duren will be used in the model. For this bed many of the primary properties are known. The shells in this bed are 3.8 cm on average, meaning that they are on the large side to represent a young mussel bed.

Based on Winter (1973) and observations during the De Vries experiments, it is assumed that the diameter of a mussel is related to its average width by a factor 0.5. If

[15] *It should be noted that some assumptions underlying the model, mainly that of the behavior of large eddies entering into the cylinder field, are based on the assumption that roughness elements are cylinders. It comes down to the fact that turbulence dissipation (dependent on the available space) is limited by horizontal pore dimensions and not the vertical. This assumption still holds for mussels. The cavities between mussels are roughly as long/wide as they are high.*

it is assumed further that the volume of a mussel can be described by a cylinder. Using these assumptions the volume (V) of a single mussel can be calculated as: $V = \pi r^2 l$, where r is the radius of the cylinder and l is the length. Given that l = 3.8 cm, then r = 0.95 cm and V = 11 cm^3 = 1.1 $\cdot 10^{-5}$ m^3. The total volume mussels per square meter are then given by: V · density = 1.1 $\cdot 10^{-5}$ · 1800 = 0.019 m^3 m^{-2}. Taking into account average mussel bed height of 0.06 m, the solidity is 32%, or the porosity is 68%. If these variables are used to generate a grid of cylinders, Figure 39 is found. It is this idealized mussel bed that is used as input for the DPM model

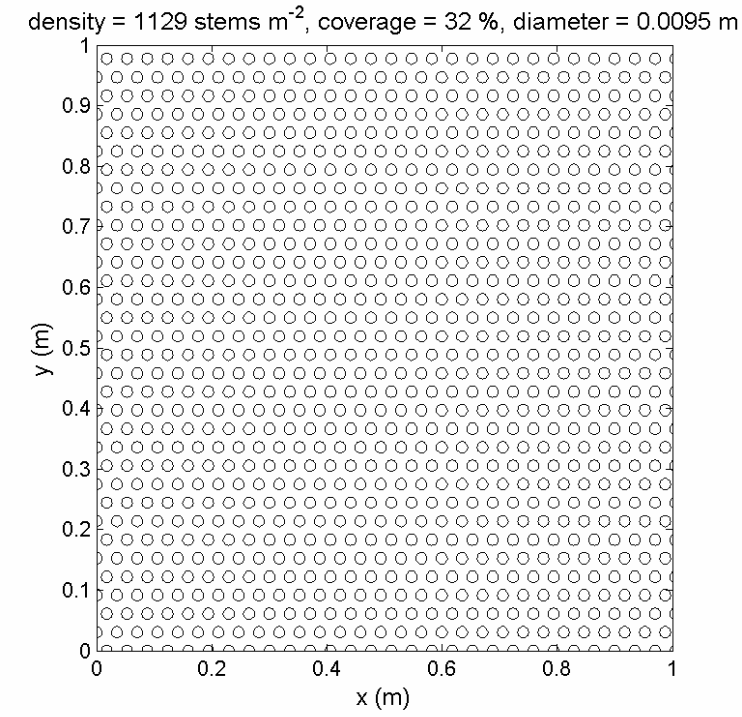

Figure 39: Top view of cylinder grid simulating the mussel bed as used in the experiments by Van Duren.

A last input parameter that is required for the DPM model is the drag coefficient of each cylinder. Although some work has been done to establish an empirical estimation of this value (Witman and Suchanek (1984); De Vries (unpublished results)), the attempts have proved either incomplete or unsuccessful. Here it is assumed – and this seems reasonable - that mussels have the same drag coefficient as smooth cylinders. This gives a drag coefficient of 1.

The flow conditions are derived using the analysis of mussel habitat as presented by Brinkman *et al.* (2002). The maximum flow velocity in the environment where mussels are found is on average 0.5 m s^{-1}. Normally maximum velocity will occur between flood tide and the ebb tide. However, considering the 40% emersion time of mussel beds and the tidal amplitude of roughly 1.5 m, a 1 m water depth seems reasonable. The roughness of the bed between the mussels needs to be specified for the model. The bed roughness is assumed to be similar to that of a sandy bed, simulating the larger particles of (pseudo-)faecal pellets: k_s = 1 mm. Actually because of the high roughness of mussels, the bed roughness is not an important factor.

Table 8.1: DPM input parameters

cylinder diameter	*0.019*	*m*
cylinder density	*1129*	*stems m^{-2}*
drag coefficient (C_D)	*1*	*-*
cylinder height	*0.06*	*m*
*water depth (*h*)*	*1*	*m*
flow velocity (U)	*0.6*	*m s^{-1}*
bed roughness height (k_s)	*1*	*mm*

A.3 Results

On flat beds with uniform flow it is the bed shear stress that can be related to erosion directly. This bed shear stress is related to the square of the velocity close to the bed and the bed roughness:

$$\tau_{bed} = \frac{\rho g u_b^{\,2}}{C_{3D}^{\,2}} \qquad (15)$$

Please note that the bed roughness C_{3D}, is not equal to the Chézy roughness coefficient[16], but is related to it via the White Colebrook formulation and:

$$C_{3D} = \frac{\sqrt{g}}{\kappa} \ln\left(1 + \frac{\Delta z_b}{2 z_0}\right) \qquad (16)$$

Where:

κ = Von Kármán constant (= 0.41) (-)

Δz_b = bed layer thickness (m)

In order to avoid becoming to specific regarding the value of the latter, here the shear velocity in the layer closest to the bed will be investigated. The results are displayed in Figure 40.

[16] *Equation (15) can be used in depth averaged cases. Instead of u_b the depth averaged U can be used. A logarithmic profile is then assumed and the normal Chézy can be used. However when near bed velocities are used a smaller roughness value is required.*

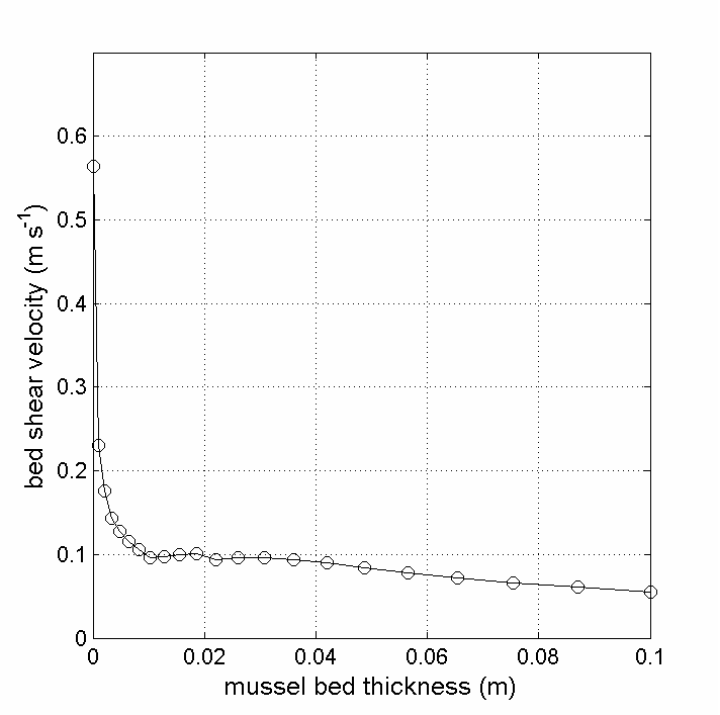

Figure 40: Velocities in vertical layer closest to the bed.

It can be concluded from Figure 40 that the bed shear stress (that is related to the square of the bed shear velocity) will diminish for any height of a mussel bed. Even at a mussel bed height of only a few millimeters the velocity over the bed is highly reduced. At ten centimeters the bed shear velocity is reduced by a factor 12. It seems save to assume that at these reductions no erosion will take place[17].

Considering the quick decrease in velocities it is safe to assume that no sediment can erode from a mussel bed, neither from the mussel mud nor from the sediment lying in between the mussels. This result is in clear contradiction with the results of Widdows *et al.* (2002), who observed that a few mussels would actually destabilize the bed through scour. And indeed scour is something that cannot be describe by time averaged bed shear stress.

It is a common misunderstanding that erosion is only dependent on the time averaged bed shear stress as forced by the shear velocity presented above. In reality the bed shear stress is not constant when turbulence is involved; turbulence can be explained simply as the variation in the instantaneous velocities. Therefore the instantaneous bed shear stress will vary in the presence of turbulence. This can well mean that for a case with a time averaged bed shear stress below critical, erosion still takes place. Consider in this respect Figure 41, two cases in which the first would normally not be expected to lead to erosion. Turbulent processes cause the probability of deviations from the mean to increase and thus to lead to erosion. This is – highly simplified – what happens when scour occurs.

[17] Perhaps it would be more convincing to give a presentation of the produced bed shear stress compared with the critical bed shear stress. For this case such an approach is riddled with uncertainty: the critical bed shear stress is heavily influenced by sticky but loose biodeposition and the roughness of the bed between the mussels is unknown. Because of those factors, calculations using equations (15) and (16) yield highly varying results.

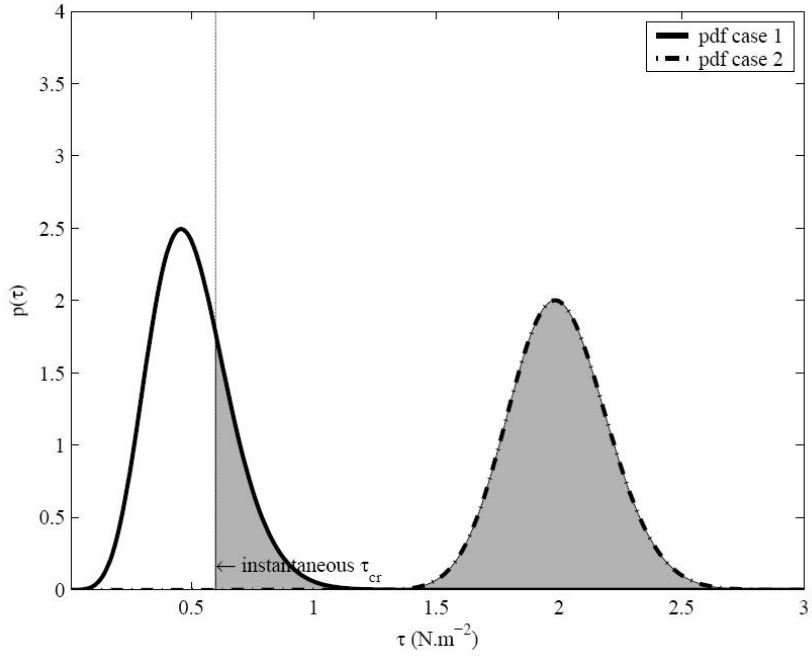

Figure 41: Probability densities for the bed shear stress of two imaginary cases, from Baptist (2005, p. 124).

Calculating the actual pick-up of sediment taking into account this process is very complex, it is described by Hofland and Battjes (2006). It will not be attempted here. However to give an idea the near bed quantity of turbulence (in the same bed layer as the velocities presented above) are given in Figure 42.

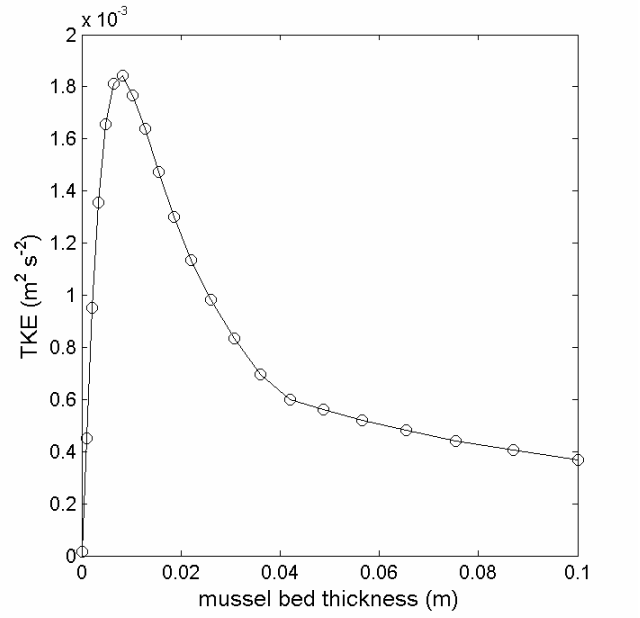

Figure 42: Turbulence in near bed layer

It is clear from this graph that there is indeed high turbulence present, especially at the lower elevations of the mussel bed. This is why, as Widdows *et al*. (2002) describe, erosion occurs from single mussel layers. It is thus very well possible that erosion of

material from in between mussels in increased as related to that same sediment from a flat bed. When the mussel bed height increases, the turbulent eddies have more difficultly penetrating to the bed. In effect it is expected that these lower turbulent levels, combined with the low shear velocities will make erosion impossible from the mussel mud.

A.4 Conclusion

The hypothesis that erosion will not play a role for the mussel bed is confirmed. Both factors causing erosion (shear velocity) and (turbulence) are decreased al positions deep in the mussel layer. Turbulence is enhanced if the mussel bed height is low – simulating that the sediment is close to the mussel tops – in such conditions erosion is possible and likely even higher than from a flat bed. If sediment is eroded from positions close to the tops of the mussels, the remaining sediment located deeper in between the mussels will be increasingly difficult to erode. Depending on how high the sediment is stacked between the mussels, erosion of that sediment can thus either increase or decrease.

B Analysis of results from laboratory experiments of flow over mussel beds

The blue mussel is sometimes called the 'white rat' of marine invertebrate zoology, because of relative ease with which they can be collected and kept alive in the laboratory (Newell, 1989). This has provided a relative wealth of experiments, some of which have been mentioned in the previous chapter. Most of these laboratory experiments focus on individual or small patches of mussels. Here the data from two experiments - aimed specifically at investigating the influence of a bed of thousands of mussels on flow and erosion processes - will be analyzed. The goal is to find mussel bed roughness from flow profiles and turbulence levels from TKE profiles. One of the experiments included erosion experiments which will be discussed briefly. The appendix ends with a conclusion, listing those results that can be used in the model implementation.

B.1 Experimental set-up

Results from two distinct experimental series are used. The first are those conducted by Mindert de Vries in 2005 in the 'Oil flume' at WL|Delft Hydraulics. The aim of this experiment was to investigate the erosion of pseudo-faecal pellets from a mussel bed under influence of currents and waves. The second experimental series has been conducted in the Racetrack flume facility at NIOO in 1998, supervised by Luca van Duren. This experiment investigated the boundary layer influence of mussels (Results from experiments using the same mussel bed and facility but measured three months later have been mentioned in section 2.3.1.2). In this section the experimental set-up of these experiments will be explained. The two series will from here on simply be referred to as the experiments by respectively De Vries and Van Duren.

B.1.1 Experimental set-up De Vries

The experiments by De Vries were conducted in the 'Oil flume' flume facility at WL|Delft Hydraulics. An overview of the experimental facility is given in Figure 43. It is in total 15 m long and 50 cm in width. For a thorough description of this facility reference is made to Delvigne (1984). In order to place mussel beds level with the rest of the flume floor, a platform was constructed along the flume of 15 cm high.

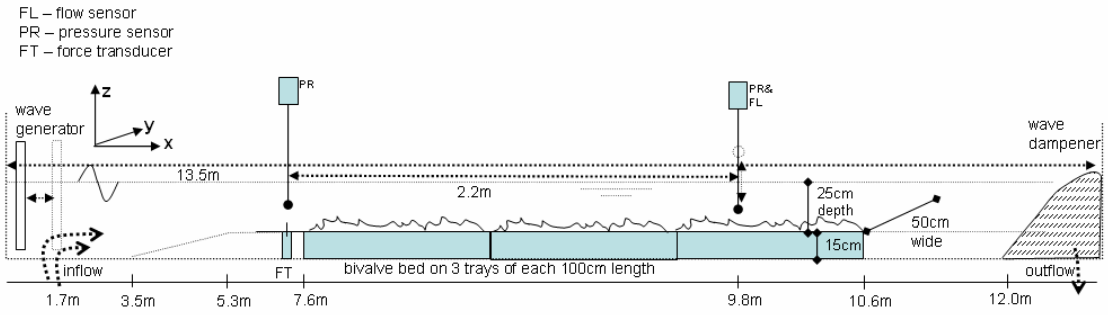

Figure 43: 'Oil flume' facility set-up as used in the experiments by De Vries. The flow sensor could be moved along the bed (image by Mindert de Vries).

The mussel beds were positioned near the back of the flume. Living and filtering mussels were left to attach to themselves and to three trays for 24 hours. During the experiments the trays of mussels were interchanged, to account for artifacts of specific mussel configurations. Mussels were alive for most of the experiments, kept that way be adding algae to the salt water. The mussel bed density was 2400 individuals m^{-2}, with an average height of 6.0 cm and a standard deviation of 2.0 cm. Actual mussel lengths were on average 6.0 cm.

Velocity measurements were taken under a variety of conditions. Conditions included both waves (wave heights 1 to 7 cm at the front of the flume) and currents (5 to 25 cm/s at the front of the flume), with waves and currents combined or separately. Measurements were done at three water depths: 12, 18 and 25 cm. Next to the hydrodynamic influence on the flow, the effect of the mussel bed on transport was investigated using couscous as a mimic for mussel pseudo-faecal pellets. These mimics were present for all flow experiments, see Figure 44. The results from these last experiments are considered briefly in section B.5. Current profiles with two velocity components (*u* and *w*, respectively in x and z direction as defined in Figure 43) were measured using a P-EMS electro magnetic flow meter at 10 Hz. For a description of this instrument, see WL|Delft Hydraulics (1990). The instrument has a probing volume of a few cubic centimeters, only the spatially averaged velocities within this volume are measured.

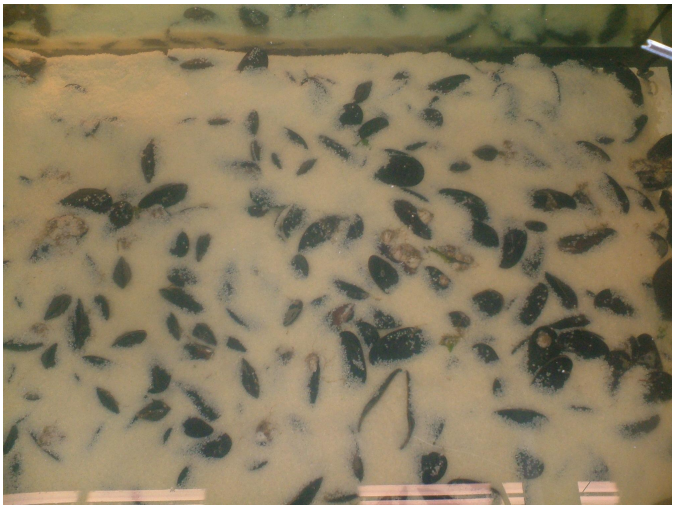

Figure 44: Couscous sediment mimics on top of mussels in test section.

B.1.2 Experimental set-up van Duren

The experiments by Van Duren were conducted in the NIOO flume. This flume is a ‘racetrack’ flume, where the flow is generated using a conveyer belt system. The test section is located on the straight at the other side. Two flow straighteners and channels in the beds aim to prevent large scale spiraling flow. A carriage is present which can be used to automatically position instruments in three dimensions along the working section of the flume. A schematic of the NIOO flume is given in Figure 45. For a more detailed description of the experiment reference is made to Van Duren *et al.* (2006).

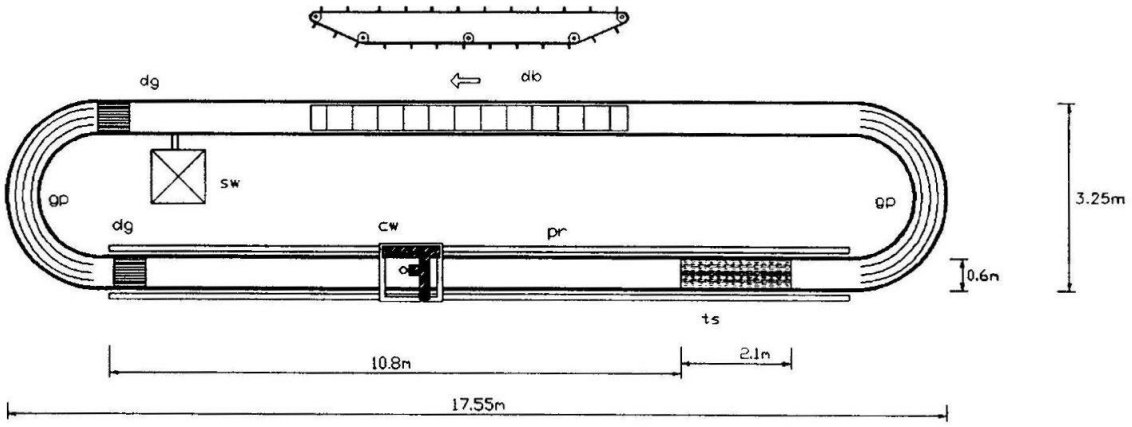

Figure 45: Top view schematic of the NIOO 'racetrack' flume. Depicted are the conveyer drive belt (db) system ate the top, the de four guided channels (gc) in the bends, the flow straighteners (fs), the measurement carriage (mc) and the test section (ts). (Source: NIOO, www.nioo.knaw.nl).

A mussel bed from an Eastern Scheldt culture bed was placed into the flume. It covered the test section and 1 m upstream from it, making a mussel bed of 3.3 m long. Mussels were kept alive by adding algae to the water. After one year of measurements roughly half of the mussels had died, however since the data set presented here was obtained at the beginning of that year it is expected that the majority of the animals was alive. The height of the mussel bed was on average 6.1 cm, with the actual height ranging from 4.9 to 8.6 cm. The mussel density was around 1800 ind m^{-2}, with average mussel length 38 cm.

For the experiments several flow rates have been investigated over the year the mussel bed was present in the flume. The data set used here contains measurements of flows with free stream velocities[18] of 4.7 cm/s, 27.5 cm/s and 39.0 cm/s. Because of the space occupied by the mussel bed, the free stream velocities in the test section were larger, respectively: 5.8 cm/s, 35.0 cm/s and 49.0 cm/s The first and second of these conditions were also used in experiments conducted at a later time and presented as the low and high velocities in Van Duren *et al.* (2006). At all velocities a water depth of 40 cm was used.

Velocity measurements were taken using an Acoustic Doppler Velocity meter (ADV), which measured in three directions, (u, v and w). The measuring frequency was 25 Hz, with a measurement volume of around 0.25 cm^3. Because ADV measurements depend on the scattering of high frequency sound by fine particles in the flow, the flume is seeded before each experiment with very fine deep-sea clay. These particles stay in suspension even at low velocities, but can be filtered out by mussel feeding activity. ADV measurements were taken at nine horizontal positions along the bed and at 33 depths at each location.

B.2 Flow over the back of the mussel bed is quasi-uniform

The data from the experiment by Van Duren allows the testing of an assumption required to hold for most of the data analysis in this appendix: the assumption of uniform flow. Of course the flow is not strictly uniform as there is a small surface slope

[18] *The free stream velocity is the velocity outside the boundary layer. Here the maximum measured velocities are used.*

to drive the current. The flow can thus only be ‘quasi-uniform’. Only if this assumption holds can bed properties be derived from the flow. The assertion can be tested by investigating the development of flow velocities along the flume. The horizontal velocities for the three measurement conditions have been plotted against the position along the flume in Figure 46.

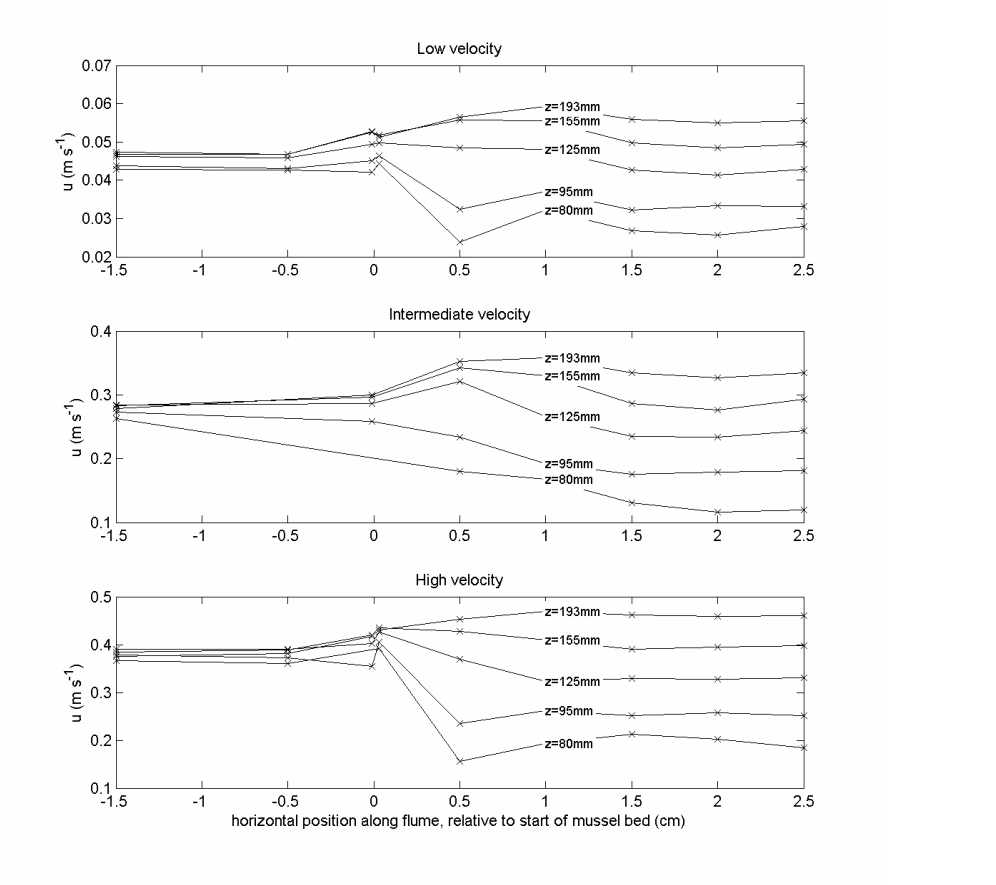

Figure 46: Development of horizontal velocities along the flume for the three different conditions. Velocities displayed for a selection of measuring heights relative to the floor of the flume (as opposed to relative to the top of the mussels).

Although some variation can be seen in the velocities at positions at the end of the flume, over all it can be concluded that for the positions at 150, 200 and 250 cm from the leading edge of the mussel bed, the profile remains unchanged. This confirms the assumption that the flow fully develops over the mussel bed and can thus be called quasi-uniform.

This confirmation allows two things: The first is that the profiles derived from data from the experiment by De Vries under similar conditions are also derived from a part of the flume that shows a fully developed flow. Secondly the profiles from the three positions of the data set by Van Duren can be averaged to find a smoother - more representative profile.

B.3 Horizontal velocity

B.3.1 Experimental results

Horizontal velocities have been measured in the experiments by both De Vries and Van Duren. The former has measured a large number of different discharges through the flume, with measurements at only few heights above the bed and only one position along the bed. Van Duren has measured only three different discharges, but for a large number of positions along the bed and for a large number of heights above the bed.

B.3.1.1 Velocity profiles from De Vries experiment

The flow profiles in the experiments by de Vries are displayed in Figure 47. Velocity profiles were measured at one position along the bed.

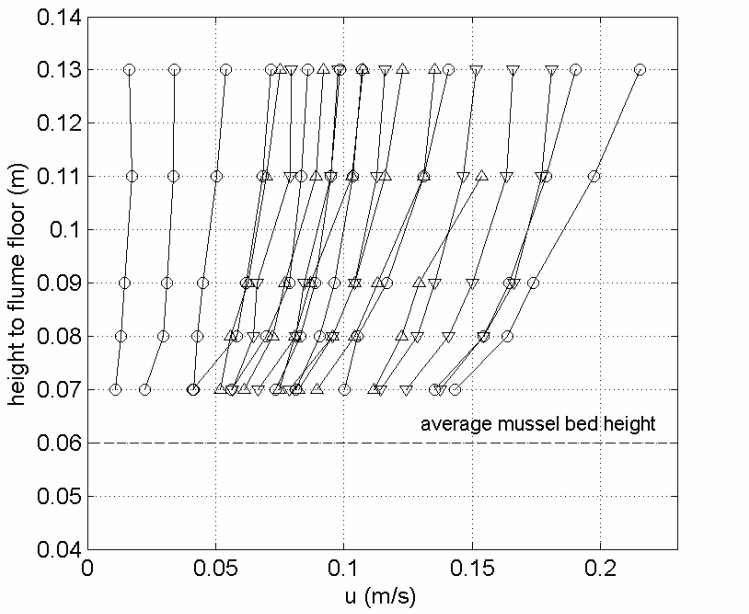

Figure 47: Horizontal velocity profiles from De Vries experiment. Measurements taken 2.2 m downstream from the mussel bed leading edge. Experiments over tray 1 are marked by a circle, over tray 2 by a triangle down and over tray 3 by a triangle up.

The profiles show more or less similar shapes, although the different discharges make comparison difficult. The measurements over the three different trays – and thus over slightly different mussel beds – show no apparent consistent deviations. It should be noted here that in fact many of the above profiles were measured at the same amount of revolutions per minute of the current generator. However due to unknown causes the rpm's do not match up with the measured velocities.

B.3.1.2 Velocity profiles from Van Duren experiment

Velocities from three measuring positions are averaged to give a smoother and more reliable profile. The results from this averaging procedure are given in Figure 48.

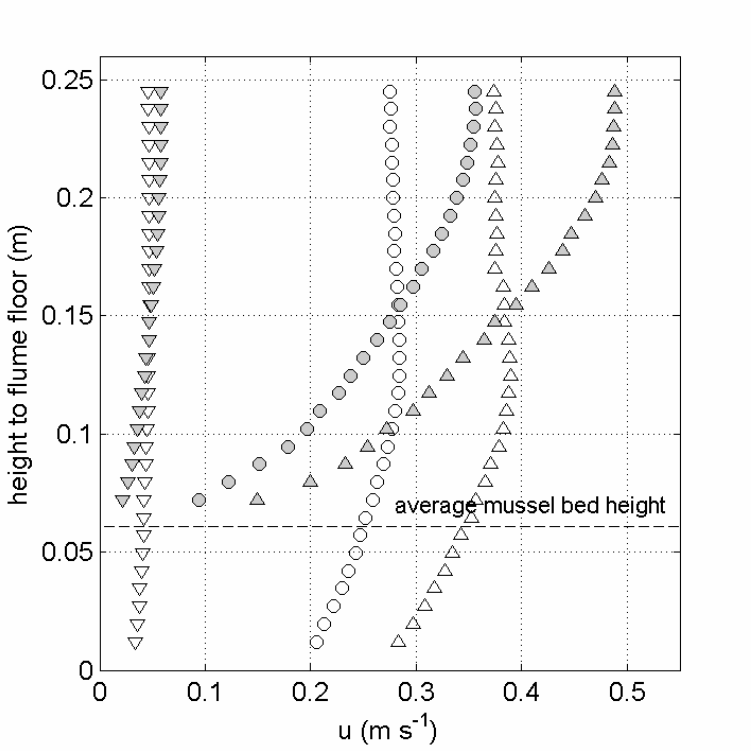

Figure 48: Averaged horizontal velocity profiles over mussel (in grey) for three different discharges from the experiment by Van Duren. Open symbols represent the measurements over flat bed.

It is clear from Figure 48 that the mussel bed causes lower current velocities near the bottom. Next to that, the elevated bed forces the water to flow higher, causing higher maximum velocities at the top. The results from flow over a flat bed show unexpected effects higher up in the water column. The flow near the surface seems to be slowed down. This could be caused by either flume wall effects, or the influence of a strong airflow present in the experimental space (Van Duren, personal communication).

B.3.2 Analysis of flow profiles

B.3.2.1 Some theory

For flow over a rough bed, the velocity increases from the bed upward. The part of the flow profile where velocities are non-uniform is called the boundary layer. Flow in the boundary layer over a rough bed, is often described by a logarithmic velocity profile ('law of the wall'):

$$u(z) = \frac{u_*}{\kappa} \ln\left(\frac{z}{z_0}\right) \qquad (17)$$

Where:

u_* = shear velocity (m s^{-1})

κ = Von Kármán constant (= 0.4) (-)

z = height above the bed (m)

z_0 = roughness height (m)

It can be seen in above equation that the velocity increases logarithmically with height. Near the bed the roughness height (z_0) above the bed is held as the zero velocity point. The rougher the bed, the higher z_0 is. Furthermore z_0 determines the gradient of the logarithmic profile. A smooth wall will lead to a small z_0 and thus a steep incline in velocities, i.e. a thin boundary layer. A rough wall is described by a large z_0 and thus a thick boundary layer. Equation (17) does not hold for cases with very large roughness elements. In such cases the flow profile will exhibit a different form (i.e. not logarithmic). Good examples of this can be found in research of flow over vegetation (see for example Baptist, 2005), or of flow over very course granular beds (see for example Hofland, 2005). However it has been noted by several researchers, including Nepf and Vivoni (2000), that flow over the top of submerged roughness elements still follows a logarithmic profile, similar to flow over a relatively flat bed. This profile can be described by:

$$u(z) = \frac{u_*}{\kappa} \ln\left(\frac{z-d}{z_0}\right) \qquad (18)$$

Where:

u_* = shear velocity (m s^{-1})

z_0 = roughness height (m)

d = zero-plane displacement (m)

The profile described in this way only holds for the flow above the roughness elements, not between them. If the flow between the roughness elements is small – as is the case with mussels – this profile can be used as an approximation for flow above roughness elements. Equation (18) is similar to equation (17), but differs in the introduction of the parameter d. This parameter describes the extent to which the profile (defined by z_0 and u_*) is lifted above the actual bed. It adjusts the reference level of the logarithmic profile to the height at which the mean representative bed shear stress appears to act. Figure 49 gives a schematic representation of this profile. Note that in this case the roughness elements are usually larger than distance d.

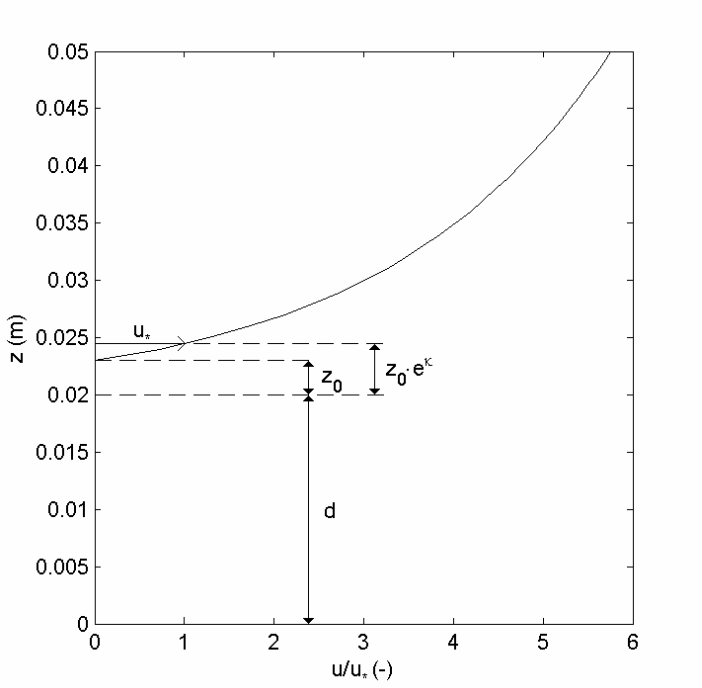

Figure 49: Schematic representation of flow profile on top of submerged vegetation. Example with d = 0.02 m and z_0 = 0.003 m. Note that this profile does not describe the flow inside the vegetation.

The roughness length z_0 is important because it can be translated into Chézy roughness (C in $m^{1/2}$ s^{-1}). The stress felt by the flow when flowing over a rough bed is proportional to u^2/C^2. (See for example Appendix C.1 for the implementation in Delft3D.) Chézy can be related to the Nikuradse roughness length (k_s in m) via the White-Colebrook equation, where k_s is (for rough beds) a constant multitude of z_0:

$$C = 18\log\left(\frac{12h}{k_s}\right) \tag{19}$$

Where:

h = water depth (m)

k_s = Nikuradse roughness length (m) = 30 · z_0

B.3.2.2 Profile shape of flat bed condition and derivation of roughness

The reliability of derived roughness values from flow profiles has been tested by investigating the profile shapes of the flat bed velocity measurements in the experiment by Van Duren[19]. In principle these profiles should exhibit a logarithmic shape and the roughness length z_0 should be very small, as one would expect for the smooth flume floor.

[19] *The measurements over flat empty bed by De Vries were not recorded properly due to equipment failure and are consequently not available.*

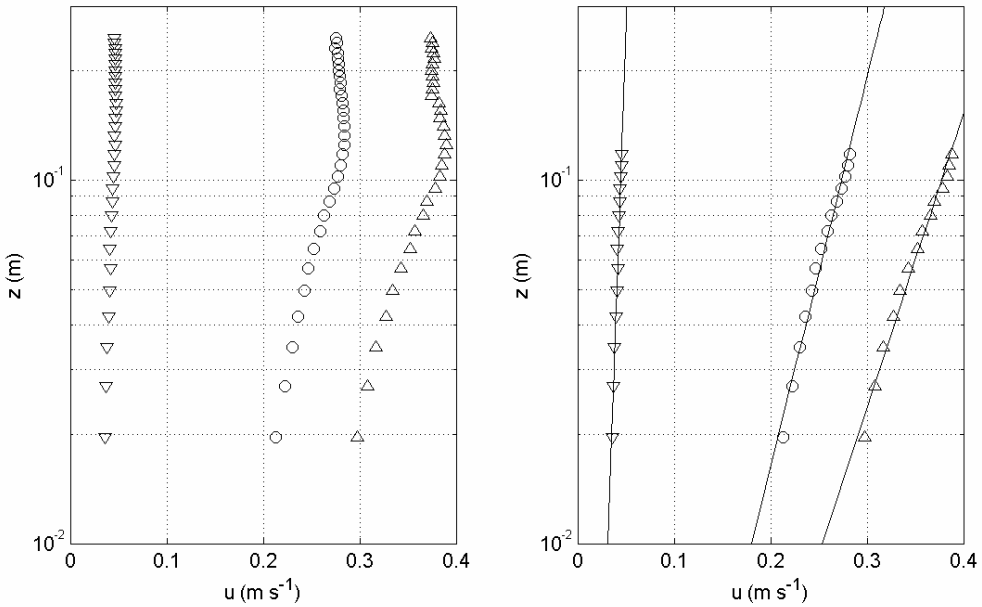

Figure 50: Figure displaying data selection for logarithmic fit and the actual fit. Displayed are three discharges measured 1.5 m before the leading edge of the mussel bed in the experiment by Van Duren.

In Figure 50 a portion of the data is selected that is clearly in the boundary layer. The fact that the other data do not follow a logarithmic profile is ignored. As can be seen in the RHS figure above the data show a trend that is not entirely logarithmic, on the log scale it shows a slight concave shape. In effect if only the data from the lower positions would be taken, a potentially different fit would be found. Neglecting this, the following values are found:

Table 8.2: Roughness and flow parameters for flow over flat bed from Van Duren

discharge	*u_* (mm s^{-1})*	*z_0 (mm)*	*k_s (30 ·z_0) (mm)*
low	*2.28*	*0.041*	*not applicable*
medium	*16.6*	*0.11*	*3.3*
high	*22.1*	*0.09*	*2.7*

For the higher two discharges, the boundary layer is clearly turbulent (otherwise z_0 would have been much smaller), hence the approximation $k_s = 30 \cdot z_0$ can be used. Indeed the found roughness heights are more or less stable. However the values of these are much higher than one would expect from a floor as smooth as the flume floor. It can thus be concluded that the NIOO race track flume does not yield profile forms that are expected from theoretical considerations[20]. This is true both of the form of the profile – only partially and then approximately logarithmic – and the size of the derived

[20] *It should be noted here that the fact that flow profiles are not logarithmic does not disqualify the results a priori. It is just that the assumptions in which the 'law of the wall' is based do not hold for the NIOO flume. Those equations thus cannot reliably be used to derive roughness values. Using a data set of flow profiles measured in the NIOO flume over beds with a known roughness, roughness values could be derived more reliably. It is not known by the author whether such a data set exists.*

variables. This means that the roughness values derived in the next section are to be interpreted with caution.

B.3.2.3 Derivation of flow and roughness parameters

It has been shown in the previous section that the NIOO flume does not yield reliable results when deriving the bed roughness from the flow profile for a flat bed. This implies that the profile that is formed does not follow the law of the wall, defined in equation (17). The following results should thus be interpreted with caution. In the case of the De Vries experiments, there are no results of a flow over a flat bed, so no test has been conducted. An analysis will nevertheless be performed. In principle a simple logarithmic profile can be fitted to the data points given in Figure 47 and Figure 48. There is one large difference with a standard case: the mussels fill up a considerable part of the space, it would thus be unwise to maintain the original flume floor as z=0. In other words the question is what value should be chosen for zero-plane displacement d in equation (18). Two different approaches are chosen. The first is to define z=0 at the mean height of the mussels, i.e. $d = h_{mus}$ (mean height mussels). This is the approach chosen by Van Duren *et al*. (2006). Theoretically d is defined at the point where vertically speaking, half of the momentum of the flow has been absorbed. Therefore d as h_{mus} seems unrealistic. An alternative approach is chosen. In this approach it is simply assumed that the profile is logarithmic. Then the value of d is chosen such that the fit of the logarithmic profile with the data is optimal. In other words the value of d is found by maximizing the combined least square goodness of fit (R^2) of the logarithmic profile to the data[21]. Both approaches yield values for z_0 and u_*.

The results are displayed in Table 8.3. For brevity not all the values for De Vries the experiments are displayed, the given values are averages of the analysis of the 20 profiles displayed in Figure 47. For the experiments by Van Duren a selection of vertical measuring positions was made, as the higher velocities deviated clearly from the profile. Also displayed is the Nikuradse length k_s, defined as $30 \cdot z_0$.

[21] *Note that with combined least square fit it is meant here that the value of* d *is found by maximizing the sum of* R^2 *of the separate conditions. For the 20 conditions by De Vries it was found that the combined* R^2 *is maximized (at 19.38) with* d = *1.4 mm. For the 3 conditions by Van Duren it was found that the combined* R^2 *is maximized (2.889) at* d = *22 mm.*

Table 8.3: Roughness parameters for different experiments and approaches

experiment	discharge	$h_{mus} - d$ (mm)	z_0 (mm)	$\sigma(z_0)$ (mm)	R^2 (-)	k_s (mm)
De Vries (n=20)	variable	0	0.16	0.12	0.967	4.8
De Vries (n=20)	variable	1.4	0.22	0.16	0.969	6.6
Van Duren	low	0	2.3	n.a.	0.985	69
Van Duren	medium	0	4.2	n.a.	0.957	126
Van Duren	high	0	3.2	n.a.	0.947	96
Van Duren	low	22	12.9	n.a.	0.998	387
Van Duren	medium	22	18.5	n.a.	0.999	555
Van Duren	high	22	15.7	n.a.	0.996	471

Now the two experiments can be compared. It becomes clear right away that the roughness in the experiments by De Vries is much less than in those by Van Duren. Furthermore the optimized logarithmic fit is hardly submerged between the mussels. This is most likely the results of the large amount biodeposition mimic (couscous) used by De Vries to investigate erosion, see Figure 44. The couscous covered the mussel almost entirely, smoothing the bed.

The analysis of the data by Van Duren gives interesting results. When $d = h_{mus}$ is chosen, the roughness height is in the order of the mussel dimensions. When the profiles are fitted, d becomes smaller and k_s becomes very large. As an example: for sediments k_s can be approximated by $3 \cdot D_{90}$ (where D_{90} is the grain size that is not exceeded by 90% of the sediment mixture). The roughness length would thus be expected to be in the order of magnitude (3x) of the roughness elements. The mussels used in de Van Duren experiment were nearly 4 cm; the found roughness lengths of ten times that value seem too large. One can doubt these results, primarily because it has been shown in section B.3.2.2 that the velocity profiles are not logarithmic to begin with. Fitting such a profile might thus not be defensible. The approach followed by Van Duren *et al.* ($d = h_{mus}$) on the other hand, yields strange curves in the logarithmic profile. This is also suggested by the lower R^2 value. These curves can not be explained by the argumentation of an internal boundary layer given by Van Duren *et al.* (2006). With a smaller zero-plane displacement (d), these curves disappear.

B.4 Turbulence profiles

This section briefly presents the profiles of Turbulent Kinetic Energy, as derived from the experimental data. It is important to describe turbulence over mussel beds, because it is the driver of turbulent mixing of fine sediment over the vertical, influencing the amount of sediment available for both normal deposition and biodeposition. Furthermore sediment higher up in the vertical is transported faster because of the higher velocities there. Also turbulent eddies can directly pick up sediment due the inherent velocity peaks, causing high instantaneous bed shear stress.

B.4.1 Turbulence and Turbulent Kinetic Energy

Turbulence is essentially best described as random and chaotic flow movements. Flow without turbulence is laminar: all layers of the flow have parallel velocities without disturbances between the layers. Turbulence is generated when the inertial forces (for example disruptions from a rough bed) are no longer compensated by viscous forces (the power of the fluid to resist changes in velocity): the laminar flow transfers into turbulent flow. In such a case, small instabilities are no longer controlled and spin out of control, generating turbulent eddies. Eddies are dissipated as they are broken up into smaller eddies and eventually spend their last energy in viscous friction. For most conditions the viscous forces in a flow are constant. Therefore increased velocities and increased disturbances (for example by roughness elements) increase turbulence.

For the specific case of flow over mussels, it is thus expected that the turbulence is highest near the tops of the mussels, where velocities are still high and the roughness of the mussels generates much turbulence. In between the mussels, the velocities decrease and the size of eddies is limited by byssal threads and shells. The reduced velocities lead to less turbulence in between the mussels and the narrow spaces mean that existing turbulent eddies are broken up quickly. Therefore theoretically, high turbulence is expected near the mussel tops and decreasing turbulence in both directions along the vertical.

In order to test whether this expectation is found in experiments, velocity time series need to be translated into turbulence values. Turbulence can be seen as random fluctuations through time in velocity *u, v* and *w*. In order to quantify this random process, it is helpful to separate the fluctuating (random) component from the mean (this is called Reynolds decomposition), for example for *u*:

$$u(t) = \bar{u} + u'(t) \tag{20}$$

Where:

u(t) = time dependent velocity (m s^{-1})

$\bar{u}$ = mean velocity, or steady component (m s^{-1})

u'(t) = deviation from the mean, or fluctuating component (m s^{-1})

A flow has not one component, but three: *u, v* and *w*. Considering that kinetic energy of each of these components can be given by E_{kin} = ½ *m* u^2, the equivalent can be done for the turbulent components. For a three-dimensional flow, the turbulent kinetic energy per unit of mass at one point in space and time can be given by:

$$TKE = \frac{1}{2}\left(u'^2 + v'^2 + w'^2\right) \tag{21}$$

Where:

TKE = Turbulent Kinetic Energy (m^2 s^{-2})

The instantaneous value of *TKE* can vary dramatically due to the fact that *u'*, *v´* and *w´* are random fluctuations. A more useful value is the mean *TKE*, usually (although confusingly) also called *TKE*, but actually more precisely described as *mTKE*, where the squared fluctuating components are averaged over time:

$$TKE = \frac{1}{2}\left(\overline{u'^2} + \overline{v'^2} + \overline{w'^2}\right) \tag{22}$$

Where:

TKE = mean Turbulent Kinetic Energy ($m^2\ s^{-2}$)

In case of velocity measurements, a discrete data set is obtained. Assuming that this data set has n measurements at a single location, the time averaged square of *u'* is approximated by the variance in the measurement series *U*:

$$\overline{u'^2} \approx \frac{1}{n}\sum_{i=1}^{n}\left(U_i - \overline{U}\right)^2 = \mathrm{var}(U) \qquad (23)$$

The variances in the velocity component can thus be used in equation (22). The variances can be derived relatively easily from the measurement time series following equation (23). Using this technique for each position of the flow a TKE profile can be determined from the measurements.

B.4.2 Experimental results

B.4.2.1 TKEpartial profiles from De Vries Experiments

The P-EMS instrument is capable of measuring only two velocity components simultaneously. In this case those components are *u* and *w*. The two components can be used to derive $TKE_{partial}$. The results are displayed in Figure 51.

$$TKE_{partial} = \frac{1}{2}\left(\overline{u'^2} + \overline{w'^2}\right) = \frac{1}{2}\left(\mathrm{var}(U) + \mathrm{var}(W)\right) \qquad (24)$$

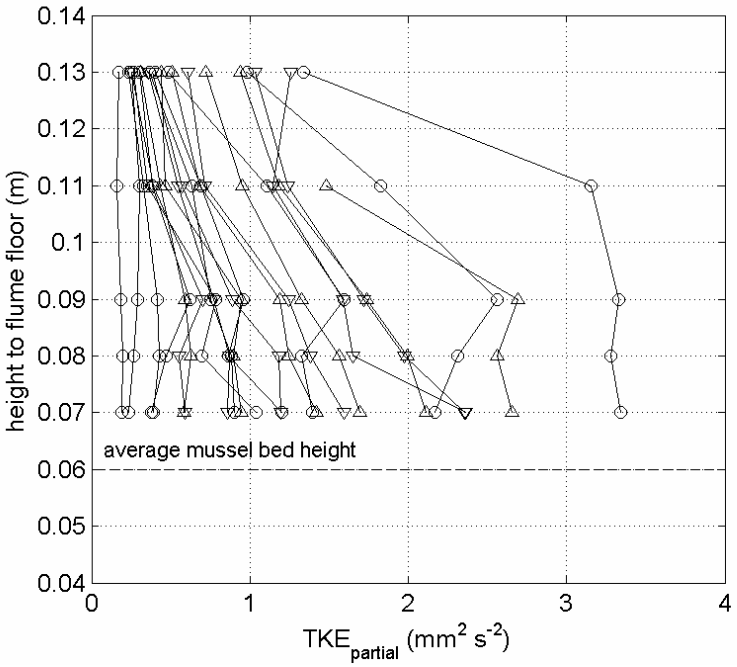

Figure 51: $TKE_{partial}$ profiles from De Vries experiment. Measurements taken 2.2 m downstream from the mussel bed edge. Experiments over tray 1 are marked by a circle, over tray 2 by a triangle down and over tray 3 by a triangle up.

It appears from Figure 51 that turbulence is highest at the top of the mussels. This is exactly as expected, turbulence is largest at the point where it is generated (the mussels). TKE values are expected to fall again in between the mussels, as explained in section B.4.1. However, measurements in these parts of the flow are very difficult and have not been attempted by De Vries.

B.4.2.2 TKE profiles from Van Duren Experiments

The experiment by Van Duren included measurements of all three velocity components. As a result the full equation (22) can be used to determine TKE values. The results are displayed in Figure 52.

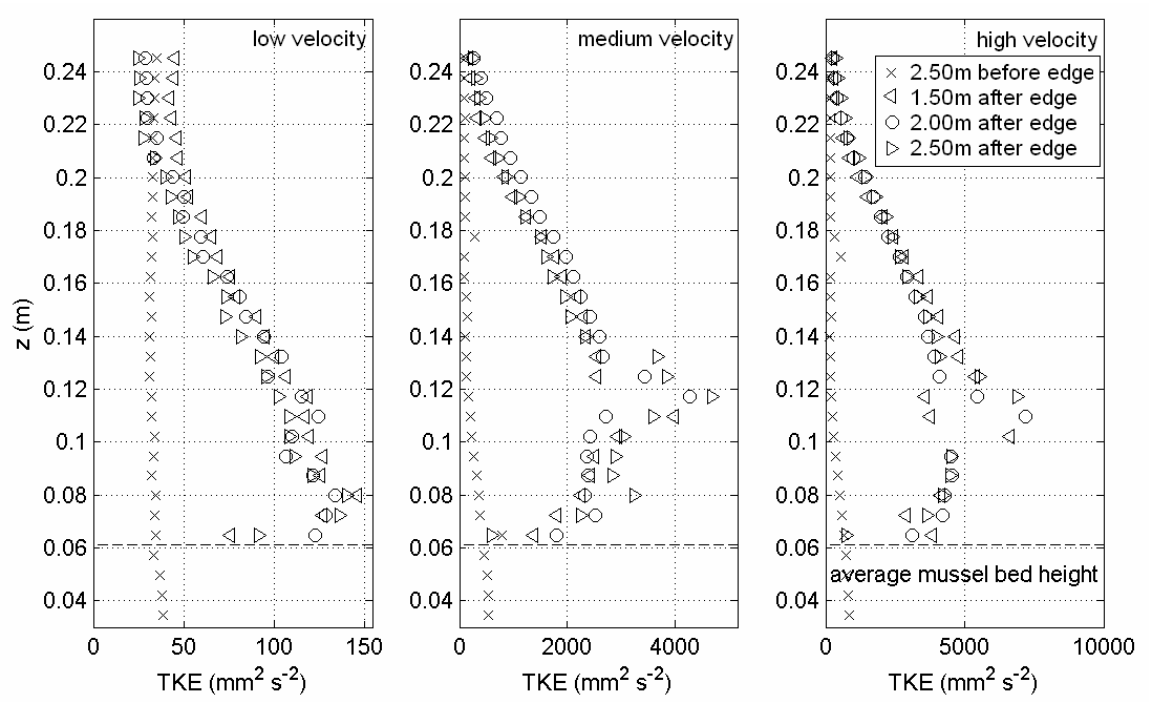

Figure 52: TKE profiles for three positions along the downstream end of the mussel bed by Van Duren. Crosses (x) represent measurements before the mussel bed and thus over flat bed. At the high velocity figure, extreme TKE values up to 20 000 mm^2 s^{-2} around z = 0.11 m are not displayed.

It is clear from Figure 52 that turbulence is much higher over a mussel bed than over a flat bed, this confirms results by Van Duren (2006). A number of other things are notable in Figure 52. First of all the peaks in the TKE near the bed are erratic. This is strange as turbulence is very diffusive; in fact it also diffuses itself. It would thus be expected that these peaks smooth themselves out. It was found that it is a known property of the ADV instrument that reflection from the bed causes strange effects at specific low heights above the bed. The turbulence peaks near the bed seen in Figure 52 are certainly examples of this phenomenon (Van Duren, personal communication) and can thus be disregarded in further analysis.

A second thing is important: it seems as if the TKE diminishes towards the mussels before reaching the mean mussel bed levels. This is not expected as explained in section B.4.1. This apparent phenomenon can be explained by the fact that the ADV has a threshold below which turbulent eddies cannot be detected. This has two reasons, the first is that small eddies can fall entirely into the measuring volume, in which case the high velocities of the eddy are averaged out. Secondly the high ambient

velocities, mainly $\bar{u}$, mean that the measuring frequency will have trouble detecting high frequency turbulence. For low velocities, where this latter phenomenon is less important, the measured turbulence increases up till close to the mussels. A part of the turbulent spectrum is thus not detected by the ADV in the experiments by Van Duren. Only a high frequency Laser Doppler Velocity meter (LDV), measuring at around 500 Hz is able to capture the entire turbulence profile. In case of the De Vries experiment, the measuring volume of the velocity meter is smaller and turbulence levels lower, which explains why similar problems do not arise to the same degree.

The turbulence levels measured by Van Duren are much larger than those measured by De Vries. Partly, this is due to the missing velocity term v. However, more important is the large difference in bed roughness between the two experiments, as established in section B.3.2.2. With little of the mussel shells exposed in the experiments by De Vries, the turbulence production is similarly low.

The final notable thing is the difference between the TKE values presented here and those published in Van Duren *et al.* (2006). The latter are around 40 % lower, while the experimental results were obtained in the same way over the same bed only a few months later. Van Duren (personal communication) suggests that a layer of deposited silt has built up during the three intermediate months between the experiments. The (bio)deposition of this material may have decreased the bed roughness in the same way as the much larger amount of couscous has done in the De Vries experiment. A second explanation is based on the fact that during the three months, mussels have died (actually after a year almost half the mussels was dead). The decreased rate of mussel feeding in the later experiment could have significantly reduced the amount of turbulence.

B.5 Erosion experiments by De Vries

The experiments by De Vries were primarily designed to investigate the erosion of biodeposition mimics (couscous) from in between the mussels. The results from these experiments have not been analyzed, mainly because the forcing hydrodynamic conditions were insufficiently known and the erosional properties of couscous not understood.

However the experiments do offer some interesting qualitative clues with regard to the resuspension of material from a mussel bed. The experiment has been conducted as follows, couscous was placed on the bed and velocities and waves were intensified each time until no further material eroded. Two significant observed qualitative phenomena are: (1) photographs of the experiments showed that even at the fastest currents and highest waves combined significant amounts of couscous remained between the mussels. This illustrates the point made in section 2.3.1.3 that sediment lying at a certain depth between the mussels cannot erode. The erosion limit marks the boundary between erosion resistant mussel mud and material still sensitive for erosion, as defined in Figure 7. (2) The second point that needs to be made here is that waves added very significantly to the amount of erosion of the couscous. Even at high velocities little of the biodeposition mimic eroded. When waves were added erosion accelerated enormously. The waves added little in terms of bed shear stress, but apparently the turbulent motions caused by waves are an important factor in lifting material from in between the mussels.

B.6 Conclusion

The first objective of this appendix was to establish a quantitative understanding of the roughness of mussel beds. It has been shown that the experiments by Van Duren showed much larger roughness values than those by De Vries. The low roughness found for the latter experiments has been shown to be mainly due to coverage of the shells by mimic pseudo-faecal pellets. The absolute values of the z_0 of the mussel bed as found by analysis of the results by Van Duren have been shown to be unreliable, because the experimental set-up does not exhibit logarithmical flow profiles. In conclusion, the results as presented here are insufficient to achieve the stated goal. An experimentally derived value for roughness cannot be given based on the results. This parameter should be estimated in another way for model implementation.

The second objective of this chapter was to find turbulence levels over mussel beds. It has been established that turbulence levels are up to ten times higher over a mussel bed than over a flat bed. The high turbulence levels make the lower area of the water column well mixed. Filtration (and capture of fine sediment) by mussels is thus less likely to cause local shortages in the water column, also because suspended sediment is concentrated near the bed.

C Delft3D-FLOW

In this appendix the hydro- and morphodynamic process based simulation tool Delft3D will be explored, with specific emphasis on the features used in the research. Delft3D is capable of solving 2D and 3D non steady flow and transport problems. Here the 2DH implementation will be presented, leaving out the unused vertical terms as much as possible. A thorough description of most of the things mentioned can be found in WL|Delft Hydraulics (2006).

First the hydrodynamic equations of the model will be explained in section C.1. Then the staggered computational grid on which the model is based is presented (section C.2). Section C.3 explores the drying and flooding algorithm. In section C.4 the trachytopes module for simulating vegetation roughness is described. Section C.5, finally, deals with the transport equations and the morphological updating.

C.1 Hydrodynamic equations

For each control volume in the computational grid, the shallow water equations are solved. These are derived from Navier-Stokes equations for incompressible free surface flow. Leaving out terms for wind stress and Coriolis force, the used equations for a depth averaged application read:

$$\frac{\partial u}{\partial t}+u\frac{\partial u}{\partial x}+v\frac{\partial u}{\partial x}+g\frac{\partial \eta}{\partial x}+\frac{g|U|u}{C^2(d+\eta)}-\upsilon\left(\frac{\partial^2 u}{\partial x^2}+\frac{\partial^2 u}{\partial y^2}\right)=0 \qquad (25)$$

$$\frac{\partial v}{\partial t}+u\frac{\partial v}{\partial y}+v\frac{\partial u}{\partial y}+g\frac{\partial \eta}{\partial y}+\frac{g|U|v}{C^2(d+\eta)}-\upsilon\left(\frac{\partial^2 v}{\partial x^2}+\frac{\partial^2 v}{\partial y^2}\right)=0 \qquad (26)$$

Where:

u, v = depths average velocity in x and y direction (m s^{-1})

g = acceleration due to gravity (m s^{-2})

η = water level above reference plane (m)

|*U*| = absolute magnitude of velocity = $\sqrt{(u^2+v^2)}$ (m s^{-1})

C = Chézy roughness coefficient ($m^{1/2}$ s^{-1})

d = water depth below reference plane (m)

υ = horizontal eddy viscosity (m^2 s^{-1})

Equation (25) describes the change in time for the u component of the horizontal depth averaged velocity (term 1). The second and third term describe the advection of velocity in x and y direction. The fourth term gives the contribution of surface slope to the acceleration of the fluid. Term 5 describes the loss term due to bed friction. The sixth and final term describes diffusion. Equation (26) is the equivalent for the change in the velocity component in y-direction *v*. A final equation that governs the system is continuity equation:

$$\frac{\partial \eta}{\partial t} + \frac{\partial (d+\eta)u}{\partial x} + \frac{\partial (d+\eta)v}{\partial y} = 0 \qquad (27)$$

This last equation ensures that the total amount of fluid remains the same. The amount of fluid going in and out of cell should be equal to the change in water level in that cell. The equations can only be solved when user specified boundary and initial conditions have been specified. Further model boundary conditions at the bed and on the surface are omitted here. For transport process at the bed the bed shear stress is important. The force of the bed on the fluid is incorporated as the fifth term in equation (25) and (26). The corresponding force on the bed is then given by:

$$\vec{\tau_b} = \frac{\rho_0 g \vec{U} |U|}{C^2} \qquad (28)$$

Where:

τ_b = bed shear stress (N m^{-2})

$\vec{U}$ = velocity vector (m s^{-1})

For certain applications it is desirable to let the bed shear stress be a vector. For the purposes relevant in this report only the magnitude is used. This means that the absolute value can simply be used.

C.2 Computational grid

In order for the explanation below to make sense, the staggered grid used in Delft3D is introduced. The equations on which Delft3D is based are applied in a so called staggered grid. This grid is presented in Figure 53. A staggered grid is used for practical, numerical and physical reasons (see WL|Delft Hydraulics, 2003, p. 10-2). This report will not get into detail regarding the specifics of the staggered gird, however. Still, in order to understand especially the way Delft3D models flooding and drying it is important to understand the basics.

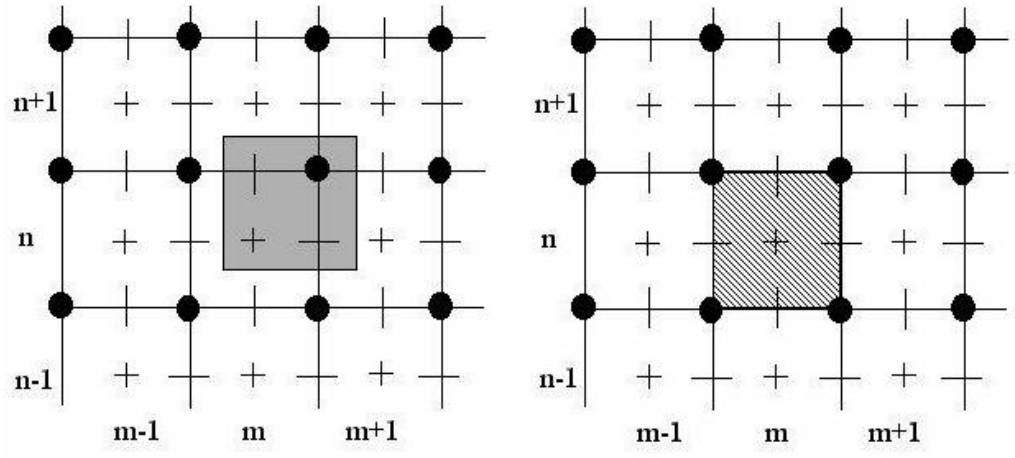

Figure 53: Computational grid as used in Delft3D, Left: items with the same array number, right: the computational control volume (source: WL|Delft Hydraulics, 2006, p. E-1). Explanation of symbols in text below.

The principle of the staggered grid is that the quantities, depth (●), water level (+), horizontal velocity in x-direction (-) and horizontal velocity in y-direction (|) are not

defined in the same point. This means that the control volume (on the right side in Figure 53) consists of a water level surrounded by four depths points defined by the bathymetry) and velocities defined at the four sides of the square made by the four depths points.

C.3 Drying and Flooding Algorithm

The intertidal flat modeled in this study is essentially a large, shallow and relatively flat area, bordered by a deeper channel. As the water is high the flat is submerged, however as the water level falls the flat is exposed and flow is constricted to the channel.

In the numerical model Delft3D (see p. 10-24 of Delft Hydraulics (2003)) the phenomenon of drying and flooding is modeled by switching off grid cells as they become dry (this state is called inactive) and switching them on as they become flooded again (active). There are three crucial items to consider when using Delft3D to calculate this drying and flooding process: (1) the way in which the bottom depth is defined at water level point, (2) the way in which the water levels is defined at the velocity points and (3) criteria for setting a velocity and/or water levels points wet (active) or dry (inactive). These items will be dealt with below in the order specified.

The bed level for a water level point (+) is defined as the mean of the surrounding four water depth points (●). Steep bed slopes can mean that the water level falls below this average leading to a negative water depth. In such a case the cell is switched off and the computational step has to be repeated, this can lead to higher computational times. For such a case it can be considered to specify the bed level as the maximum of the four depth points: Dpsopt= #MAX#.

The second item that is to be considered carefully is the definition of the total water depths at the velocity points (- and | in Figure 53). To establish velocities, the total depth available for flow is required. Normally this is obtained from the difference between the mean of the depth points bordering the velocity point and the mean of the water level points bordering the velocity point. However one can imagine that when large gradients are concerned this may lead to similar problems as explained in the previous paragraph. Here also there are a number of options that can be chosen. In this context it is wise to opt for an up wind scheme. That takes the water level depending on where the flow is coming from. This means that grid cells can always empty, even if the destination cell is already dry. The downside is, is that discharges are on average overestimated. The upwind scheme can be selected by specifying DCO = +999.

Finally the criteria for defining a cell as either dry or wet are to be specified. The first criterion is the threshold depth. In principle when the water depth falls below this value the cell is considered dry and if it rises above it is considered wet again[22]. Because of the reasons explained above it is undesirable to let the control volume become negative. In order to prevent this, the threshold depth should be chosen in such a way that it is larger than the maximum distance the water level can fall over half time step (the time which the flooding and drying algorithm uses). In this way it becomes impossible for the water level to fall from above the threshold to negative in half a time step. The criteria can be defined as follows:

[22] *In order to prevent the system from rapidly switching from wet to dry, the grid cell is only considered dry if the water level falls below half the threshold depth. It is only considered wet again when the water level rises above the entire threshold depth.*

$$\delta \geq \frac{\partial \zeta}{\partial t}\frac{\Delta t}{2} \tag{29}$$

Where:

δ = Threshold depth (m)

ζ = Water level relative to reference (m)

t = Time (s)

Any threshold depth larger then this fulfils the destined function, although choosing a value too large will make the system unrealistic, i.e. grid cells become dry when substantial amounts of water are still present.

C.4 Trachytopes functionality

Trachytopes (a combination of the Greek words for rough and roughness) can be used to implement the hydraulic roughness of diverse ecotopes in 2DH computations. This can be implemented in a variety of ways, one of these contains the equations proposed by Baptist (2005). His approach is based on the assumption that vegetation can be modeled as rigid cylinders; this provides the vegetation variables: density m, diameter D, height k and drag coefficient C_D. The formulation for representative roughness obtained by genetic programming (Baptist *et al.*, 2006) has been incorporated:

$$C_r = \sqrt{\frac{1}{C_b^{-2} + (2g)^{-1} C_D m D k}} + \frac{\sqrt{g}}{\kappa}\ln\left(\frac{h}{k}\right) \tag{30}$$

Where:

C_r = representative Chézy roughness coefficient ($m^{1/2}\ s^{-1}$)

C_b = bed Chézy roughness ($m^{1/2}\ s^{-1}$)

C_D = drag coefficient of vegetation structure (-)

m = number of cylinders per unit area (m^{-2})

D = diameter of cylinders (m)

k = height of vegetation

κ = Kármánn's constant (-)

h = water depth (m)

An equation for the bed shear stress has been derived by the relatively simple reduction factor approach (see Baptist, 2005, p.48). This approach assumes that the flow through the vegetation is uniform in vertical direction. The equation reads:

$$\tau_{bv} = \frac{1}{1 + \frac{C_D m D k C_b^{\ 2}}{g}} \cdot \tau_t \tag{31}$$

Where:

τ_{bv} = bed shear stress on a vegetated bed ($N\ m^{-2}$)

τ_t = total stress on bed and vegetation calculation using the representative roughness C_r ($N\ m^{-2}$) substituted in equation (28):

$$\tau_t = \frac{\rho g}{C_r^{\,2}} |U|^2 \tag{32}$$

Equations (30) and (31) have been implemented in Delft3D in a slightly different way, maintaining the same results. The main idea is that there is a total stress on the bed (τ_t) also used in (31), of which only a part is actually exerted on the bed, the rest is absorbed by the vegetation. Tot this end the representative roughness C_r is split into two parts, the first due to the vegetation and the second due to the bed (C_b'), such that:

$$\tau_{bv} = \frac{\rho g}{(C_b')^2} |U|^2 \tag{33}$$

Where:

C_b' = *effective* Chézy bed roughness ($m^{1/2}\ s^{-1}$)

Substituting (31) in the left hand argument of (31)and using C_r as described by (30) in (32) and substituting this into the right hand argument of (31), the following expression for C_b' can be obtained:

$$C_b' = C_b + \frac{\sqrt{g}}{\kappa} \ln\left(\frac{h}{k}\right) \sqrt{1 + \frac{C_D m D k C_b^2}{2g}} \tag{34}$$

Using this equation the bed shear stress can be computed as normal in Delft3D, see equation (28), but now with the normal equation for bed shear stress and the *effective* bed roughness under vegetation C_b'.

The functionality can be applied in a model by specifying a type of vegetation (or multiple) defined by four variables: k, mD, C_D and C_{bed}. In another file the indices of grid cells containing this type vegetation are specified. In the main Delft3D input file the time step with which the roughness is updated can be specified, as the roughness is dependent on the time dependent variable water depth (h). For the purpose of this report the representative roughness is not expressed as C but as Nikuradse roughness height k_s which is independent of water depth (h). If C_r is substituted into the White Colebrook formulation (8), the following expression is found[23]:

$$k_s = \frac{12h \cdot k^{\frac{\sqrt{g}}{18\kappa}\ln(10)}}{10^{\frac{C_1}{18}} h^{\frac{\sqrt{g}}{18\kappa}\ln(10)}} \approx \frac{12k \cancel{h}}{10^{\frac{C_1}{18}} \cancel{h}} = \frac{12k}{10^{\frac{C_1}{18}}} \tag{35}$$

Where:

C_1 = $\sqrt{\dfrac{1}{C_b^{-2} + (2g)^{-2} C_D n D k}}$ ($m^{1/2}\ s^{-1}$)

$\dfrac{\sqrt{g}}{18\kappa}\ln(10)$ = 1.0017 ≈ 1

[23] *The fact that the found expression is independent of water depth (h) is both coincidental and convenient.*

C.5 Transport equations

This section gives on overview of the model implementation of sediment transport in Delft3D. In older versions of this software, the formulations were implemented in a separate model Delft3D-MOR, nowadays this module in integrated into Delft3D. As an effect a more complete picture of the formulation and implementations is given in the FLOW manual (WL|Delft Hydraulics, 2006).

Delft3D schematizes the different sediments as either 'mud', 'sand' or 'bed load'. For all of these a large amount of fractions can be specified. The first is modeled only as suspended transport, the last only as bed load transport. 'Sand' transport is a combination of both suspended and bed load transport. As this study focuses on fine sediments, this section will deal primarily with 'mud'.

C.5.1 Suspended load sediment transport

Two-dimensional suspended sediment transport is calculated by solving the following advection diffusion equation for each control volume for each sediment fraction:

$$\frac{\partial c}{\partial t}+\underbrace{\frac{\partial uc}{\partial x}+\frac{\partial vc}{\partial y}}_{advection}\underbrace{-\frac{\partial}{\partial x}\left(\varepsilon_{s,x}\frac{\partial c}{\partial x}\right)-\frac{\partial}{\partial y}\left(\varepsilon_{s,y}\frac{\partial c}{\partial y}\right)}_{diffusion}=E-D \qquad (36)$$

Where:

c = mass concentration of sediment (kg m^{-3})

u, v = flow velocity components (m s^{-1})

$\varepsilon_{s,x}, \varepsilon_{s,y}$ = eddy diffusivities in three directions (m^2 s^{-1})

E = erosion source term (kg m^{-3} s^{-1})

D = deposition sink term (kg m^{-3} s^{-1})

Settling velocities can be adjusted for the phenomenon of hindered settling (i.e. at high concentrations particles cannot settle as fast as in isolation because they are hindered by other particles).

C.5.2 Initial and boundary conditions

Equation (36) can only be solved if all the boundary conditions are specified. These include the condition at the start of the computation (initial condition), at the horizontal boundaries of the system, at the water surface and at the bed. The initial condition specifies what the concentration of sediment is in each grid cell at t=0. The surface condition ensures no sediment can enter or leave the model from there. The second boundary condition is the one at the bed. The exchange of material through this boundary is modeled by the fluxes between the bed water layer (in a depth averaged model this is the only layer) and the bed. The erosion and deposition are applied as a sink (D, in kg m^{-2} s^{-1}) and source (E, in kg m^{-2} s^{-1}) term for each cell.

The open boundaries can be separated into inflow and outflow boundaries. For inflow a time dependent concentrations can be specified for each layer for each boundary, furthermore the concentration can be varied linearly spatially along the boundary. In contrast an outflow boundary is not prescribed, sediment is simply transported (by advection) outside the model domain. A 'Thatcher-Harleman' return time can be specified for boundaries where inflow and outflow are alternating in a single boundary.

The change in concentration in the boundary can be abrupt as the outflow may be much lower than the boundary inflow condition, when the return time is specified the inflow concentration adjusted gradually over that time from the old outflow concentration to the new boundary condition.

C.5.3 Cohesive sediment

Cohesive sediment is one of the sediment types that can be described by the above presented general formulations. The most important equations specific to cohesive sediment are those describing erosion and deposition. Flocculation is ignored here. Focus is on the erosion (*E*) and deposition (*D*) terms in equation (36).

The fluxes between sediment suspended in the water and deposited on the bed are calculated using the Partheniaes-Krone formulations:

$$E = M \cdot \max\left(0, \frac{\tau_b}{\tau_{e\_crit}} - 1\right) \tag{37}$$

$$D = w_s \cdot c \cdot \max\left(1 - \frac{\tau_b}{\tau_{d\_crit}}, 0\right) \tag{38}$$

Where:

E = resuspension flux (g m^{-2} d^{-1})

M = first order erosion rate (kg m^{-2} d^{-1})

τ_{e_crit} = critical bed shear stress for erosion (N m^{-2})

D = deposition flux of suspended matter (kg m^{-2} d^{1})

w_s = settling velocity of suspended, note unit: (m d^{-1})

τ_b = bed shear stress (N m^{-2})

τ_{d_crit} = critical bed shear stress for deposition (N m^{-2})

The bed shear stress used here is the magnitude of τ_b computed in equation (28).. Two notes have a place here. First, it has been shown by Winterwerp and Van Kesteren (2004) that the Krone deposition equation (38) actually incorporates resuspension via the critical bed shear stress for deposition. Therefore, deposition is better described as simply $w_s \cdot c_{z=0}$. This can be achieved by setting the critical bed shear stress for deposition to a very high value. Secondly it should be noted that in a depths averaged calculation the deposition is calculated as if the concentrations are uniform over depth. In reality in most cases there is more suspended sediment near the bed which can be deposited more easily. The effect is that for depth averaged applications, the deposition term underestimates deposition.

D Model grid and parameter settings

D.1 Model area dimensions

The model area should be large enough to situate morphological boundary effects sufficiently far from the mussel bed area of interest. Flow velocities in the model will be around 0.5 m s^{-1} parallel to the channel and 0.05 m s^{-1} transverse to the channel. Furthermore a maximum water depth of 2 m and a 0.5 mm s^{-1} settling velocity are considered[24]. On average, with a uniform concentration profile, the suspended sediment is located at half the water depth. If the sediment can settle half the depth the situation is assumed to be sufficiently adjusted. This means that in the channel parallel direction, there should be ((1 m / 0.0005 m s^{-1}) · 0.5 m s^{-1} =) 1000 m. For the transverse direction it follows that the adjustment distance should be ((1 m / 0.0005 m s^{-1}) · 0.05 m s^{-1} =) 100m. The mussel bed area should be positioned at least these adjustment lengths away from the model boundaries. Considering this, the model dimensions are chosen as 2250 x 300 m

D.2 Computational grid

Two grid have been set-up for this study a coarse and a fine one. The fine grid is only applied where the mussel bed patterns are implemented. A coarse grid is used in the other applications because of the much smaller computation time. Both models used small grid cells in the center (10 x10m and 2 x 2m for the coarse and fine grid respectively) and elongated grid cells (10 x 100) near the model boundaries. The grids have respectively 64 x 32 = 2048 and 137 x 63 = 8631 cells. The choice in grid cell dimensions is motivated by the mussel bed dimensions. In order to model the influence of bathymetric and roughness features on the flow, a certain feature – for example a mussel patch – should be covered by at least 5 grid cells. Figure 54 gives an overview of both grids used in this study.

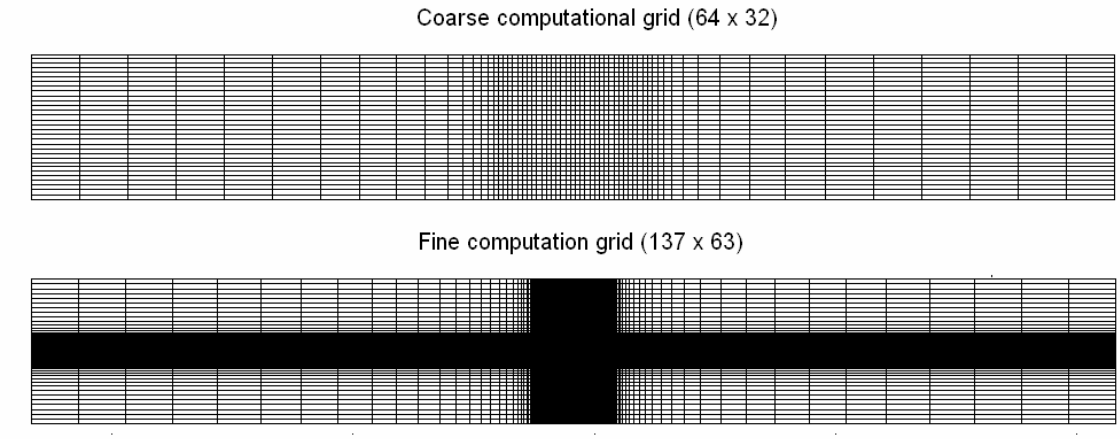

Figure 54: Computational grids.

[24] *These values have been obtained from test computations and conform to values found later in the model used in this report.*

There are two quality criteria applying to a rectangular grid: (1) aspect ratio and (2) smoothness. The first entails that the ratio between the length of the grid cell and the width should be within 0.5 – 2 (WL|Delft Hydraulics, 2006, p. 4-13) in the area of interest. The second criterion concerns the smoothness of the grid, in other words the ratio between the width (or length) of one cell and the width (or length) of a neighboring cells. This value should be smaller than 1.2 in the area of interest (WL|Delft Hydraulics, 2006, p. 4-13). Both criteria are met with the grid used here.

D.3 Numerical settings

A variety of numerical parameters prescribes how Delft3D is to compute the hydrodynamic motions. Perhaps most important is the time step. A guideline in choosing this parameter can be determined using the Courant number. This number implies that a water particle should not travel in more than 2 grid cells in one time step:

$$Cr = \frac{u \cdot \Delta t}{\Delta x} < 1 \qquad (39)$$

Considering the fine grid with minimum grid dimensions of 2 m and the coarse grid with dimensions of 10 m and using a velocity of 0.5 m s^{-1} the time step should be smaller than respectively 4 and 20 s. Accordingly the chosen time steps are 3 and 15 s. Smaller time steps did not significantly affect results.

Because the mudflat is an intertidal area a good implementation of the drying and flooding algorithm is required. This algorithm is explained in Appendix C.3. There are two things important: the value of the control volume in a cell should not become negative in a computation cycle and the discharge through a cell is described correctly. Parameter values and settings have been chosen to take these requirements into account. The most important is the threshold depth, which is set at 5 mm. Essentially, cells where the water falls below this level are considered dry and are taken out of the computation.

D.4 Hydrodynamic parameters

- Time step: 15 s (coarse grid) 3 s (fine grid)
- Layers: 1
- Initial uniform water level: 1.5 m
- Physical parameters:
  - Constants:
    - Gravitational acceleration: 9.81 m s^{-2}
    - Water density: 1000 kg m^{-3}
    - Water temperature: 15 °C
    - Salinity: 31 ppt
  - Roughness: k_s: 0.005 m
  - Uniform horizontal eddy viscosity: 1 m^2 s^{-1}

- Uniform horizontal eddy diffusion coefficient: 1 m^2 s^{-1}
- Numerical parameters:
  - Depth at grid cell centers: MAX
  - Threshold depth: 0.005 m
  - Marginal depth: +999
  - Smoothing time: 0 min
- Harmonic boundary conditions (as given in *.bnd and *.bch file):
  - Channel (water level boundary)
    - Frequency: 30°
    - Amplitude: 1.5 m
    - Phase difference between west and east: 5.5°
  - West (water level boundary)
    - Frequency: 30°
    - Amplitude: 1.5 m
    - Phase relative to channel: 0
  - East (water level boundary)
    - Frequency: 30°
    - Amplitude: 1.5 m
    - Phase relative to channel: 5.5°

D.5 Morphological parameters

- Number of sediments: 1:
  - Type: Mud
  - Density: 2650 kg m^3
  - Settling velocity: $5 \cdot 10^{-4}$ m s^{-1}
  - Critical bed shear stress for sedimentation: 1000 N m^{-2}.
  - Critical bed shear stress for erosion: 0.5 N m^{-2}
  - Erosion rate: $1 \cdot 10^{-4}$ kg m^{-2} s^{-1}
- Process parameters:
  - Morphological scale factor: 10
- Spin-up interval before morphological changes: 0 min
- Minimum depth for sediment calculation 0.05 m
- Initial condition:
  - Uniform concentration in water column: 0.04 kg m^3

D.6 Standard mussel bed parameters

- Multiplication factor for settling velocity over a mussel bed: 2

- Trachytope vegetation characteristics:
  - vegetation height: 0.03 m
  - density · diameter: 5.45 m^{-1}
  - Drag coefficient: 0.641
  - Chézy coefficient for bed in between mussels = 17.57 $m^{1/2}$ $s^{—1}$
  - These values correspond to k_s = 0.09 m and equal bed shear stress on the sediment as a flat bed under similar conditions at 75 cm water depth.
- Erosion rate (spatially applied by *.ero): $4 \cdot 10^{-4}$ kg m^{-2} s^{-1}
- Critical bed shear stress for erosion (spatially applied by *.tce): 0.5 m^{-2}

E Flow conditions and suspended sediment concentration at observation points

Observation points can be defined in Delft3D where model output is written to file with a certain time interval. A number of these points have been defined. For seven observation points on the model boundary the observed flow conditions and suspended sediment concentration are presented in this appendix. These points are situated on the model domain as displayed in Figure 55. Note that the water levels are the exact boundary conditions as imposed.

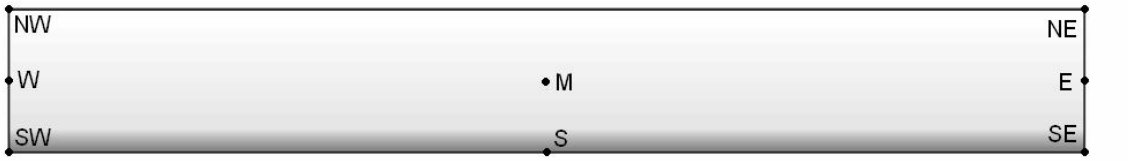

Figure 55: Observation points, note that these 'points' actually correspond to grid cells.

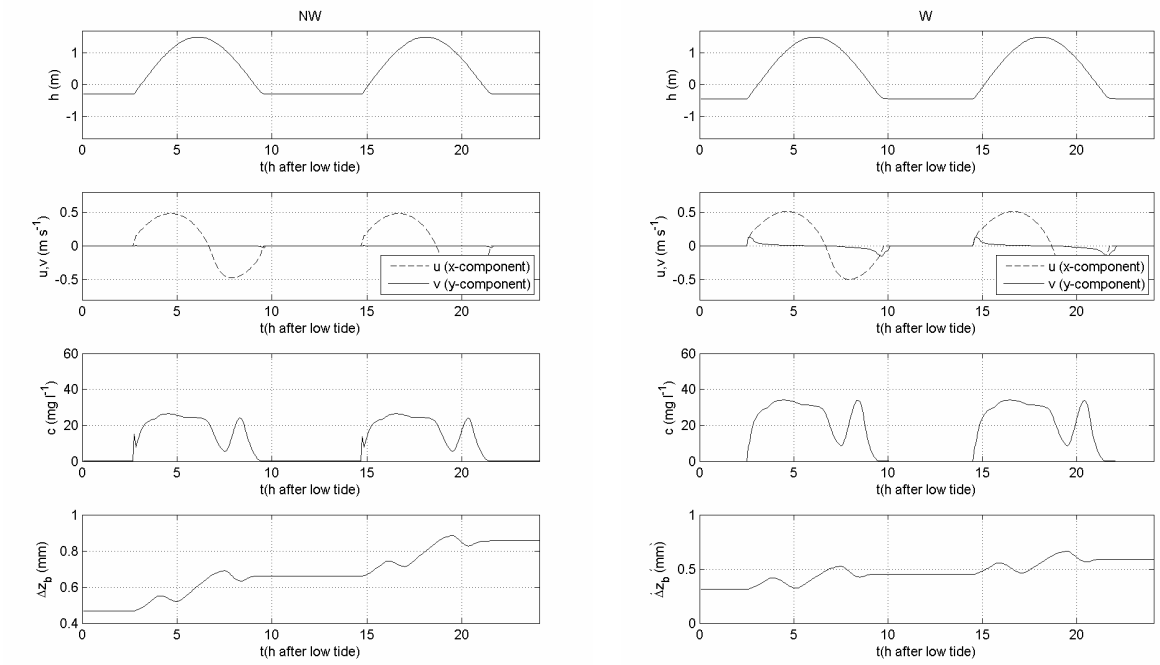

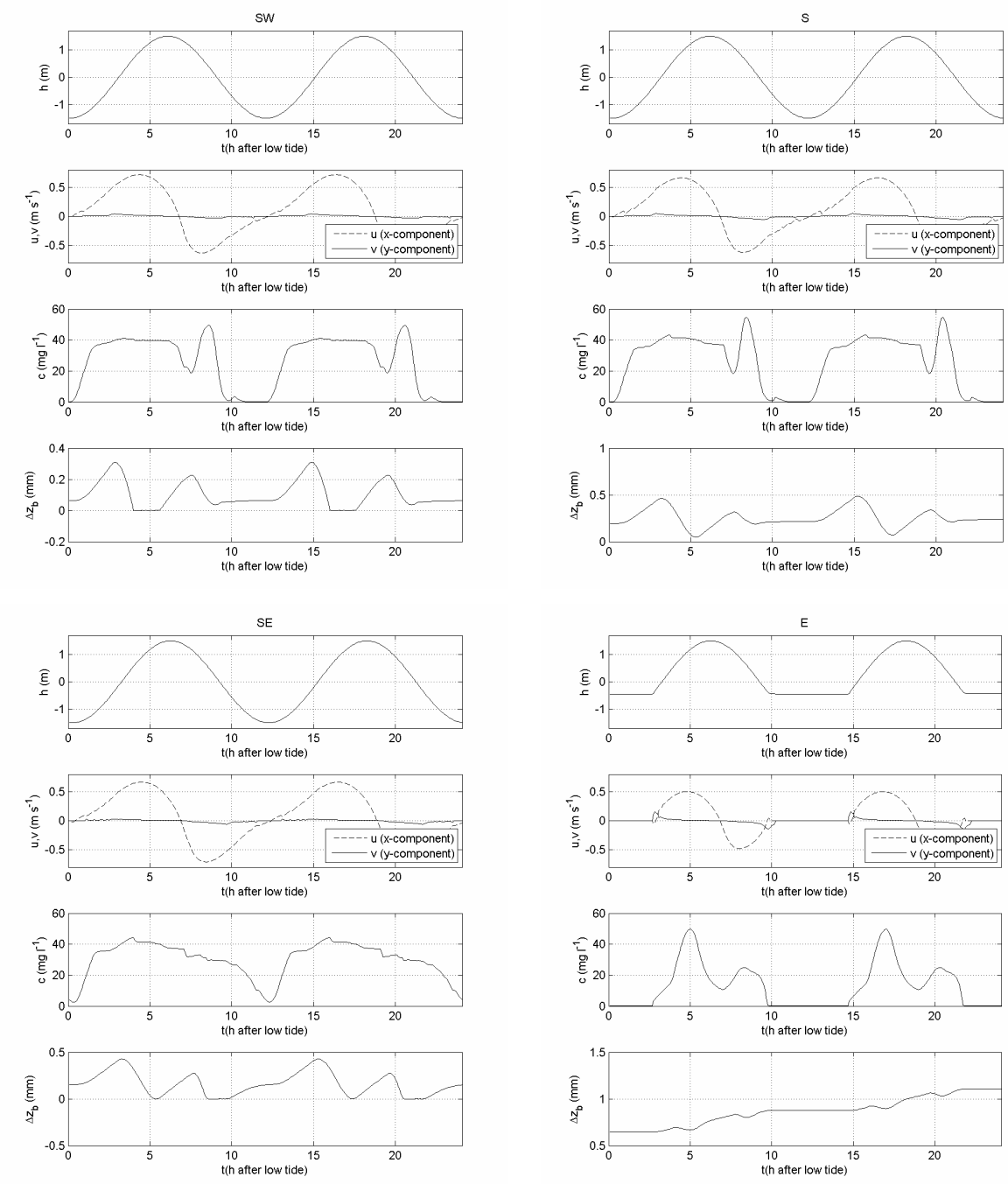
SW
S
SE
E
h (m)
u,v (m s-1)
c (mg l-1)
Δzb (mm)
t(h after low tide)
u (x-component)
v (y-component)

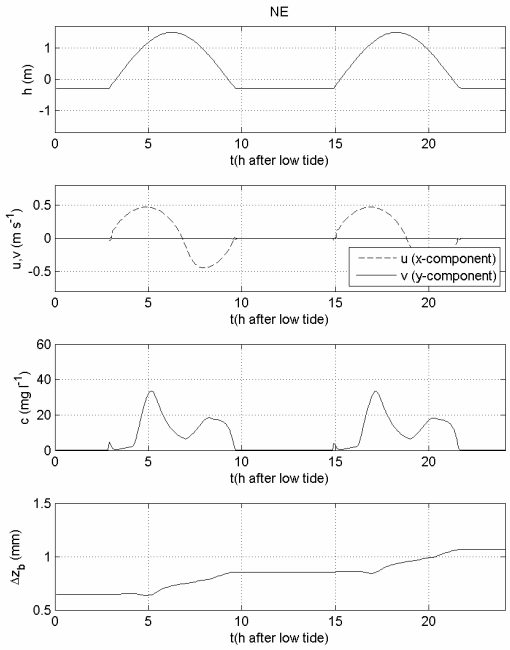

Figure 56: Water level (h), flow velocity components (u, v) and suspended sediment concentration (c) in seven observation points during a double tidal cycle following low tide in the reference situation.

F Contour plots of deposition in case of different mussel bed patterns

The accretion in the area of interest in cases of different mussel bed patterns is presented. The mussel bed area is depicted by a thick dotted line.

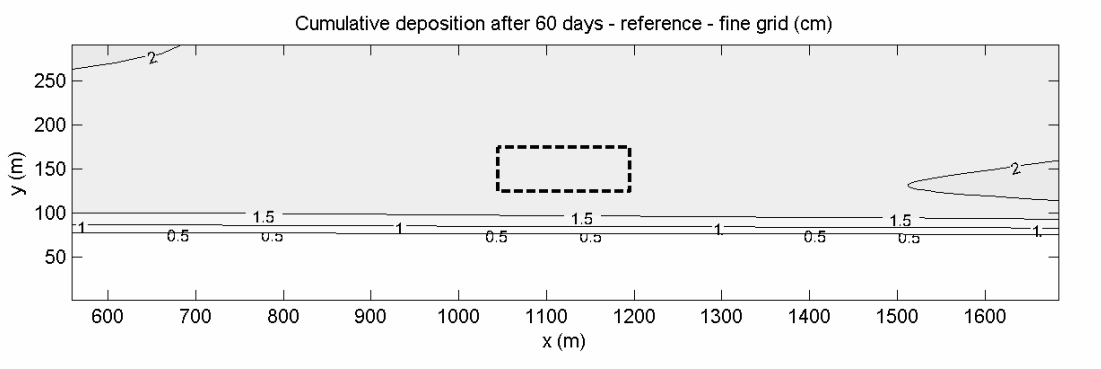

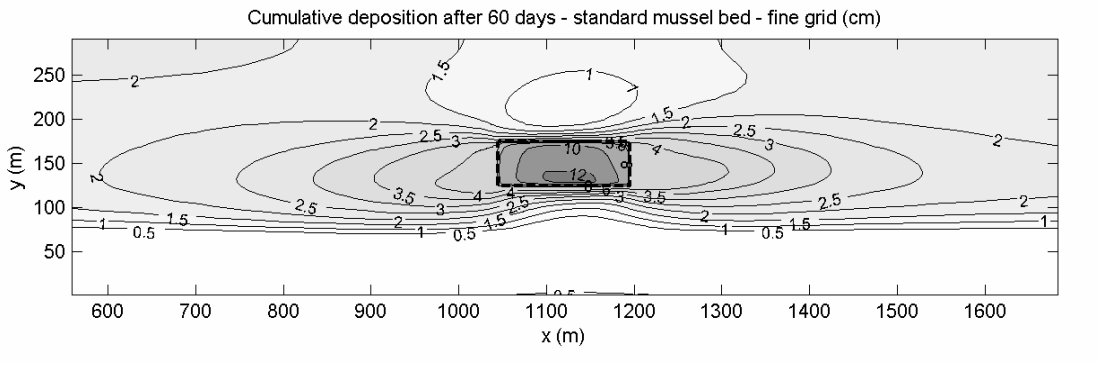

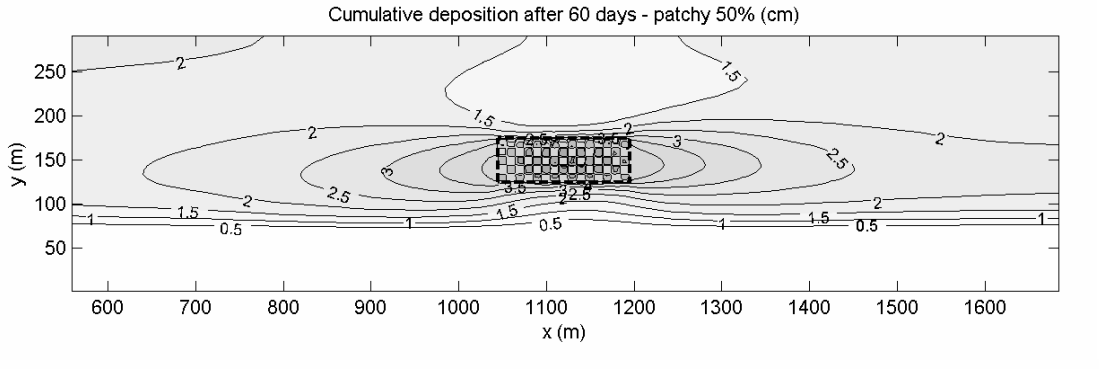

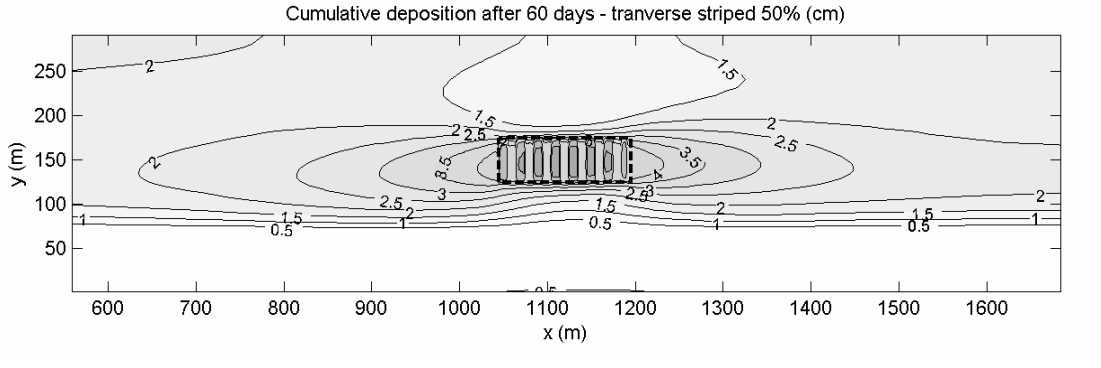

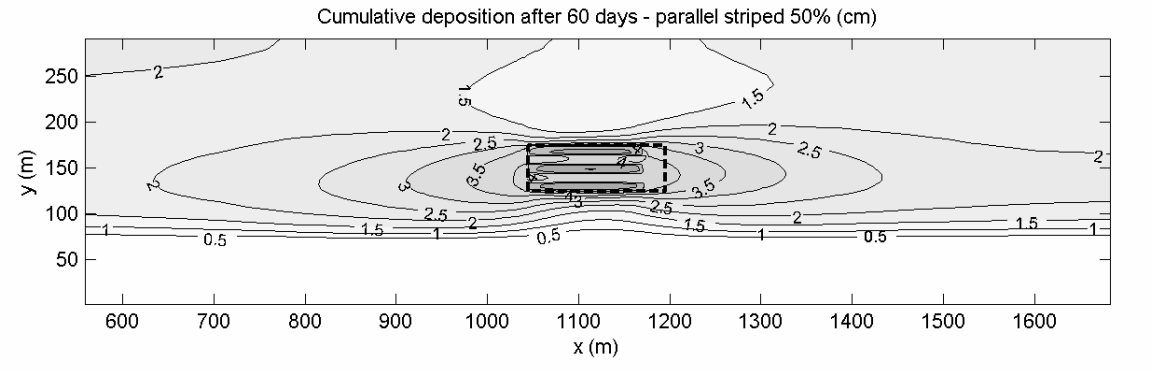
Cumulative deposition after 60 days - parallel striped 50% (cm)
y (m)
x (m)

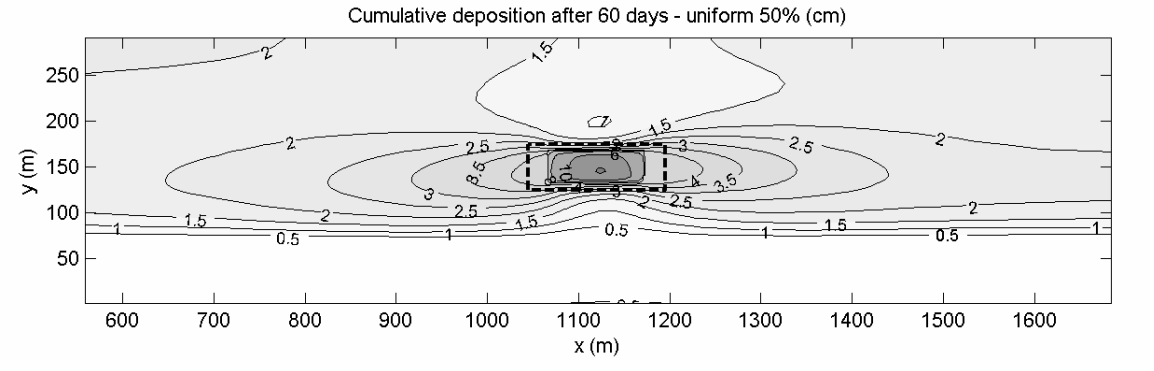
Cumulative deposition after 60 days - uniform 50% (cm)
y (m)
x (m)

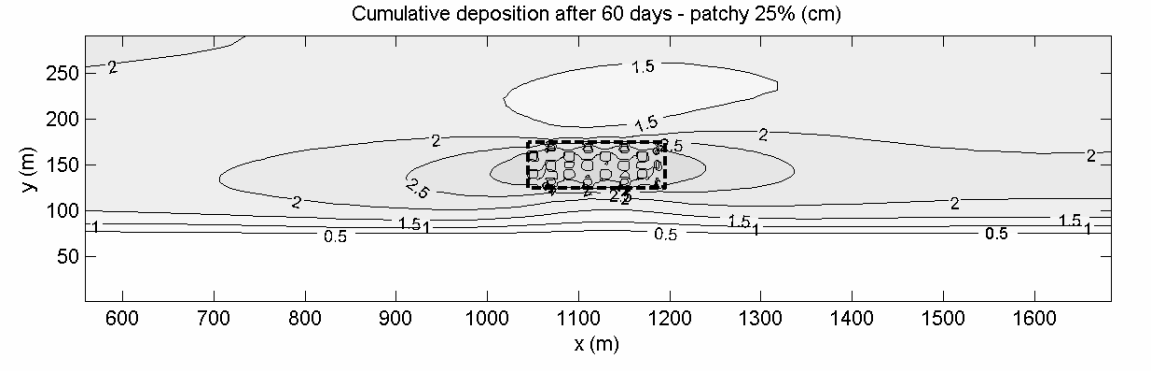
Cumulative deposition after 60 days - patchy 25% (cm)
y (m)
x (m)

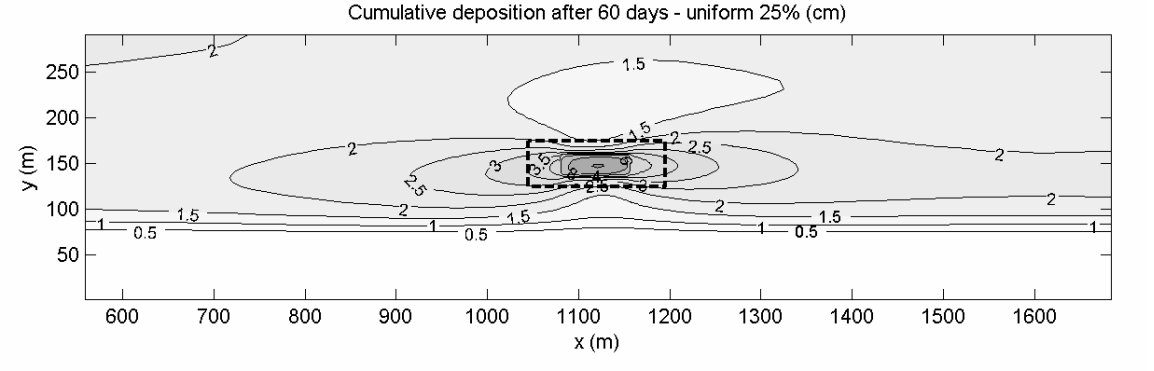
Cumulative deposition after 60 days - uniform 25% (cm)
y (m)
x (m)